REGULATING VALVULAR INTERSTITIAL CELL PHENOTYPE BY BOUNDARY STIFFNESS

A Dissertation Presented

By

Mehmet Hamdi Kural

Submitted to the Faculty of Worcester Polytechnic Institute, Department of Biomedical Engineering,

Worcester in partial fulfillment of the requirements for the degree of

Doctor of Philosophy

May 19, 2014

Biomedical Engineering

REGULATING VALVULAR INTERSTITIAL CELL PHENOTYPE BY BOUNDARY STIFFNESS

A Dissertation

Submitted to the Faculty of

WORCESTER POLYTECHNIC INSTITUTE

in

Biomedical Engineering

May 2014

by

_____

Mehmet Hamdi Kural

APPROVED:

_____

Kristen L. Billiar, PhD
Associate Professor, *Thesis Advisor*
Biomedical Engineering Department
Worcester Polytechnic Institute

_____

Glenn R. Gaudette, PhD
Associate Professor,
Biomedical Engineering Department
Worcester Polytechnic Institute

_____

Raymond L. Page, PhD
Assistant Professor,
Biomedical Engineering Department
Worcester Polytechnic Institute

_____

Nima Rahbar, PhD
Assistant Professor,
Civil and Environmental Engineering Department
Worcester Polytechnic Institute

_____

Narendra Vyavahare, PhD
Professor
Bioengineering Department
Clemson University

To my lovely wife...

ACKNOWLEDGEMENTS

I want to thank my advisor Prof. Kristen Billiar for trusting me and giving me the chance to work with him. Thank you for being a very good role model as a scientist, an engineer and a teacher. Thank you for being very understanding and encouraging all the time.

I want to thank my thesis committee members Prof. Glenn Gaudette, Prof. Raymond Page, Prof. Narendra Vyavahare and Prof. Nima Rahbar for their valuable comments and suggestions about this thesis.

I want to thank my colleagues Heather Cirka, John Favreau, Tracy Hookway, Jacques Guyette, Jon Grasman, Zoe Reidinger, Amanda Clement, Jennifer Molignano, Jason Forte, Tuba Bas, Denis Kole, Olga Kashpur, Sarah Hernandez for training me and sharing their experience.

I want to thank BME faculty members Marsha Rolle, George Pins, Anjana Jain, Tanja Dominko and Dirk Albrecht for their advice and use of their lab equipment.

I want to thank Victoria Huntress for helping me with microscopy and imaging.

I want to thank Hans Snider for helping me with histology.

I want to thank Christoper Chen for generously donating micro-tissue gauge stamps and Thomas Boudou, Michael Borochin, Mahmut Selman Sakar and Adrian West for sharing their experiences with micro-tissue gauge method.

I want to thank NIH for funding my projects (grant number: 1R15-HL087257-01A2).

I want to thank my brother Comert Kural and my sister in law Suheda Kural for being my guides in the US.

I want thank my mother Beyhan Kural and father Rifat Kural for their endless support through my entire life. Thank you for watching over me, giving me strength and sending your love from thousands of miles away.

And I want to thank my wife, Nurhan Canpulat Kural for always loving me, for always being right by my side, for sharing the life with me and for making it beautiful for me.

ABSTRACT

A quantitative understanding of the complex interactions between cells, soluble factors, and the biological and mechanical properties of biomaterials is required to guide cell remodeling towards regeneration of healthy tissue rather than fibrocontractive tissue. The goal of this thesis was to elucidate the interactions between the boundary stiffness of three-dimensional (3D) matrix and soluble factors on valvular interstitial cell (VIC) phenotype with a quantitative approach.

The first part of the work presented in this thesis was to characterize the combined effects of boundary stiffness and transforming growth factor-β1 (TGF-β1) on cell-generated forces and collagen accumulation. We first generated a quantitative map of cell-generated tension in response to these factors by culturing VICs within micro-scale fibrin gels between compliant posts (0.15-1.05 nN/nm) in chemically-defined media with TGF-β1 (0-5 ng/mL). The VICs generated 100 to 3000 nN/cell after one week of culture, and multiple regression modeling demonstrated, for the first time, quantitative interaction (synergy) between these factors in a 3D culture system. We then isolated passive and active components of tension within the micro-tissues and found that cells cultured with high levels of stiffness and TGF-β1 expressed myofibroblast markers and generated substantial residual tension in the matrix yet, surprisingly, were not able to generate additional tension in response to membrane depolarization signifying a state of continual maximal contraction. In contrast, negligible residual tension was stored in the low stiffness and TGF-β1 groups indicating a lower potential for shrinkage upon release. We then studied if ECM could be generated under the low tension environment and found that TGF-β1, but not EGF, increased *de novo* collagen accumulation in both low and high tension environments roughly equally. Combined, these findings suggest that isometric

cell force, passive retraction, and collagen production can be tuned by independently altering boundary stiffness and TGF-β1 concentration.

In the second part, by using the quantitative information obtained from the first part, we investigated the effects of dynamic changes in stiffness on cell phenotype in a 3D protein matrix, quantitatively. Our novel method utilizing magnetic force to constrain the motion of one of two flexible posts between which VIC-populated micro-tissues were cultured effectively doubled the boundary stiffness and resulted in a significant increase in cell-generated forces. When the magnetic force was removed, the effective boundary stiffness was halved and the tissue tension dropped to 65-87% of the peak value. Surprisingly, following release the cell-generated forces continued to increase for the next two days rather than reducing down to the homeostatic tension level of the control group with identical (but constant) boundary stiffness. The rapid release of tension with the return to baseline boundary stiffness did not result in a decrease in number of cells with α-SMA positive stress fibers or an increase in apoptosis. When samples were entirely released from the boundaries and cultured free floating (where tension is minimal but cannot be measured), the proportion of apoptotic cells in middle region of the micro-tissues increased more than five-fold to 31%. Together, these data indicate that modest temporary changes in boundary stiffness can have lasting effects on myofibroblast activation and persistence in 3D matrices, and that a large decrease in the ability of the cells to generate tension is required to trigger de-differentiation and apoptosis.

Table of Contents

Table of Figures

Table of Tables

CHAPTER 1: Introduction

1.1 Introduction

Due to heart valve diseases, approximately 300,000 patients have heart valve replacement surgery each year [1]. Although previously believed to be a passive degenerative process, it is now becoming clear that valvular interstitial cells (VICs) play an active role in heart valve disease, yet there are no treatments short of replacement. To develop therapies, it is critical to understand the mechanisms leading to heart valve diseases.

VICs play a vital role in healthy function of heart valves by synthesizing, remodeling, and repairing the valvular extra cellular matrix (ECM) [2]. In healthy adult heart valves, the majority of VICs resemble quiescent fibroblasts. However, VICs have a highly plastic nature and can differentiate (i.e., activate) into the highly contractile myofibroblast phenotype which is recognized by α-smooth muscle actin (α-SMA) rich stress fibers, increased force generation and collagen production. In excessive numbers, myofibroblasts can compact surrounding matrix aggressively and stiffen tissues by generating large forces and secreting large amounts collagen, which are associated with pathological fibrosis [3, 4] and calcification [5].

Tissue engineered heart valves (TEHVs) are promising, since they have potential to remodel, grow and be produced completely autologous, especially for pediatric patients who have to have reoperations through their growth era.

The most recent TEHV technology employs biodegradable synthetic polymers or natural scaffolds seeded with cells. There is a variety of options for both scaffold material and cell source. Poly(lactic acid) (PLA) and poly(glycolic acid) PGA are most commonly used synthetic materials, while collagen, fibrin or hyaluronic acid (HA) are the natural materials used as TEHV scaffolds. Mechanical conditioning of cell seeded scaffolds in

bioreactors provides *in vitro* tissue formations [6-10]. In addition to this, animal model studies showed that remodeling into native-like tissues occurs in implanted TEHVs [11, 12]. Although these studies showed that TEHVs have feasibility, still, there are drawbacks that prevent clinical trials. One of the most common problems is the tissue retraction or shrinkage due to cell traction forces and residual stress in extra cellular matrix (ECM), created by forces applied by cells. The reason for the retraction is that the remodeled ECM is not stiff and strong enough to carry that load, after the degradation of the scaffold. Tissue retraction problem was observed both *in vitro* [6, 10] and *in vivo* studies [12-14]. In most of the *in vivo* studies the regurgitation caused by tissue retraction is mentioned as mild, but it is still one of the obstacles to clinical trials.

VICs are activated to the myofibroblastic phenotype as a result of changes in mechanical stresses exerted on valves. These stresses are elevated during embryonic development [15], disease states such as hypertension, hyperglycemia, and hyperlipidemia, and with disruption of the ECM structure (damage) [16]. Along with stress transferred to and generated by cells, transforming growth factor beta (TGF-β) is known to be necessary for myofibroblast activation in all types of fibroblasts [17-19]. Further evidence indicates that that TGF-β and mechanical tension have a synergistic effect on myofibroblast activation in VICs [20, 21]. It appears that increased external loads result in amplification of intrinsic tension at the cell level, which, in turn, increases the sensitivity of cells to TGF-β and triggers myofibroblast activation. Intracellular tension has also been shown to increase with to resistance cell traction forces (i.e., stiffness) of two-dimensional (2D) substrates [22] and three-dimensional (3D) matrices [23] .

In particular, in 3D fibroblast-populated collagen gel matrices which are anchored to flexible beams, the stiffness of beams (tissue boundary) has been shown to be correlated

positively with the homeostatic tension generated by the cells and myofibroblast markers [24, 25]. However, the combined effect of boundary stiffness and soluble factors on differentiation has not been systematically studied for VICs or any cell type. Further, reducing the number of myofibroblasts by apoptosis [26, 27] and phenotypic reversal to a quiescent state [28] is thought to play an important role in wound healing and may be critical for the development of heart valve therapies. However, the effect of tension in determining myofibroblast fate (between persistence, apoptosis or de-differentiation) has not been studied in a 3D matrix. A quantitative knowledge of the relationships between 3D matrix stiffness, growth factor sensitivity, and VIC fate are needed for rational design of therapies for heart valve disease and for the development of tissue engineered valves.

The goal of this thesis is to determine the role of mechanical stiffness of the tissue boundary in the activation of VICs to the myofibroblast phenotype within a three-dimensional ECM environment, and further to investigate the effects of reduced boundary stiffness in real time on VIC fate. In *Chapter 2*, background relevant to heart valve structure, the effect of mechanical and soluble cues on VIC activation and research techniques to investigate the effect of mechanical factors on cell behavior in 3D matrices are presented. *Chapter 3* describes our quantitative characterization of the combined effect of stiffness and growth factors on VIC phenotype within 3D fibrin gels in a micro-well format. Here we cultured VICs in fibrin micro-tissues with multiple boundary stiffness and TGF-β concentrations. VIC-generated forces were measured and quantitative dose-response relationships including interactions between stiffness and growth factor concentration were determined utilizing design of experiment (DOE) methods. Results showed that these two factors increase VIC-generated forces synergistically, but moderate levels of both factors are required for a significant effect. The information provided in Chapter 3 determined our starting point for *Chapter 4*,

which describes our studies of the effects of reduced boundary stiffness on myofibroblast persistence in 3D. In this study, we cultured myofibroblastic VICs in fibrin micro-tissues and altered the boundary stiffness in real time using magnetic forces. Consistent with the results of our comprehensive stiffness study (Chapter 3), cell-generated forces were elevated with increased boundary stiffness in real time, yet surprisingly, the forces continued to increase following real-time reduction of boundary stiffness. Increased apoptosis was only observed with complete freeing of the tissues from the posts, not from the 2-fold real-time decrease in stiffness in the cultured tissues. Although the reasons for the sustained persistence of highly contractile myofibroblasts remain elusive, the persistence does not appear to be due to a substantial increase in local tissue modulus (stiffness). In *Chapter 5*, the contribution of this thesis to the literature is summarized and implications of our findings and suggestions for future directions are presented.

References

[1] Vesely I. Heart Valve Tissue Engineering. Circulation Research. 2005;97:743-55.
[2] Schoen FJ. Evolving concepts of cardiac valve dynamics: the continuum of development, functional structure, pathobiology, and tissue engineering. Circulation. 2008;118:1864-80.
[3] Cushing MC, Liao J-T, Anseth KS. Activation of valvular interstitial cells is mediated by transforming growth factor-β1 interactions with matrix molecules. Matrix Biol. 2005;24:428-37.
[4] Hinz B. Tissue stiffness, latent TGF-beta1 activation, and mechanical signal transduction: implications for the pathogenesis and treatment of fibrosis. Current rheumatology reports. 2009;11:120-6.
[5] Jian B, Narula N, Li QY, Mohler ER, 3rd, Levy RJ. Progression of aortic valve stenosis: TGF-beta1 is present in calcified aortic valve cusps and promotes aortic valve interstitial cell calcification via apoptosis. The Annals of thoracic surgery. 2003;75:457-65; discussion 65-66.
[6] Mol A, Rutten MCM, Driessen NJB, Bouten CVC, Zünd G, Baaijens FPT, et al. Autologous Human Tissue-Engineered Heart Valves: Prospects for Systemic Application. Circulation. 2006;114:I-152-I-8.
[7] Kortsmit J, Driessen NJB, Rutten MCM, Baaijens FPT. Real Time, Non-Invasive Assessment of Leaflet Deformation in Heart Valve Tissue Engineering. Ann Biomed Eng. 2009;37:532-41.
[8] Jiang H, Rhee S, Ho C-H, Grinnell F. Distinguishing fibroblast promigratory and procontractile growth factor environments in 3-D collagen matrices. The FASEB Journal. 2008;22:2151-60.
[9] Knapp DM, Tower TT, Tranquillo RT, Barocas VH. Estimation of cell traction and migration in an isometric cell traction assay. AIChE Journal. 1999;45:2628-40.
[10] Flanagan TC, Cornelissen C, Koch S, Tschoeke B, Sachweh JS, Schmitz-Rode T, et al. The in vitro development of autologous fibrin-based tissue-engineered heart valves through optimised dynamic conditioning. Biomaterials. 2007;28:3388-97.
[11] Hoerstrup SP, Sodian R, Daebritz S, Wang J, Bacha EA, Martin DP, et al. Functional Living Trileaflet Heart Valves Grown In Vitro. Circulation. 2000;102:Iii-44-Iii-9.
[12] Gottlieb D, Kunal T, Emani S, Aikawa E, Brown DW, Powell AJ, et al. In vivo monitoring of function of autologous engineered pulmonary valve. The Journal of Thoracic and Cardiovascular Surgery. 2010;139:723-31.
[13] Flanagan TC, Sachweh JS, Frese J, Schnoring H, Gronloh N, Koch S, et al. In vivo remodeling and structural characterization of fibrin-based tissue-engineered heart valves in the adult sheep model. Tissue engineering Part A. 2009;15:2965-76.
[14] Syedain ZH, Meier LA, Bjork JW, Lee A, Tranquillo RT. Implantable arterial grafts from human fibroblasts and fibrin using a multi-graft pulsed flow-stretch bioreactor with noninvasive strength monitoring. Biomaterials. 2011;32:714-22.
[15] Butcher JT, McQuinn TC, Sedmera D, Turner D, Markwald RR. Transitions in early embryonic atrioventricular valvular function correspond with changes in cushion biomechanics that are predictable by tissue composition. Circulation research. 2007;100:1503-11.
[16] Miller M, Stone NJ, Ballantyne C, Bittner V, Criqui MH, Ginsberg HN, et al. Triglycerides and Cardiovascular Disease: A Scientific Statement From the American Heart Association. Circulation. 2011;123:2292-333.

[17] Desmouliere A, Geinoz A, Gabbiani F, Gabbiani G. Transforming growth factor-beta 1 induces alpha-smooth muscle actin expression in granulation tissue myofibroblasts and in quiescent and growing cultured fibroblasts. J Cell Biol. 1993;122:103-11.
[18] Tomasek JJ, Gabbiani G, Hinz B, Chaponnier C, Brown RA. Myofibroblasts and mechano-regulation of connective tissue remodelling. Nature reviews Molecular cell biology. 2002;3:349-63.
[19] Gabbiani G. The myofibroblast in wound healing and fibrocontractive diseases. The Journal of pathology. 2003;200:500-3.
[20] Walker GA, Masters KS, Shah DN, Anseth KS, Leinwand LA. Valvular myofibroblast activation by transforming growth factor-beta: implications for pathological extracellular matrix remodeling in heart valve disease. Circulation research. 2004;95:253-60.
[21] Merryman DL, H.D.;Long, R.A.; Engelmayer, G.C.; Hopinks, R.A; Sacks, M.S.;. Synergistic Effects of Cyclic Tension and Transforming Growth Factor Beta-1 on the Aortic Valve Myofibroblast. Cardiovasc Pathol. 2007;16:8.
[22] Goffin JM, Pittet P, Csucs G, Lussi JW, Meister JJ, Hinz B. Focal adhesion size controls tension-dependent recruitment of alpha-smooth muscle actin to stress fibers. J Cell Biol. 2006;172:259-68.
[23] Provenzano PP, Keely PJ. Mechanical signaling through the cytoskeleton regulates cell proliferation by coordinated focal adhesion and Rho GTPase signaling. J Cell Sci. 2011;124:1195-205.
[24] Legant WR, Pathak A, Yang MT, Deshpande VS, McMeeking RM, Chen CS. Microfabricated tissue gauges to measure and manipulate forces from 3D microtissues. Proceedings of the National Academy of Sciences. 2009;106:10097-102.
[25] John J, Quinlan AT, Silvestri C, Billiar K. Boundary stiffness regulates fibroblast behavior in collagen gels. Annals of biomedical engineering. 2010;38:658-73.
[26] Grinnell F, Zhu M, Carlson MA, Abrams JM. Release of mechanical tension triggers apoptosis of human fibroblasts in a model of regressing granulation tissue. Experimental cell research. 1999;248:608-19.
[27] Carlson MA, Longaker MT, Thompson JS. Wound splinting regulates granulation tissue survival. The Journal of surgical research. 2003;110:304-9.
[28] Wang H, Haeger SM, Kloxin AM, Leinwand LA, Anseth KS. Redirecting Valvular Myofibroblasts into Dormant Fibroblasts through Light-mediated Reduction in Substrate Modulus. PLoS ONE. 2012;7:e39969.

CHAPTER 2: Background

Excerpted from two published reviews:

Kural, M.H. and Billiar, K.L., "Regulating tension in three-dimensional culture environments." (Invited review) Experimental Cell Research, 319(16), 2013. 2447-2459 (See Appendix-I for permission)

Cirka, H.A., **Kural, M.H**., and Billiar, K.L., "Mechanoregulation of Aortic Valvular Interstitial Cell Life and Death" Journal of Long-Term Effects of Medical Implants, *Accepted for publication*.

2.1 Heart Valve Physiology

In this chapter, background on heart valve physiology and literature describing methods for studying the effect of mechanical factors in 3D cell culture environments are presented. In the first part, we briefly describe the native environment of VICs in heart valves, pathological conditions and current tissue engineered heart valve technology. In the second part, we present a review of techniques for modify tension in 3D matrices to manipulate cell behavior which provides rationale for the choice of the culture system utilized in this thesis.

2.1.1 Heart valves and the mechanical environment of heart valve cells

There are four valves in our hearts which maintain the unidirectional blood flow (Figure 2.1). Atrioventricular valves- mitral and tricuspid valves- prevent backflow form ventricles into atrium. Mitral valve (bicuspid valve) separates left atrium and left ventricular while tricuspid valve separates right atrium and right ventricle. Both atriovetricular valves are attached ventricular wall with tendon cords (chordae tendineae). Chordae tendineae are pulled by papillary muscles which provides constant tension on the cords. Semilunar valves- aortic valve and pulmonary valve- prevent back flow from arteries to ventricles. Pulmonary valve is located at the base of pulmonary trunk, and aortic valve is at the base of aorta.

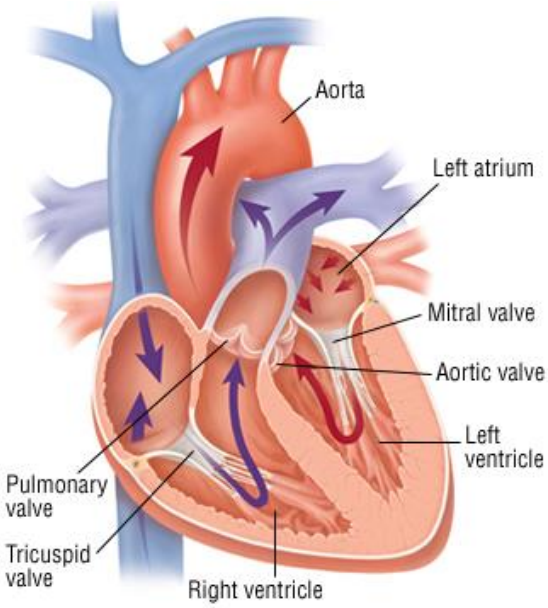

Figure 2. 1 Locations of four heart valves in the heart (www.drugs.com).

Heart valve leaflets have a complex structure in terms of extra cellular matrix (ECM) composition and cell type distribution. All of the four kinds of valves have a similar layered structure. On the outflow surface there is a collagen fiber-rich layer which provides mechanical strength. In the in the center there is loose connective tissue layer. Finally under the in-flow surface there is an elastin-rich layer. For the aortic valve, these layers are called as fibrosa, spongiosa and ventricularis (Figure 2.2). Blood-contacting surfaces of valve leaflets are covered with a monolayer of valvular endothelial cells (VECs). VECs provide thromboresistance and mediate inflammation [1]. . Deep to surface and through all the layers, there are valvular interstitial cells (VICs) which are responsible for synthesize, remodeling and repair of valve ECM including collagen, elastin, and amorphous ECM (predominately glycosaminoglycans [GAGs]) [1].

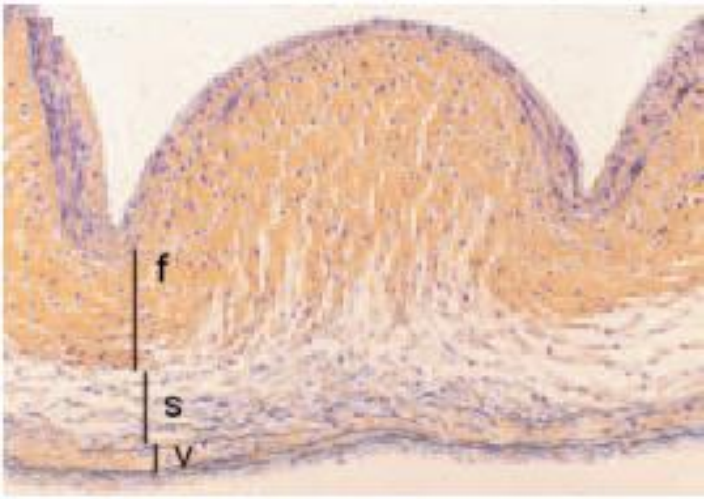

Figure 2. 2 Cross-sectional view of an aortic valve: Blood-contacting surfaces are covered with VECs. VICs are located in all layers. Fibrosa layer (f) contains collagen fibers. The spongiosa (s: in the core) is composed of loose connective tissue ECM. Ventricularis (v) layer has an elastin-rich structure [1].

Depending upon their location within the aortic valve, VICs experience a multitude of forces and mechanical properties which differentially regulate their phenotype (Figure 2.3). During ventricular filling (diastole), the valve leaflets are stretched to form a tight seal which prevents the back flow of blood from the aorta to the left ventricle. When the pressure in the left ventricle is greater than that in the aorta (systole), the valve opens by leaflet shortening and flexion allowing blood to flow out of the heart. During a normal cardiac cycle, the valve tissue and resident cells are exposed to a variety of mechanical stresses including stretching due to transvalvular pressure, shear stress due to blood flow, and cyclic flexure. Due to the rapid opening and closing, the rates of loading are particularly high.

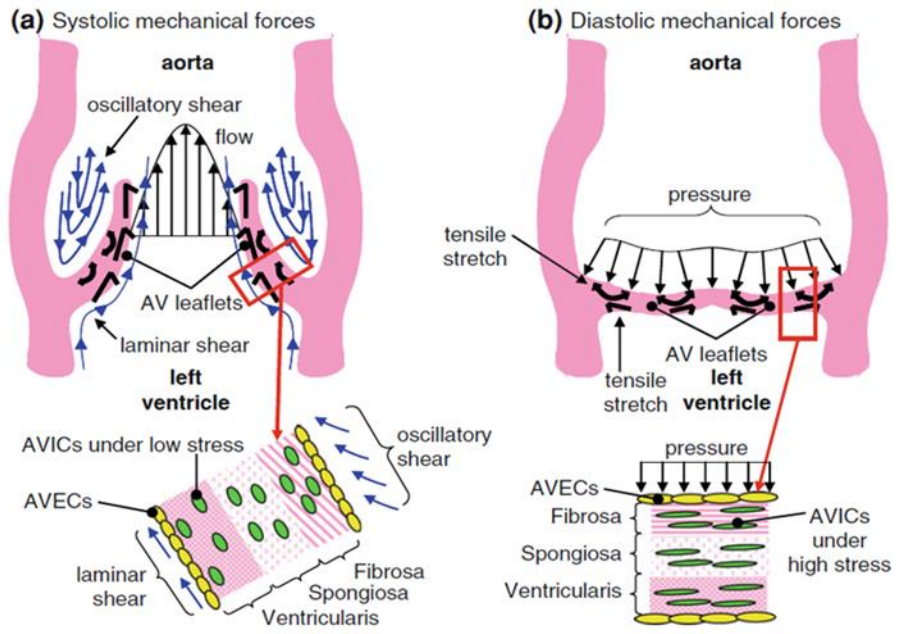

Figure 2. 3 An illustration showing the mechanical fotces that aortic VICs are exposed during cardiac cycle [2].

Different layers of valves have specific protein compositions resulting in unique mechanical properties and transfer of forces. Specifically, the ventricularis and fibrosa are fibrous in composition (collagen and elastin) and resist tensile forces, whereas the glycosaminoglycan (GAG)-rich spongiosa acts as a lubricating and shock absorbing layer between the ventricularis and fibrosa. Mechanical properties differ between the valve leaflet layers. Reported values for the fibrosa range from 4.7 kPa to 13 kPa [2, 3] and those of the ventricularis range from 3.7 kPa to 7.3 kPa [2, 3]. Despite these macroscopic measurements, the local extracellular matrix modulus which the VICs experience is not known.

2.1.2 VICs and Valve Diseases

In healthy adult heart valves, VICs have a quiescent nature. They are at rest and maintain normal valve physiology. Due to change in mechanical environment (disease and injury), VICs are activated and start to express characteristics of myofibroblasts, a highly

contracting and synthetic phenotype. Activated VICs (aVICs, i.e., myofibroblasts) remodel the valve ECM by applying high large traction forces, synthesizing increased amount of ECM proteins, or enzymatically degrading the ECM. At the end of normal remodeling, aVICs are removed by apoptosis. Dysfunction of aVIC apoptosis, together with excessive ECM synthesis and abnormal remodeling can result in pathological fibrosis, angiogenesis or calcification [4].

With advanced valve disease, the stratified structure of the valve is destroyed resulting in protein disarray. The valve thickens [5] and VICs activate to the myofibroblast phenotype. ECM composition may regulate VIC phenotype either by directly changing ligand signaling pathways or by altering the transfer of loads and hence the mechanical environment. In addition to protein changes, calcified valves also have altered cell distribution throughout the leaflet. In a healthy valve, VICs are found dispersed evenly through all three layers [5]. In diseased valves the cells form aggregates within the tissue.

Under normal physiologic conditions, VICs do not usually come into contact with one another as they are embedded in large amounts of extracellular matrix. Focal adhesions on the cell serve as attachment point to ECM proteins. Focal adhesions grow larger when loaded, e.g., by pulling with micro-beads [6, 7] or substrate stretch [8]. With increasing tension, fibroblasts transition to proto-myofibroblasts; this phenotype expresses α-SMA-negative stress fibers [9]. The myofibroblast phenotype is characterized by *de novo* expression of α-SMA sequestered within the stress fibers [10, 11]. Although shown in a different cell type than VICs, the tension generation capacity of myofibroblasts is much greater than that of fibroblasts due to α-SMA incorporation into stress fibers [12]. It remains an open research question if the integrins expressed by myofibroblasts differ

from those expressed by fibroblasts; transforming growth factor- beta (TGFβ), a potent myofibroblast activator, up-regulates the expression of many integrins [13].

Extensive experimental evidence suggests that VIC phenotype is sensitive to the elastic modulus of the substrate on which the cells are cultured [14-16] and substrate modulus is known to regulate the amount of tension a cell can generate [17]. When VICs are cultured on compliant substrates (less than 3 kPa), they have a rounded morphology with little α-SMA incorporation into the cytoskeleton [14]. Spread area, which is correlated with cell generated tension in other cell types [18] is also smaller for VICs on more compliant substrates. However, on high modulus substrates (greater than 10 kPa), VICs are elongated and spindle shaped with α-SMA incorporation into the stress fibers [14].

Several research groups have attempted to identify a "transitional" stiffness where VICs differentiate from quiescent fibroblast-like cells to highly contractile myofibroblasts and/or below which they de-differentiate [14, 19]. Quinlan et al. activated VICs to the myofibroblast phenotype by culturing them for two days on stiff tissue culture plates before transfer to collagen-coated polyacrylamide hydrogels. Identification of transitional stiffness was accomplished by using eleven different substrates with moduli that ranged from 0.15 kPa-150 kPa [14]. The transitional modulus was found to be 2.5 kPa-7kPa [14]. Anseth and colleagues also demonstrated that the activated VIC phenotype is reversible [19, 20]. Specifically, myofibroblasts were cultured for three days on photodegradable hydrogels then irradiated to reduce the modulus from 32 kPa to 7 kPa. Within two days after modulus reduction, myofibroblasts reverted to quiescent VICs without significant changes in cell viability [19, 20]. Additionally, myofibroblasts that have reverted to the fibroblast state maintained the potential to activate the expression of myofibroblast genes in response to TGF-β1 and to proliferate in response to growth

stimuli, indicating a reversible fibroblast state [20].These data indicate that myofibroblasts can be de-differentiated without inducing apoptosis which has implications for the development of treatments of CAVD and fibrotic diseases; however, a better understanding of the precise magnitude of stiffness and/or cell tension reduction required for phenotypic regulation is needed, especially in a more biomimetic three-dimensional culture environment.

2.2 Regulation of Tension in 3D Culture Environments

2.2.1 Background of Mechanobiology in 3D

In the 1980s, soft wrinkling culture surfaces [21], tunable stiffness substrates [22], and dynamic stretching devices [23] were developed which allow systematic study of how cells apply traction to their surroundings and how external loads affect cell behavior [24]. However, the importance of tension on cell behavior was actually highlighted in 3D matrix culture much earlier. Cell behavior has been studied in 3D matrices of clotted plasma and lymph since the early 1900s (see review by Grinnell and Petroll [25]), and over 50 years ago Weiss [26] demonstrated that cells locally reorganize fibers in a fibrin gel clot model between cell explants indicating long-range effects of traction forces. In the early 1970s, Elsdale and Bard [27] cultured cells on and in reconstituted collagen gels and found that they retain *in vivo*-like bipolar spindle morphology indicating lines of tension, and Bell [28] systematically studied the effect of free-floating and rigidly anchored boundaries on the structure of collagen gels compacted by fibroblasts of different proliferative potential. In the next decade, Stopak and Harris [29] found that fibroblast traction in 3D collagen matrices is sufficient to form patterns of tension,

compression, and fiber alignment with similarities to wrinkling caused by cell traction on thin polymer membranes [21].

These biopolymer culture models provide a tissue-like spatial arrangement missing in 2D culture, and reveal many differences in cell behavior on flat surfaces and within a fibrous matrix. Most notably, cell morphology is markedly different in gels than on 2D surfaces [30-32]. Cell growth [27], motility [31, 33], differentiation [34], tumorigenicity [35], and response to soluble factors are also altered when cells are extracted from 3D tissues and cultured on 2D substrates [36]. Reasons for discrepancies in cell behavior between 2D and 3D environments are an active topic of debate in the literature [37]. "Dimensionality" itself is not an independent stimulus, rather a complex set of factors that must be decoupled to better understand the critical determinants of cell behavior (see reviews [38] and [39]). Cell-generated tension in 3D matrices, the focus of the present review, is affected by many factors including cell morphology, adhesion, soluble factors, and the resistance of the cells surroundings to deformation (effective stiffness), all of which differ between 2D and 3D systems. Cell morphological states and migration are restricted by the fibrous meshwork such that cells spread and align along fibers and cells need to squeeze through (ameboid-like) or enzymatically degrade the proteins if the fiber mesh is dense and/or cross-linked [25]. Further, specialized cell–matrix adhesions [40] are formed in 3D systems with more symmetric adhesions over the surface of the cell which alters the concentration of ligands available for binding [41]. Diffusion of nutrients and growth factors is also limited in 3D gels in a protein density-dependent manner, and the matrix can act as a repository of factors which can be enzymatically released by the cell in a tension-dependent manner [42].

Combinations of ECM components and biological hydrogels (e.g., collagen and fibrin [43], collagen and agarose [44], etc.) are utilized as 3D models of varied complexity to mimic specific tissues and to facilitate particular cell-matrix interactions; however, single protein matrices of collagen or fibrin remain the most widely utilized model systems for the study of mechanobiology in 3D (as reviewed by Pedersen and Swartz [38]). Type I collagen is the most abundant protein found in interstitial tissue and is widely used in tissue engineering applications. Collagen monomers can be obtained as small aggregates by acidic digestion of connective tissues (e.g., rat tail tendon, bovine cartilage, and skin) and by pepsin extraction [30]. Collagen monomers form *in vitro* by self-assembly when the pH is brought to physiologic level, a process accelerated with increasing temperature (generally 4-37°C). Although the reconstituted collagen gel has much weaker mechanical properties than collagen structures in native tissues, it has proved useful both for fundamental cell-matrix studies and for clinically available engineered tissues (e.g., Apligraf®, Organogenesis Inc.). Fibrin is the major component of the provisional matrix during wound healing and is a widely utilized model matrix as reviewed by Janmey et al. [45]. Fibrin matrices are formed by polymerization of fibrinogen (obtained from blood) with thrombin in the presence of calcium. Fibrin matrices actively bind growth factors, heparin, and different integrin types making them suitable tools for researching fibroplasia [46], stem cell differentiation [47], tumor angiogenesis, and tissue engineering [48, 49]. The cell tension within these compliant gels can be modulated locally by modifying the intrinsic properties and globally by modifying the boundary conditions, as reviewed in the following sections.

2.2.2 Free-floating, Rigidly Anchored and Released Gels

Most commonly, cell-populated gels are either anchored to a rigid culture surface or cultured freely floating in the media following polymerization. When cells are cultured

at sufficiently high density (typically 0.1 – 3 million cells/ml) within protein gels for extended culture duration (hours), they act collectively and the forces they generate are transmitted through the matrix to other cells and to the boundaries of the tissue [28, 50, 51]. As the population of cells compact the matrix globally, how the edges of the tissue are constrained (or released from constraint) determines the overall resistance of matrix deformation i.e., effective stiffness. This resistance regulates the traction forces that the cells are able to generate and sustain within the matrix.

The resulting cell morphology, migration, contractility and protein secretion are markedly different under "free" (floating) and "fixed" (rigidly anchored) boundary conditions, despite identical *initial* protein and cell density [52]. The matrix can also be released from a rigid boundary which leads to a decrease in tension within gel and further changes in cell behavior (Figure 2.4). The tension that populations of cells generate against stiff boundaries are many fold greater than against soft boundaries [36, 53], and tension in free gels, although not directly measurable, is likely to be negligible in the center of a floating gel compared to an anchored gel. For this reason, anchored matrices are termed "mechanically loaded," "high tension," or "stressed" gels, and free floating matrices are termed "unloaded," "low tension," or "unstressed" gels. Differences in the ability of the cells to generate tension against these boundary conditions also lead to substantial variations in the resulting microstructure of the gels which may affect cell behavior. Differences between the volume of floating and anchored gels [54, 55] result in dramatic variances in the ECM density, pore size, diffusional coefficients and distances between cells [56-58] (although actual gel volume and structural parameters are seldom measured experimentally). The behavioral differences under the different boundary conditions have also been attributed to the relatively high intrinsic stiffness of anchored gels compared to floating gels due to greater anisotropic compaction [54, 59]. Further, the

organization of the fibers is quite different between these two cases due to the altered direction of compaction [36]. These confounding factors hinder efforts to decouple the effects of tension from the architecture and properties of protein gels and have led to extensive development of synthetic polymer systems for studying mechanobiology in 3D [44, 60]. Regardless of these limitations, cell behavior and fate in free floating, rigidly anchored, and released collagen gels have been studied extensively and have added greatly to our understanding of cell mechanics and motility (as reviewed by Grinnell and Petroll [25]).

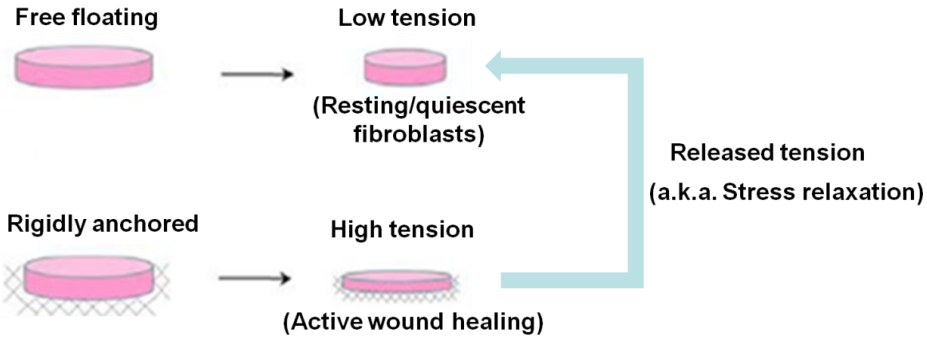

Figure 2. 4 Fibroblasts in free floating gels resemble the quiescent cells. Fibroblasts in free floating gels resemble the quiescent cells in interstitial tissues, while cells in anchored gels are activated and differentiate into myofibroblasts (in the presence of TGF-β) as observed in active wound healing. Releasing anchored gels simulate the accelerated completion of wound healing.

In freely floating gels (zero radial force at outer boundary), cells contract the 3D gels by two mechanisms: initial cell elongation and spreading and cell traction forces due to cell locomotion [61]. Cells are in round shape when they are first trypsinized and re-suspended in gel solution. Within hours they elongate and branch and apply traction forces to the surrounding material. Following elongation and spreading, they apply traction to the matrix while they migrate. In free gels, fibroblasts have a dendritic morphology similar to those in native interstitial tissues rather than the pancake-like shape observed in 2D monolayers [52, 62, 63] and they do not express stress fibers [64-

66] or require fibronectin for stress generation or compaction [62, 67, 68]. Instead, the cells generate force by α- and α-actinin constituting the cortical cytoskeleton [31, 69]. Since there is low resistance to collagen translocation, cells are not able to generate significant tension and thus are not exposed to tension generated by other cells. Due to the low tension in the center of the gel (generally the area analyzed), fibroblasts do not differentiate into to myofibroblasts, a highly contractile and synthetic phenotype, and they do not express organized α-SMA rich stress fiber structures, even in the presence of transforming growth factor-β (TGF-β) [65, 67]. At the edges of free-floating fibroblast-populated collagen gels, the cells and collagen are aligned circumferentially suggesting anisotropic stresses in these areas and a portion of the cells are α-SMA+ indicating heightened tension, as predicted by analytical analyses [70, 71].

Inside anchored matrices (zero radial displacement at the outer boundary), cells initially appear similar to cells in free floating matrices and migratory forces dominate contractile forces for short culture duration [72]. With cooperative cell remodeling of the matrix over many hours, the cells become extended and stellate or bipolar [51, 65], and the tension in the gel rises rapidly over 24 hours followed by an equilibrium "homeostatic" tension generated [73]. Under these conditions, cells can generate sufficient tension against the fixed boundary to differentiate into phenotypes observed on stiff substrates; however, the means by which they achieve the high tension differ in 2D and 3D systems. In soft protein gels, as in wound granulation tissue [74], the cells generate tension between each other via the matrix which must be restrained at the boundaries. On 2D substrates, single cells can generate high levels of tension against the stiff material, as occurs in stiff fibrotic tissues. In both systems, fibroblasts initially form α-SMA negative stress fibers, generate contractile forces via Rho kinase (contractile remodeling), and have a stellate-like morphology; these cells are termed proto-myofibroblasts by Tomasek et al. [64]. In

the presence of TGF-β, proto-fibroblasts become differentiated myofibroblasts as defined by expression of α-SMA+ stress fibers and by generation of increased contractile forces [51, 54, 64, 75]. The actions of growth factors such as TGF-β are strongly regulated by the tension that the cell can generate within the ECM. For example, in the low tension environment of floating matrices, TGF-β stimulates fibroblast contraction directly as an agonist; in anchored matrices TGF-β stimulates differentiation into the myofibroblast phenotype and increases generation of residual stress in the matrix [76].

To decrease the tension in cell-populated gels, an anchored gel may be released after compacting for a period of time (generally 3-5 days) (Figure 2.4) [77]. This experimental condition, often termed stress relaxation but more aptly called release, is thought to represent an accelerated transition between granulation tissue and late-stage wound healing where the cells are shielded from extrinsic stress [67, 74, 78]. Following release from rigid constraints, the tissue rapidly contracts (retracts) due to a combination of passive residual stress [79] and active cell contraction involving a stress-fiber dependent smooth muscle-like mechanism [77] (Figure 2.5). The rate and magnitude of retraction are often utilized as metrics of the cells ability to generate contractile force [80]; however, these metrics should be interpreted cautiously as the immediate retraction is due to residual stress stored in the matrix, not active muscle-like contraction. Further, the ensuing change in shape depends both on the stress that the cells can actively generate and on the compressive stiffness of the matrix against which they contract, thus even if the cells are able to generate substantial force, little retraction will be observed if the matrix is very stiff due to extensive remodeling. Methods for measuring tension (described in Section 5) are more reliable means of determining the contractile ability of the cell population. Upon retraction, the cell morphology changes profoundly, cell proliferation and collagen synthesis decrease [81], cells switch from an active remodeling

to a quiescent phenotype [81], and myofibroblasts de-differentiate and/or apoptose [82, 83]. The magnitude and rate of the drop of tension required for phenotypic switching and other biological sequel following release are not currently known as experimental systems have not been developed for this purpose.

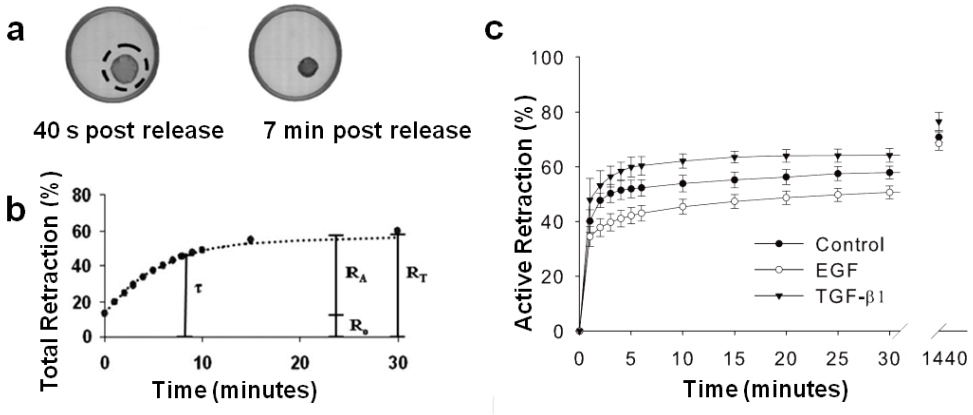

Figure 2. 5 (a) Photographs of a fibroblast-populated fibrin gel floating within a 24 mm diameter culture well 40 seconds and seven minutes post release showing the decrease in area from the constrained size (indicated by dotted circle) due to retraction. (b) Total retraction in the tissue, [1-(A/A0)]*100%, where A and A_0 are final and initial areas of the gel, increases roughly exponentially with time to an equilibrium value with a time constant of approximately eight minutes. To determine the active cell component (R_A) of the observed total retraction (R_T), the immediate passive retraction (R_0) can be subtracted from R_T. (c) Growth factors differentially affect active cell retraction. From [84] (a & b) and [79] (c).

In the majority of studies utilizing collagen and fibrin gels, a circular well is utilized with uniform radial boundary conditions. Mixed boundary conditions (alternating free and anchored regions) and different shapes (square, rectangular, annular, cruciform, tubular, etc.) allow researchers to alter the patterns of tension in the samples as the cells compact protein matrices and to correlate the stress field with cell behaviors such as matrix deposition. The cells and collagen fibers in rectangular and annular gels become highly aligned parallel to the free surfaces, indicating the lines of tension [85]. In cruciform gels, *de novo* collagen fibrils in cell-laden fibrin gels align parallel to the free edges in the direction of highest tension [86], and the degree of alignment can be controlled by the relative width of the arms [87]. When cells are embedded in fibrin gels in a cross-shaped

mold with different arm widths, collagen production is higher in narrower arms where the stress is higher (as computed by multi-scale models [86]).

Nested collagen matrices are another innovative means for investigating cell-matrix interactions with mixed boundary conditions [88, 89] (Figure 2.6a). In this system, a dermal equivalent, obtained by the compaction of a free-floating collagen gel by fibroblasts, is embedded in an acellular collagen gel. Cells migrate into the outer acellular matrix and collagen is pulled by the cells towards dense dermal equivalent. In free floating nested gels, the collagen flow from the outer region to the cell-populated inner region is more pronounced than for attached nested gels, while cell migration is lower (Figure 2.6 b & c). These results highlight the fact that cell migration and collagen translocation in a collagen gel depend on the overall resistance of the matrix to traction forces applied by cells [89], i.e., the effective stiffness. Similar cell-matrix interactions are observed when the resistance of the matrix near a cell in a collagen gel is altered by applying compressive local strain. When collagen fibers are pushed towards the front of a cell, the tension the cell can generate decreases and the cell temporarily shortens, then the cell extends again by reprotrusion and pulls the collagen fibrils inward to reestablish a homeostatic tension level [25].

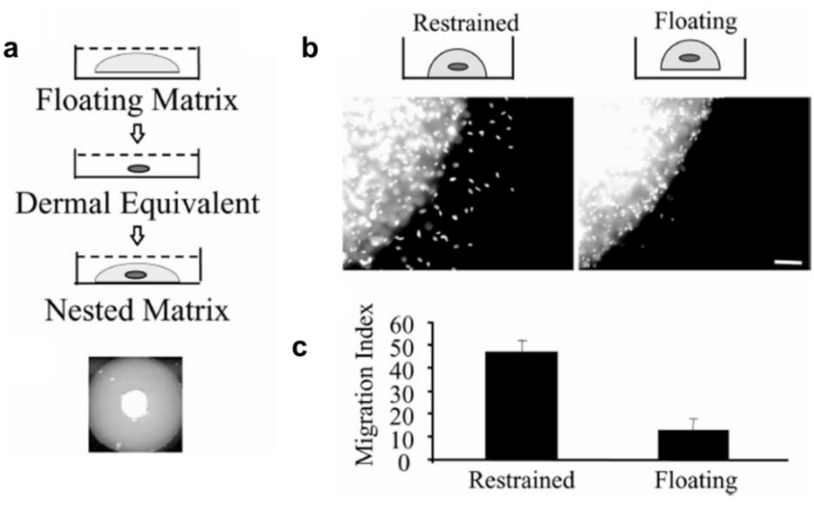

Figure 2. 6 (a) Nested collagen matrices contain contracted floating collagen matrices re-embedded in cell-free matrices which can be anchored to the culture surface or floating as shown in (b). (b & c) Cell migration into the acellular region is more extensive into anchored nested gels. From [89].

Comparison of the cell-matrix interactions in floating and anchored nested gels illustrates that proximity to the lower boundary, not just lateral boundaries, also affects the ability of cells to generate tension within a protein gel. Feng et al. [90] recently reported on a microfluidic system created to investigate the effects of gel thickness and fiber alignment in thin stacked gels. The authors found that cell morphology and motility of cells in 3D gels were affected by both fiber alignment and substrate thickness and attributed the changes to an increase in effective stiffness of the thin gels relative to the thick gels. By culturing cells on the surface of anchored gels of varied thickness, we have also observed a progressive increase in cell spreading with proximity to the stiff underlying boundary. Enhanced spreading is observed even when the boundary is over 100 microns from the cell, indicating long-range tethering of the fibers which limits collagen translocation and facilitates the generation of cell traction [91].

2.2.3 Refined Control and Measurement of Tension: Adjustable Boundary Conditions

As discussed in the previous section, free-floating and rigidly anchored boundary conditions result in very different states of tension within cell-populated collagen and fibrin gels which strongly affect cell behavior. The rate and extent of gel initial compaction and retraction upon release [79, 81] provide relative measures of cell activity in these systems, yet these are indirect measures of motility and contractility. For refined mechanobiological investigations, methods for quantitatively measuring and controlling tension within cell-populated collagen and fibrin gels have been developed as described below.

To measure forces generated by cells in cell-populated collagen gels, Lapiere and colleagues [92] and Kolodney and Wysolmerski [93] developed culture force monitors (CFMs) in the early 90's. A CFM consists of a cell-populated collagen gel suspended in media between a highly sensitive isometric force transducer and a rigidly fixed anchor (Figure 2.7). The cell-generated tension is propagated hundreds of microns through the fibrous matrix between cells and to the attached boundaries [69] and can be measured externally if the cell density is sufficiently high and if the matrix is compliant enough to avoid stress shielding [51]. Initially, when cells are resuspended in the gels, the force generated increases rapidly due to traction applied to collagen fibrils by cells during migration [94, 95]. After approximately 24 hours, the tension reaches a plateau as the compaction phase ends and the remodeling phase commences. In the remodeling phase, the cells crosslink the collagen in the new compacted arrangement and lock in residual stresses [96]. To further investigate the effects of the boundaries on the cell tension, Brown, Eastwood and colleagues [51] modified the CFM such that one side could be actuated, and they found that cells quickly respond to extension and retraction of the rigid

boundary to maintain a level of tensional homeostasis [51]. The particular homeostatic tension level developed by a population of cells is dependent upon soluble and mechanical factors such as growth factors, initial protein concentration, and boundary conditions [36, 53, 97]. To determine the contractile potential of the cells, the cells can be stimulated by depolarization (e.g., with potassium chloride) or by vasoactive agents (lysophosphatidic acid, thrombin, etc.). The basal tension can be eliminated by agents which disrupt the cytoskeleton (e.g., Cytochalasin-D) to determine the residual stress that is built up in the matrix a result of remodeling [36, 53].

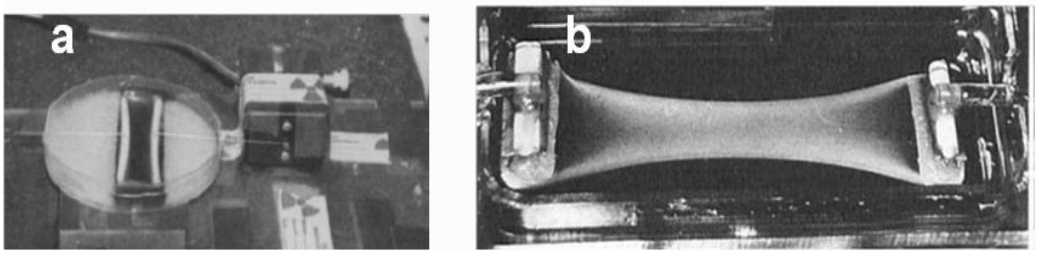

Figure 2. 7 Culture force monitors with (a) low aspect ratio and (b) high aspect ratio. Modified from [93] (a) and [92] (b).

Whether comparing cell types, the effects of soluble factors, or cell-matrix interactions, the most important metric from culture force measurements is the force generated per cell. The force per cell is generally calculated by dividing the total measured tension by the number of cells in the gel [92, 94]. Using this calculation, dermal and cardiac fibroblasts generate 0.1-10 mN per million cells (i.e., 0.1-10 nN per cell) in both uniaxial [92, 94] and biaxial [36, 98] systems. Although straightforward, this calculation assumes that all cells act in parallel, which is clearly an oversimplification (see schematic, Figure 2.8a). On the other extreme, if we assume that all of the cells act in series, the total force measured would be equal to the force generated by a single cell, which is clearly an overestimate (Figure 2.8b). Since the cells are distributed approximately uniformly throughout a cell-populated collagen gel, cells act in parallel with some cells and in series

with others. In practice, systems which utilize a high aspect ratio (Figure 2.7b) [92] yield a lower force per cell than those using a low aspect ratio (Figure 2.7a) [93] for the same cell density and contractile activity and produce different levels of cell and matrix alignment [72]. As an improvement to simple parallel and series models, Kolodney and Wysolmerski [93] divide the measured uniaxial force by the cell cross-sectional area measured from histological cross-sections to calculate cell stress (they term tension). Alternatively, calculating the stress in the tissue can be used to normalize the total force to the cross-sectional area of both cells and gel. This method is appropriate for comparing the cell contractility of cells within gels with similar cell density; however, if the cell density is markedly different, changes in cell activity may be misinterpreted. For example, as shown schematically in Figure 2.8c, for two tissues with identical cross-sectional area and measured force, if one tissue has twice the force per cell but only half of the cell density, the calculated stresses would be identical; thus the stress measure would mask the difference in individual cell contractile force. As a relatively straight-forward solution that does not require histological analysis, a representative volume element (RVE) containing one cell and the surrounding volume of ECM (equal to the total volume divided by the total cell number) (Figure 2.8d) can be used where total force measured is equal to the sum of forces for all RVEs in a perpendicular cross-section. Assuming all cells are aligned in the direction of the measured force, the force per cell, F_C, is simply equal to the total force, F_T, divided by the number of RVEs in parallel (n_E). Using this method for a biaxial configuration (where the total force is divided by two to account for random cell orientation [36]), dermal fibroblasts generate 17 to 100 nN per cell for low and high stiffness boundary conditions, respectively, after three days of culture in standard media.

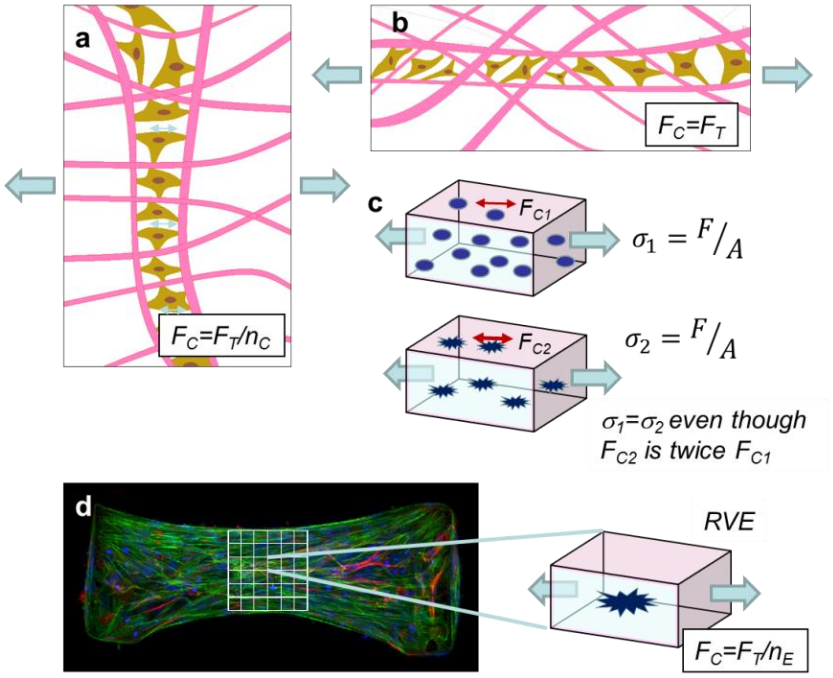

Figure 2. 8 Schematic representing idealized arrangements of cells in a collagen gels in (a) parallel and (b) series formations for the purpose of estimating the force per cell, FC, from total measured force, FT, from the total number of cells, n_C, assuming uniaxial strain (c) Hypothetical volume elements with identical cross-sectional area the upper element has twice the cell density of the lower element but each cell generates half of the force; in the case of equal cross-sectional area, *A*, the calculated stress would be the same for both elements. This calculation would not reflect the higher contractile activity of the cells in the lower relative to the upper element demonstrating the flaw of tissue stress calculations for the estimation of cell contractility. (d) Micrograph of a uniaxially constrained cell-populated fibrin gel showing a representative volume element (RVE) containing one cell within its associated volume which is equal to the tissue volume in the central region divided by the cell number in the central region. n_E = number of RVEs in parallel in a given cross section. Note that F_C is lowest in (a), highest in (b), and in between in (d).

Another approach to study the effects of tension on cell behavior is to apply a force boundary condition which is resisted by cell-generated forces [98]. This method has the benefit of being able to prescribe the total force generated by the population of cells, including anisotropic loading (different weights on each axis); however, there is a very limited range of weights that can be applied. If the load is too low, the cells will compact the gel similar to a free gel, and if too high for the cells to generate an equal and opposite force, the cell-populated gel will stretch out until the anchors hit the rigid stops [98]. Costa and colleagues [99] utilized this method to study the effect of altering the axis of tension and found, for the first time, that cell realignment precedes collagen fiber

realignment indicating that a change in global loading can overcome local contact guidance.

The tension within a cell-populated protein matrix may be modulated more subtly by anchoring the boundaries with compliant beams which are able to bend with cell-generated forces. This method also provides the ability to monitor the tension by measuring beam deflection which is proportional to applied force. Flexible beams were first used to measure the force generated by fibroblasts seeded in collagen-glycosaminoglycan sponges [100], and Freyman et al. report force per cell values of ~1 nN regardless of overall stiffness of the system (intrinsic matrix stiffness plus beam stiffness). We developed an analogous system utilizing thin stainless steel wires as compliant anchors to modulate the boundary stiffness of suspended collagen gels in a biaxial configuration [36]. In this system, the resistance to deformation can be tuned from negligible stiffness (free-floating) to infinite stiffness (rigidly anchored) boundary conditions (Figure 2.9) [36]. In contrast to the aforementioned study in collagen-GAG sponges [101], we found that increased boundary stiffness (0.048 to 0.64 mN/mm) elicits enhanced basal tension and potassium-stimulated active contractile force from fibroblasts. Remodeling of the collagen matrix also increases the intrinsic matrix stiffness as a function of boundary stiffness indicating stiffness-dependent phenotypic regulation of the cells which is synergistically enhanced by growth factors (e.g., TGF-β1). An analogous compliant-boundary system has been developed utilizing cantilevered silicone posts for the development and characterization of uniaxial millimeter-scale engineered cardiac tissues. Cell-populated fibrin [102] and collagen gels [103] are suspended between 3-3.5 mm high PDMS posts, and the beating force generated by neonatal rat cardiomyocytes has been measured by dynamically tracking the post deflections.

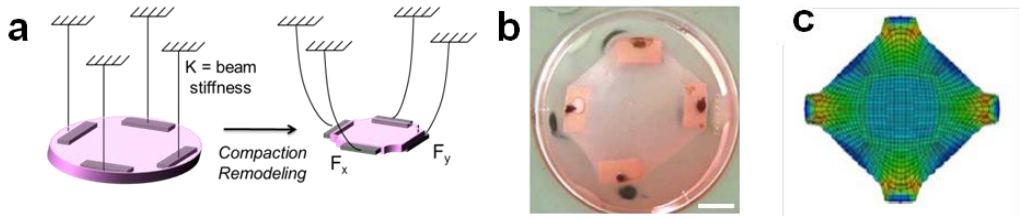

Figure 2. 9 Schematic view of a compliant-boundary system. (b) Bottom view of compacted collagen gel after culturing for three days (scale bar 10 mm). (c) Finite analysis of distribution of stresses generated by cells compacting the gel against four stiff boundaries (simulated by decreasing the temperature of the linear elastic material in the FE software). Adapted from [36].

Utilizing the same principle of controlled-stiffness boundaries but on a smaller scale, Chen and colleagues [53] developed an array of silicon elastomer-based microwells (< 1 mm in length) containing PDMS cantilevers (termed micro-tissue gauges, μTUGs) to culture cell-populated collagen gels between compliant anchors in a more high-throughput manner (Figure 2.10). The small size of the samples offers the advantage of low material costs, reduced diffusion limitations, and ability to utilize powerful optical microscopy methods. Using the μTUG system, NIH 3T3 fibroblasts and rat cardiomyocytes have been shown to generate greater force per cell against stiff anchors than soft anchors [53, 97]. Higher initial collagen density (which increases intrinsic stiffness) results in higher total force but lower tissue stress due to decreased compaction [53, 97]. The same system has also been used to measure changes in tension as a response to chemical [104], electrical [97], and optical [105] stimuli in airway smooth muscle cell-, cardiomyocyte-, and myoblast- populated collagen gels, respectively. The intrinsic stiffness of the micro-tissues can be measured by attaching magnetic beads to one of the cantilevers in each well and pulling the tissues by magnetic force [106]. Combining this technique with treatments to eliminate cell contraction, the authors determined that the tissue stiffness is not affected significantly by the active cell tension. They also note that residual tension remains in the tissue following cell deactivation, indicating substantial collagen remodeling during the culture period [106].

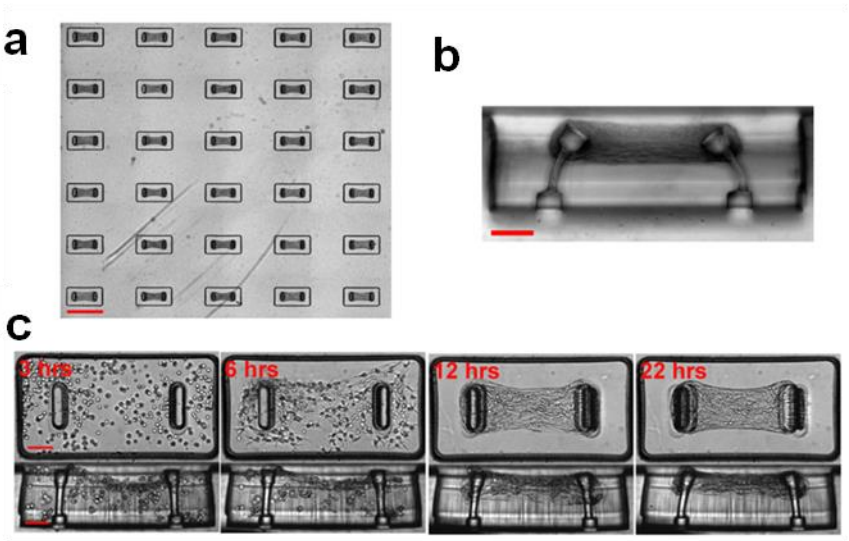

Figure 2. 10 (a) Arrays of micro-tissues are simultaneously generated ina PDMS substrate. (b) Cross-section view of a single micro-tissue gauge well. (c) Representative images depicting the time-course of a contracting micro-tissue. (Scale bars: *A*, 800 μm; *B* and *C*, 100 μm). From [53].

While uTUGs and other spring-anchored gels systems provide to ability to measure and regulated tension in 3D, VIC stiffness dependence has not been studied in these system, and there has been no systematic study of any cell type with multiple (>2) stiffness levels and multiple growth factor concentration levels. Further, although there is some evidence in 2D systems that the VIC phenotype may be modulated by reducing 2D culture surface modulus, there has been no dynamic modulation of the stiffness of the posts to alter stiffness in 3D. Our studies to fill these gaps in the literature will be described in the next 2 chapters.

References

[1] Schoen FJ. Evolving Concepts of Cardiac Valve Dynamics: The Continuum of Development, Functional Structure, Pathobiology, and Tissue Engineering. Circulation. 2008;118:1864-80.
[2] Vesely I, Noseworthy R. Micromechanics of the fibrosa and the ventricularis in aortic valve leaflets. Journal of biomechanics. 1992;25:101-13.
[3] Stella JA, Sacks MS. On the biaxial mechanical properties of the layers of the aortic valve leaflet. Journal of biomechanical engineering. 2007;129:757.
[4] Redden RA, Doolin EJ. Collagen crosslinking and cell density have distinct effects on fibroblast-mediated contraction of collagen gels. Skin Res Technol. 2003;9:290-3.
[5] Hinton RB, Lincoln J, Deutsch GH, Osinska H, Manning PB, Benson DW, et al. Extracellular matrix remodeling and organization in developing and diseased aortic valves. Circulation research. 2006;98:1431-8.
[6] Choquet D, Felsenfeld DP, Sheetz MP. Extracellular matrix rigidity causes strengthening of integrin–cytoskeleton linkages. Cell. 1997;88:39-48.
[7] Suter DM, Errante LD, Belotserkovsky V, Forscher P. The Ig superfamily cell adhesion molecule, apCAM, mediates growth cone steering by substrate–cytoskeletal coupling. The Journal of cell biology. 1998;141:227-40.
[8] Sawada Y, Sheetz MP. Force transduction by Triton cytoskeletons. The Journal of cell biology. 2002;156:609-15.
[9] Hinz B, Gabbiani G. Cell-matrix and cell-cell contacts of myofibroblasts: role in connective tissue remodeling. Thrombosis and haemostasis. 2003;90:993-1002.
[10] Hinz B, Celetta G, Tomasek JJ, Gabbiani G, Chaponnier C. Alpha-smooth muscle actin expression upregulates fibroblast contractile activity. Molecular biology of the cell. 2001;12:2730-41.
[11] Hinz B, Mastrangelo D, Iselin CE, Chaponnier C, Gabbiani G. Mechanical tension controls granulation tissue contractile activity and myofibroblast differentiation. The American journal of pathology. 2001;159:1009-20.
[12] Chen J, Li H, SundarRaj N, Wang JHC. Alpha-smooth muscle actin expression enhances cell traction force. Cell motility and the cytoskeleton. 2007;64:248-57.
[13] Ignotz RA, Massagué J. Cell adhesion protein receptors as targets for transforming growth factor-β action. Cell. 1987;51:189-97.
[14] Quinlan AM, Billiar KL. Investigating the role of substrate stiffness in the persistence of valvular interstitial cell activation. Journal of Biomedical Materials Research Part A. 2012;100:2474-82.
[15] Yip CYY, Chen J-H, Zhao R, Simmons CA. Calcification by valve interstitial cells is regulated by the stiffness of the extracellular matrix. Arteriosclerosis, thrombosis, and vascular biology. 2009;29:936-42.
[16] Kloxin AM, Benton JA, Anseth KS. In situ elasticity modulation with dynamic substrates to direct cell phenotype. Biomaterials. 2010;31:1-8.
[17] Marinković A, Mih JD, Park J-A, Liu F, Tschumperlin DJ. Improved throughput traction microscopy reveals pivotal role for matrix stiffness in fibroblast contractility and TGF-β responsiveness. American Journal of Physiology-Lung Cellular and Molecular Physiology. 2012;303:L169-L80.
[18] Califano JP, Reinhart-King CA. Substrate stiffness and cell area predict cellular traction stresses in single cells and cells in contact. Cellular and molecular bioengineering. 2010;3:68-75.

[19] Kloxin AM, Benton JA, Anseth KS. < i> In situ</i> elasticity modulation with dynamic substrates to direct cell phenotype. Biomaterials. 2010;31:1-8.
[20] Wang H, Haeger SM, Kloxin AM, Leinwand LA, Anseth KS. Redirecting valvular myofibroblasts into dormant fibroblasts through light-mediated reduction in substrate modulus. PloS one. 2012;7:e39969.
[21] Harris AK, Wild P, Stopak D. Silicone rubber substrata: A new wrinkle in the study of cell locomotion. Science 1980;208:177-9.
[22] Pelham RJ, Jr., Wang Y. Cell locomotion and focal adhesions are regulated by substrate flexibility. PNAS. 1997;94:13661-5.
[23] Leung DY, Glagov S, Mathews MB. Cyclic stretching stimulates synthesis of matrix components by arterial smooth muscle cells in vitro. Science. 1976;191:475-7.
[24] Discher DE, Janmey P, Wang YL. Tissue cells feel and respond to the stiffness of their substrate. Science. 2005;310:1139-43.
[25] Grinnell F, Petroll WM. Cell motility and mechanics in three-dimensional collagen matrices. Annu Rev Cell Dev Biol. 2010;26:335-61.
[26] Weiss P. Cellular Dynamics. Reviews of Modern Physics. 1959;31:11-20.
[27] Elsdale T, Bard J. Collagen substrata for studies on cell behavior. J Cell Biol. 1972;54:626-37.
[28] Bell E, Ivarsson B, Merril C. Production of a tissue-like structure by contraction of collagen lattices by human fibroblasts of different proliferative potential in vitro. PNAS. 1979;76(3):1274-8.
[29] Stopak D, Harris AK. Connective tissue morphogenesis by fibroblast traction. I. Tissue culture observations. Dev Biol. 1982;90:383-98.
[30] Billiar KL. The Mechanical Environment of Cells in Collagen Gel Models. In: Gefen A, editor. Cellular and Biomolecular Mechanics and Mechanobiology: Springer Berlin Heidelberg; 2011. p. 201-45.
[31] Walpita D, Hay E. Studying actin-dependent processes in tissue culture. Nat Rev Mol Cell Biol. 2002;3:137-41.
[32] Grinnell F. Fibroblast-collagen-matrix contraction: Growth-factor signalling and mechanical loading. Trends Cell Biol. 2000;10:362-5.
[33] Roy P, Petroll WM, Chuong CJ, Cavanagh HD, Jester JV. Effect of cell migration on the maintenance of tension on a collagen matrix. Ann Biomed Eng. 1999;27:721-30.
[34] Hay ED. Extracellular matrix alters epithelial differentiation. Curr Opin Cell Biol. 1993;5:1029-35.
[35] Petersen OW, Rønnov-Jessen L, Howlett AR, Bissell MJ. Interaction with basement membrane serves to rapidly distinguish growth and differentiation pattern of normal and malignant human breast epithelial cells. PNAS. 1992;89:9064-8.
[36] John J, Quinlan AT, Silvestri C, Billiar K. Boundary stiffness regulates fibroblast behavior in collagen gels. Ann Biomed Eng. 2010;38:658-73.
[37] Schwartz MA, Chen CS. Cell biology. Deconstructing dimensionality. Science. 2013;339:402-4.
[38] Pedersen JA, Swartz MA. Mechanobiology in the third dimension. Ann Biomed Eng. 2005;33:1469-90.
[39] Baker BM, Chen CS. Deconstructing the third dimension: how 3D culture microenvironments alter cellular cues. J Cell Sci. 2012;125:3015-24.
[40] Cukierman E, Pankov R, Stevens DR, Yamada KM. Taking cell-matrix adhesions to the third dimension. Science. 2001;294:1708-12.
[41] Gieni RS, Hendzel MJ. Mechanotransduction from the ECM to the genome: are the pieces now in place? Journal of cellular biochemistry. 2008;104:1964-87.

[42] Wipff P-J, Rifkin DB, Meister J-J, Hinz B. Myofibroblast contraction activates latent TGF-beta1 from the extracellular matrix. J Cell Biol. 2007;179:1311-23.
[43] Cummings CL, Gawlitta D, Nerem RM, Stegemann JP. Properties of engineered vascular constructs made from collagen, fibrin, and collagen-fibrin mixtures. Biomaterials. 2004;25:3699-706.
[44] Ulrich TA, Jain A, Tanner K, MacKay JL, Kumar S. Probing cellular mechanobiology in three-dimensional culture with collagen–agarose matrices. Biomaterials. 2010;31:1875-84.
[45] Janmey PA, Winer JP, Weisel JW. Fibrin gels and their clinical and bioengineering applications. J R Soc Interface. 2009;6:1-10.
[46] Tuan TL, Song a, Chang S, Younai S, Nimni ME. In vitro fibroplasia: matrix contraction, cell growth, and collagen production of fibroblasts cultured in fibrin gels. Exp Cell Res. 1996;223:127-34.
[47] Willerth SM, Arendas KJ, Gottlieb DI, Sakiyama-Elbert SE. Optimization of fibrin scaffolds for differentiation of murine embryonic stem cells into neural lineage cells. Biomaterials. 2006;27:5990-6003.
[48] Ye Q, Zünd G, Jockenhoevel S, Hoerstrup SP, Schoeberlein a, Grunenfelder J, et al. Tissue engineering in cardiovascular surgery: new approach to develop completely human autologous tissue. Eur J Cardiothorac Surg. 2000;17:449-54.
[49] Grassl ED, Oegema TR, Tranquillo RT. Fibrin as an alternative biopolymer to type-I collagen for the fabrication of a media equivalent. J Biomed Mater Res. 2002;60:607-12.
[50] Ahlfors JE, Billiar KL. Biomechanical and biochemical characteristics of a human fibroblast-produced and remodeled matrix. Biomaterials. 2007;28:2183-91.
[51] Brown RA, Prajapati R, McGrouther DA, Yannas IV, Eastwood M. Tensional homeostasis in dermal fibroblasts: Mechanical responses to mechanical loading in three-dimensional substrates. J Cell Physiol. 1998;175:323-32.
[52] Grinnell F. Fibroblast biology in three-dimensional collagen matrices. Trends Cell Biol. 2003;13:264-9.
[53] Legant WR, Pathak A, Yang MT, Deshpande VS, McMeeking RM, Chen CS. Microfabricated tissue gauges to measure and manipulate forces from 3D microtissues. PNAS. 2009;106:10097-102.
[54] Arora PD, Narani N, McCulloch CA. The compliance of collagen gels regulates transforming growth factor-beta induction of alpha-smooth muscle actin in fibroblasts. Am J Pathol. 1999;154:871-82.
[55] Germain L, Jean A, Auger FA, Garrel DR. Human Wound Healing Fibroblasts Have Greater Contractile Properties Than Dermal Fibroblasts. J Surg Res. 1994;57:268-73.
[56] Yamato M, Adachi E, Yamamoto K, Hayashi T. Condensation of collagen fibrils to the direct vicinity of fibroblasts as a cause of gel contraction. J Biochem. 1995;117:940-6.
[57] Sieminski AL, Hebbel RP, Gooch KJ. The relative magnitudes of endothelial force generation and matrix stiffness modulate capillary morphogenesis in vitro. Exp Cell Res. 2004;297:574-84.
[58] Knapp DM, Tower TT, Tranquillo RT, Barocas VH. Estimation of cell traction and migration in an isometric cell traction assay. AIChE Journal. 1999;45:2628-40.
[59] Galie Pa, Westfall MV, Stegemann JP. Reduced serum content and increased matrix stiffness promote the cardiac myofibroblast transition in 3D collagen matrices. Cardiovasc Pathol. 2011;10.1016/j.carpath.2010.10.001.
[60] Park JS HN, Kurpinski KT, Patel S, Hsu S, Li S. Mechanobiology of mesenchymal stem cells and their use in cardiovascular repair. Front Biosci. 2007;12:5098-116.

[61] Dallon JC, Ehrlich HP. A Review of Fibroblast Populated Collagen Lattices. Wound Repair Regen. 2008;16:472–9.
[62] Tamariz E, Grinnell F. Modulation of fibroblast morphology and adhesion during collagen matrix remodeling. Mol Biol Cell. 2002;13:3915-29.
[63] Dean DM, Rago AP, Morgan JR. Fibroblast elongation and dendritic extensions in constrained versus unconstrained microtissues. Cell Motil Cytoskeleton. 2009;66:129-41.
[64] Tomasek JJ, Gabbiani G, Hinz B, Chaponnier C, Brown RA. Myofibroblasts and mechano-regulation of connective tissue remodelling. Nature reviews Molecular cell biology. 2002;3:349-63.
[65] Grinnell F, Ho CH, Tamariz E, Lee DJ, Skuta G. Dendritic fibroblasts in three-dimensional collagen matrices. Mol Biol Cell. 2003;14:384-95.
[66] Hinz B, Gabbiani G. Cell-matrix and cell-cell contacts of myofibroblasts: Role in connective tissue remodeling. Thromb Haemost. 2003;10.1160/th03-05-0328.
[67] Grinnell F. Fibroblasts, myofibroblasts, and wound contraction. Journal of cellular biochemistry. 1994;124:401-4.
[68] Carlson MA, Longaker MT. The fibroblast-populated collagen matrix as a model of wound healing: A review of the evidence. Wound Repair Regen. 2004;12:134-47.
[69] Vanni S, Lagerholm BC, Otey C, Taylor DL, Lanni F. Internet-based image analysis quantifies contractile behavior of individual fibroblasts inside model tissue. Biophys J. 2003;84:2715-27.
[70] Simon DD, Humphrey JD. On a Class of Admissible Constitutive Behaviors in Free-Floating Engineered Tissues. Int J Non Linear Mech. 2012;47:173-8.
[71] Simon DD, Horgan CO, Humphrey JD. Mechanical restrictions on biological responses by adherent cells within collagen gels. J Mech Behav Biomed Mater. 2012;14:216-26.
[72] Eastwood M, Porter R, Khan U, McGrouther G, Brown R. Quantitative analysis of collagen gel contractile forces generated by dermal fibroblasts and the relationship to cell morphology. J Cell Physiol. 1996;166:33-42.
[73] Kolodney MS, Elson EL. Correlation of myosin light chain phosphorylation with isometric contraction of fibroblasts. J Biol Chem. 1993;268:23850-5.
[74] Hinz B, Mastrangelo D, Iselin CE, Chaponnier C, Gabbiani G. Mechanical tension controls granulation tissue contractile activity and myofibroblast differentiation. The American journal of pathology. 2001;159:1009-20.
[75] Hinz B, Phan SH, Thannickal VJ, Galli A, Bochaton-Piallat ML, Gabbiani G. The myofibroblast: one function, multiple origins. Am J Pathol. 2007;170:1807-16.
[76] Grinnell F, Ho CH. Transforming growth factor beta stimulates fibroblast-collagen matrix contraction by different mechanisms in mechanically loaded and unloaded matrices. Exp Cell Res. 2002;273:248-55.
[77] Tomasek JJ, Haaksma CJ, Eddy RJ, Vaughan MB. Fibroblast contraction occurs on release of tension in attached collagen lattices: dependency on an organized actin cytoskeleton and serum. Anat Rec. 1992;232:359-68.
[78] Carlson MA, Longaker MT, Thompson JS. Wound splinting regulates granulation tissue survival. J Surg Res. 2003;110:304-9.
[79] Grouf JL, Throm AM, Balestrini JL, Bush KA, Billiar KL. Differential effects of EGF and TGF-beta1 on fibroblast activity in fibrin-based tissue equivalents. Tissue Eng. 2007;13:799-807.
[80] Vaughan MB, Howard EW, Tomasek JJ. Transforming growth factor-beta1 promotes the morphological and functional differentiation of the myofibroblast. Exp Cell Res. 2000;257:180-9.

[81] Mochitate K, Pawelek P, Grinnell F. Stress relaxation of contracted collagen gels: Disruption of actin filament bundles, release of cell surface fibronectin, and down-regulation of DNA and protein synthesis. Exp Cell Res. 1991;193:198-207.
[82] Grinnell F, Zhu M, Carlson MA, Abrams JM. Release of mechanical tension triggers apoptosis of human fibroblasts in a model of regressing granulation tissue. Exp Cell Res. 1999;248:608-19.
[83] Chipev CC, Simon M. Phenotypic differences between dermal fibroblasts from different body sites determine their responses to tension and TGFbeta1. BMC Dermatol. 2002;2:13.
[84] Balestrini JL, Billiar KL. Magnitude and duration of stretch modulate fibroblast remodeling. J Biomech Eng. 2009;131:051005.
[85] Costa KD, Lee EJ, Holmes JW. Creating alignment and anisotropy in engineered heart tissue: Role of boundary conditions in a model three-dimensional culture system. Tissue Eng. 2003;9:567-77.
[86] Sander EA, Barocas VH, Tranquillo RT. Initial fiber alignment pattern alters extracellular matrix synthesis in fibroblast-populated fibrin gel cruciforms and correlates with predicted tension. Ann Biomed Eng. 2011;39:714-29.
[87] Jhun CS, Evans MC, Barocas VH, Tranquillo RT. Planar biaxial mechanical behavior of bioartificial tissues possessing prescribed fiber alignment. J Biomech Eng. 2009;131:081006.
[88] Grinnell F, Rocha LB, Iucu C, Rhee S, Jiang H. Nested collagen matrices: A new model to study migration of human fibroblast populations in three dimensions. Exp Cell Res. 2006;312:86-94.
[89] Miron-Mendoza M, Seemann J, Grinnell F. Collagen Fibril Flow and Tissue Translocation Coupled to Fibroblast Migration in 3D Collagen Matrices. Mol Biol Cell. 2008;19:2051-8.
[90] Feng CH, Cheng YC, Chao PH. The influence and interactions of substrate thickness, organization and dimensionality on cell morphology and migration. Acta Biomater. 2013;9:5502-10.
[91] Rudnicki MS, Cirka HA, Aghvami M, Sander EA, Wen Q, Billiar KL. Nonlinear strain stiffening is not sufficient to explain how far cells can feel on fibrous protein gels. Biophys J. 2013;105:11-20.
[92] Delvoye P, Wiliquet P, Leveque JL, Nusgens BV, Lapiere CM. Measurement of mechanical forces generated by skin fibroblasts embedded in a three-dimensional collagen gel. J Invest Dermatol. 1991;97:898-902.
[93] Kolodney MS, Wysolmerski RB. Isometric contraction by fibroblasts and endothelial cells in tissue culture: a quantitative study. J Cell Biol. 1992;117:73-82.
[94] Eastwood M, McGrouther DA, Brown RA. A culture force monitor for measurement of contraction forces generated in human dermal fibroblast cultures: Evidence for cell-matrix mechanical signalling. Biochim Biophys Acta. 1994;1201:186-92.
[95] Marenzana M, Wilson-Jones N, Mudera V, Brown RA. The origins and regulation of tissue tension: identification of collagen tension-fixation process in vitro. Exp Cell Res. 2006;312:423-33.
[96] Eastwood M, McGrouther DA, Brown RA. Fibroblast responses to mechanical forces. Proc Inst Mech Eng H. 1998;212:85-92.
[97] Boudou T, Legant WR, Mu A, Borochin MA, Thavandiran N, Radisic M, et al. A microfabricated platform to measure and manipulate the mechanics of engineered cardiac microtissues. Tissue Eng Part A. 2012;18:910-9.

[98] Knezevic V, Sim AJ, Borg TK, Holmes JW. Isotonic biaxial loading of fibroblast-populated collagen gels: a versatile, low-cost system for the study of mechanobiology. Biomechan Model Mechanobiol. 2002;1:59-67.
[99] Lee EJ, Holmes JW, Costa KD. Remodeling of engineered tissue anisotropy in response to altered loading conditions. Ann Biomed Eng. 2008;36:1322-34.
[100] Freyman TM, Yannas IV, Pek YS, Yokoo R, Gibson LJ. Micromechanics of fibroblast contraction of a collagen-GAG matrix. Exp Cell Res. 2001;269:140-53.
[101] Freyman TM, Yannas IV, Yokoo R, Gibson LJ. Fibroblast contraction of a collagen-GAG matrix. Biomaterials. 2001;22:2883-91.
[102] Hansen A, Eder A, Bonstrup M, Flato M, Mewe M, Schaaf S, et al. Development of a drug screening platform based on engineered heart tissue. Circ Res. 2010;107:35-44.
[103] Serrao GW, Turnbull IC, Ancukiewicz D, Kim do E, Kao E, Cashman TJ, et al. Myocyte-depleted engineered cardiac tissues support therapeutic potential of mesenchymal stem cells. Tissue Eng Part A. 2012;18:1322-33.
[104] West AR, Zaman N, Cole DJ, Walker MJ, Legant WR, Boudou T, et al. Development and characterization of a 3D multicell microtissue culture model of airway smooth muscle. Am J Physiol Lung Cell Mol Physiol. 2013;304:L4-16.
[105] Sakar MS, Neal D, Boudou T, Borochin MA, Li Y, Weiss R, et al. Formation and optogenetic control of engineered 3D skeletal muscle bioactuators. Lab Chip. 2012;12:4976-85.
[106] Zhao R, Boudou T, Wang WG, Chen CS, Reich DH. Decoupling cell and matrix mechanics in engineered microtissues using magnetically actuated microcantilevers. Advanced materials (Deerfield Beach, Fla). 2013;25:1699-705.

CHAPTER 3: Mechanoregulation of VIC Phenotype in 3D

Excerpted from published journal article with permission (Appendix-I):

Kural, M.H. and Billiar, K.L., "Mechanoregulation of VIC Phenotype in the 3rd Dimension" Biomaterials, 35(4), 2014, 1128–1137.

3.1 Introduction

Advanced scaffolds for tissue engineering and regenerative medicine have the potential to be remodeled by cells and thus be adapted to the patient's local chemomechanical environment. However, complex interactions between soluble factors, the biological properties of the biomaterial (such as polymer/protein type and ligand density), and the mechanical properties of biomaterial [1, 2] govern the cells' ability to degrade the biomaterial, synthesize extracellular matrix (ECM), and generate forces. Approaches aimed at increasing the rate of growth in tissue engineered structures often result in unstable and uncontrolled fibrocontractive remodeling involving excessive contraction of the resident cells [3], build-up of residual stress [4], and ECM synthesis (i.e., scarring) [5] rather than regeneration of normal tissue. To achieve the desired tissue regeneration, there is a need to understand how biochemical and mechanical signals interact in the regulation of cell-generated forces and ECM remodeling.

Neo-tissue bulking [6-9] and retraction [10, 11] resulting from fibrocontractive remodeling are especially detrimental in the development of tissue engineered heart valves (TEHV), since even a slight shortening or thickening of the leaflets can lead to regurgitation (back flow) [3, 10, 11]. Leaflet thickening, excessive active cell contraction, and passive residual tension in the tissue [4, 10, 11] have been attributed to large numbers of myofibroblasts in TEHV leaflets since they are a highly contractile and synthetic phenotype. Excessive activation of myofibroblasts and an increase in ECM stiffness are also associated with fibrosis and calcification of native heart valves [12]. Myofibroblast activation is triggered when TEHVs are mechanically conditioned in bioreactors and/or treated with growth factors to accelerate the development of *de novo* tissue [13].

Activation is also observed in native heart valves as a result of abrupt changes in pressure loading [14].

Mechanical tension and transforming growth factor-β1 (TGF-β1) are the two main regulators of myofibroblast activation [5, 15, 16]. Culture conditions involving externally applied stress or high substrate elastic modulus lead to formation of stress fibers in the cytoplasm which in turn generate intracellular tension [15-17]. Under high intracellular tension, TGF-β1 stimulates recruitment of α-SMA in the stress fibers [18], the defining hallmark for the myofibroblast phenotype, which contributes to further increased intracellular tension [19]. Few studies explicitly quantify the forces involved in myofibroblast activation, however it has been shown that cell-generated tension and expression of α-SMA in stress fibers are positively correlated to substrate modulus [20, 21] over certain modulus thresholds [17, 22, 23] and below saturation limits at high modulus levels [17]. TGF-β1 also increases fibroblast traction forces in a dose-dependent manner if the substrate is sufficiently stiff [21]. Analogous to two-dimensional (2D) substrate modulus, the ability of three-dimensional (3D) scaffolds to resist deformation due to cell-generated tension also strongly regulates myofibroblast activation. Most strikingly, TGF-β1 induces α-SMA expression in cells in anchored collagen gels but not in floating gels [24, 25]. TGF-β1 acts as an agonist which increases the rate of compaction of free-floating gels (to smaller diameter) [26-28] and anchored gels (to lower thickness) [29] in a dose-dependent manner. Further, when cells are pre-treated with TGF-β1 prior to seeding into collagen gels, they compact the floating gels to a higher extent, which indicates an increased ability to generate traction [28]. Similarly, TGF-β1 treatment of VICs [30] and fibroblasts [28] for several days results in higher rate and extent of gel retraction upon release of anchored gels.

While high tension resulting from myofibroblast activation is undesired in tissue engineering, TGF-β1 and mechanical stimulation are potent stimulants of ECM production and are widely used in tissue engineering to augment growth [31-33]. For example, collagen production by nenonatal smooth muscle cells increases 4 fold with 1 ng/mL TGF-β1 treatment [34]. ECM protein expression increases when cells are cyclically stretched [35-37] and decreases when contraction is inhibited in fibroblasts [38]. These findings demonstrate that both growth factors and tension modulate ECM production, but how growth factor stimulation of ECM production is regulated by tension in 3D remains understudied. It is possible that optimal combinations of these two factors - tension and growth factors - may be utilized to induce the formation of robust tissue without excessive active contraction or residual matrix stress

The most direct and functional measure of a cell's contractile state is the force it generates against the substrate or scaffold. However, in the majority of collagen gel assays the cell forces have not been directly measured, thus quantitative relationship between tension and myofibroblast differentiation have not been determined in 3D gels. Whereas measurement of the traction exerted by single cells against compliant 2D substrates utilizing traction force microscopy (TFM) is now commonplace, measuring single-cell traction force in 3D scaffolds remains challenging [39]. Alternatively, culture force monitors and compliant-anchored systems have been developed to directly measure cell-generated forces of populations of cells within biopolymer gels [40, 41]. Compliant-anchored systems have the additional benefit of allowing one to modulate the cell-generated tension by altering the resistance to cell-generated forces. Using these systems, we and others [42-44] have shown that increasing boundary stiffness leads to an increase in the cell contractile force and an increased sensitivity of fibroblasts to TGF-β1 [42]. In these investigations, a very limited number of stiffness levels and soluble factor

concentrations have been studied (generally “low” and “high”). Establishment of quantitative relationships between cell behavior and specific biochemical and mechanical stimuli requires each factor to be tested at multiple levels in combination.

The goal of the present study is to quantitatively characterize the combined effects of boundary stiffness and TGF-β1 on VIC-generated forces within a 3D matrix. To this end, we cultured VICs in fibrin gels under graded levels of boundary stiffness with multiple concentrations of TGF-β1 in a micro-scale compliant-anchored system and measured cell-generated isometric force, stimulated contraction and residual matrix tension. We also investigated the combined effects of boundary stiffness and growth factors on the cells’ ability to accumulate collagen. The findings of this study provide fundamental relationships between mechanical and chemical stimuli which will guide future research focused on determining optimum tension and growth factor conditions for controlled tissue remodeling in TEHVs.

3.2 Materials and Methods

3.2.1 Isolation of valvular interstitial cells

Pig hearts were obtained from a local slaughter house. Aortic VICs were isolated according to a reported protocol [45] within two hours of death. Briefly, aortic valve leaflets were removed from the aortic root, and washed with cold sterile Dulbecco’s phosphate buffered saline (DPBS, Cellgro, Manassas, VA). Leaflets were submerged in cold collagenase solution made up of 600 U/mL solution of Type II collagenase (Worthington Biochemical, Lakewood, NJ) in Dulbecco’s Modified Eagle’s Medium (DMEM, Life Technologies, Grand Island, New York) with 1% penicillin/ streptomycin/ ampothericin B (PSA, Life Technologies, Grand Island, New York) and 10% fetal bovine

serum (FBS, Life Technologies, Grand Island, New York). Valvular endothelial cells were removed by rubbing the leaflet surfaces using sterile cotton swabs, and the valve leaflets were washed with cold collagenase solution once more and incubated in collagenase solution at 37°C overnight. After enzymatic digestion of the leaflets, cells were plated on tissue culture flasks in DMEM with 1% PSA and 10% FBS. VICs at passage 5-8 were used for all experiments.

3.2.2 Micro-tissue gauges

To modulate and measure the forces applied by cells in a 3D environment, sub-millimeter-sized VIC-populated fibrin gels were cultured suspended between flexible posts. To create the posts and micro-culture wells, the micro-tissue gauge (μTUG) system was used as described by Legant et al. [46] (molds generously provided by Prof. Chris Chen, University of Pennsylvania). This system is composed of an array of micro-wells (dimensions of each well: 800 μm x 400μm x 250μm) containing two flexible cantilevered posts made of poly(dimethylsiloxane) (PDMS, Dow Corning, Midland, MI) (Figure 3.1). Cells were suspended in a biopolymer gel solution within the micro-wells. As cells compacted the gel, 3D constructs were formed between the flexible posts (Figure 3.1C), and the total force applied by the cells was calculated using post deflections and beam bending equations (Appendix-II). Force-per-cell values were calculated by dividing the force exerted on one post by the average number of representative volume elements (RVEs) spanning a cross-sectional area in the middle of micro-tissues [47]. An RVE contains one cell and surrounding volume of ECM (see Appendix-II for detailed description of RVEs). The cell number was determined by counting the nuclei in the

central region which are stained with Hoechst (Figure 1D).

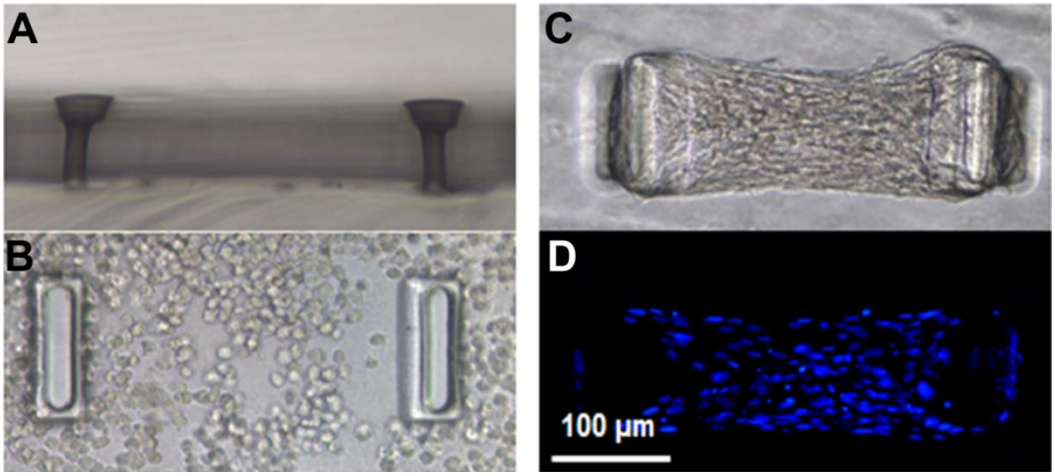

Figure 3. 1 Micro-tissue gauge (µTUG) well shown A)from the side without cells and gel, B) from the top filled with a cell-populated gel at t=1 hours and C & D) at t=72 hours. In (D) the nuclei are stained by Hoechst to facilitate cell counting utilizing fluorescent microscopy. All panels imaged at 20X.

To obtain different boundary stiffness values, the PDMS post elastic modulus was modulated by the monomer-to-curing agent ratios and heat treatments (Appendix-III, Table S1). PDMS moduli were measured by uniaxial tensile testing (EP1000, Instron, Norwood, MA).

3.2.3 Fabrication of VIC-seeded fibrin gel micro-tissues

Empty µTUG wells were treated with 1% Pluronic F-127 (Invitrogen, Eugene, Oregon) for 8 minutes to create a hydrophobic surface and prevent cell attachment to the PDMS. VICs (300,000 cells/mL final concentration) were re-suspended in a fibrin gel solution consisting of fibrinogen from bovine plasma (Sigma, St. Louis, MO, 3.25 mg/mL final concentration) and 1 U/mL thrombin (Sigma, St. Louis, MO), and this suspension was centrifuged into the µTUGs. After centrifugation, excess gel solution was aspirated and the micro-tissues were incubated at 37°C for 1 hour to allow for polymerization of the fibrinogen. Following the polymerization period, chemically defined media with different growth factor concentrations were added into µTUG dishes. A defined medium

previously reported by our group [48] was selected over serum-containing media to avoid masking the effects of exogenous growth factors while allowing robust cell contraction and matrix production. The defined medium consists of a 3:1 ratio of DMEM (high glucose; 4.5 g/L) and Ham's F12 with the addition of 5 µg/ml insulin, 5 ng/ml selenious acid, 10^{-4} M ethanolamine, 250 µg/ml L-ascorbic acid phosphate magnesium salt n-hydrate, $2x10^{-10}$ M L-3,3',5-triiodothyronine, $4x10^{-3}$ M of Glutamax™ (Life Technologies, Grand Island, New York), and 1% penicillin/ streptomycin/ amphotericin B. To prevent premature fibrin degradation, 20 µg/mL Aprotinin (Sigma, St. Louis, MO) was added to the media. The lowest PDMS stiffness utilized was 600 kPa since softer posts collapse, and the highest stiffness value was kept under 5000 kPa to allow visually detectable deflection of the posts. TGF-β1 concentrations were chosen between zero and 5 ng/mL, a concentration range reported in tissue engineering applications [31, 33, 49]. Epidermal growth factor (EGF, Sigma, St. Louis, MO) supplementation was utilized as an alternative supplement to stimulate matrix production without myofibroblast activation [26, 50, 51]. We previously demonstrated that the concentration of EGF chosen for this study (5 ng/mL) stimulates maximal ECM production from dermal fibroblasts [50, 51].

3.2.4 VIC-generated force measurements

VIC-populated gels were cultured under four different post stiffness levels (0.15, 0.33, 0.56 and 1.05 nN/nm) and with four different TGF-β1 concentrations (zero, 0.05, 0.5 and 5 ng/mL). Homeostatic tissue tension was measured every 24 hours for seven days by monitoring the post deflections as previously described [46]. In a separate set of experiments, micro-tissues were cultured with two levels of post stiffness (0.15 and 1.05 nN/nm) and two levels of TGF-β1 (zero and 5 ng/mL) for four days. On day 4, micro-tissues were stimulated with 90 mM potassium chloride (KCl) for 10 minutes to measure

the maximal cell contraction. KCl depolarizes the cell membrane and activates contraction in muscle or muscle-like cells [52, 53]. Following the stimulated contraction measurements, the micro-tissues were treated with 6 mM Cytochalasin-D (Cyto-D) for two hours to inhibit F-actin polymerization and eliminate active cell tension to determine the residual matrix tension. The residual tension is a functional metric for cell-mediated matrix remodeling [54, 55]. In the present study we defined stimulated contraction as the increase in force-per-cell above the homeostatic tension in response to KCl ($F_{STIMULATED}$). The passive and active components of homeostatic tissue tension were defined as active-isometric cell force (F_{CELL}) and residual tension. Active-isometric cell force is equal to the difference between the homeostatic tissue tension at a certain remodeling time (F_{STATIC}) and residual tension ($F_{RESIDUAL}$); i.e., $F_{CELL} = F_{STATIC} - F_{RESIDUAL}$.

In an additional set of experiments aimed at comparing the effects of TGF-β1 and EGF on cell-generated forces and collagen synthesis, micro-tissues were cultured with either soft (k = 0.15 nN/nm) or stiff (k = 1.05 nN/nm) posts. TGF-β1+ groups were supplemented with 5 ng/mL TGF-β1, and EGF+ groups were supplemented with 5 ng/mL EGF. Homeostatic tissue tension was measured on day 4.

3.2.5. Inhibition of contraction by Blebbistatin

In one set of experiments, cell-generated forces were inhibited by adding 5 μM Blebbistatin (Myosin II inhibitor, Sigma, St Louis, MO) to the culture media on the second day of culture. Micro-tissues were then cultured with either 0 or 5 ng/mL TGF-β1 and either 0 or 5 μM Blebbistatin for five days. *De novo* collagen accumulation was assessed as described below.

3.2.6 Immunofluorescent staining

Micro-tissues were fixed in 4% paraformaldehyde for 15 minutes and permeabilized with 0.25% Triton X-100 (Sigma) for 20 minutes. To visualize α-SMA or collagen, tissues were blocked with 1.5% normal goat serum in PBS for 30 min, and incubated with primary anti-α-SMA (Sigma, St. Louis, MO) or anti-collagen (Abcam, Cambridge, MA) antibody, respectively, for one hour. Fluorescently labeled secondary antibody (Alexa-546, Invitrogen, Carlsbad, CA) was then applied and imaged with Leica SP5 point scanning confocal/DMI6000 inverted microscope. In a subset of experiments, the *de novo* collagen accumulation was semi-quantitatively measured by using fluorophore intensity in confocal images (Figure 3.6A). The mean intensity of the collagen stain in region of interest (ROI) with equal area in the central part of each micro-tissue was calculated using the Leica Application Suit software. The mean intensity was divided by the total number of cells in the ROI to calculate collagen intensity per cell. F-actin was labeled by Phalloidin (Alexa-488, Life Technologies, Grand Island, New York).

3.2.7 Statistical analysis

All values are reported as mean ± standard deviation. Statistical comparisons were made using two-way analysis of variance (ANOVA) with $p < 0.05$ considered significant. When a significant difference was found, experimental groups were compared with Tukey's HSD (Honestly Significant Difference) post-hoc test (Sigmaplot 11.0, Systat Software).

The entire force data set from the 16-group stiffness/TGF-β1 experiment was fit with a 2-factor interaction model to quantitatively describe the effects of stiffness and TGF-β1 concentration (and their interactions) on the force generated per cell (Eqn. 1). A log transformation was applied to the TGF-β1 concentration levels normalized to the

maximum concentration level (5 ng/mL). Design of experiment (DOE) software was utilized to design the study and to model and plot the data (Design-Expert 8.0.7.1, Stat-Ease, Inc., MN). The model with the minimum number of parameters which fit the data with lowest p-value and highest R^2 value was determined by the analysis to be:

$$F([TGF\beta], k) = c_1 + c_2 Log([TGF\beta]/5ng/mL) + c_3 k + c_4 Log([TGF\beta]/5ng/mL) \times k \quad (1)$$

where F is force per cell (nN), $[TGF\beta]$ is TGF-β1 concentration (ng/mL), k is post stiffness (nN/nm), and $c_1..c_4$ are model parameters (fitting constants).

3.3 Results

3.3.1 Micro-tissue generation

VICs compact the fibrin gels and form dense dog bone-shaped micro-tissues between the cantilevered posts within 20-30 hours (Figure 3.1C). Due to compositional differences in our micro-tissues from those in previous studies [43, 46, 56] (pure fibrin, VICs, and chemically-defined media (without serum)), the μTUG system methodology was substantially modified. For direct comparisons between the groups, the seeding conditions were kept constant despite wide ranges of stiffness and growth factors; this constraint lead to large differences in force and ECM generation between the treatment groups and, consequently, the rate of success in forming tissues was lower than previously reported. The success rate of micro-tissues lasting more than four days was as low as 10% in groups with high TGF-β1 concentration and 20-30% in other groups.

3.3.2 Tension generation by VICs within micro-tissues

Posts are visibly deflected by the tension within the tissue during gel compaction as a function of both TGF-β1 concentration and post stiffness. Under soft boundaries, force-

per-cell values reach a maximum after 24-36 hours then start to decrease slightly on the 2nd day without TGF-β1 (Figure 3.2).

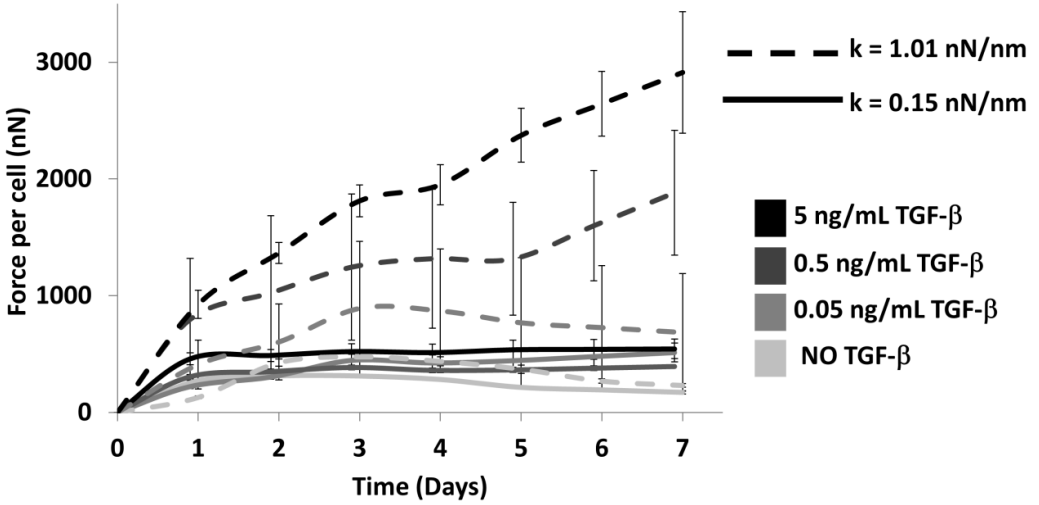

Figure 3. 2 Average force-per-cell values over seven days of culture (n=8-12 per group). Under soft boundary homeostatic tissue tension reaches a plateau after second day at any TGF-β1 concentration.Under stiff boundary, tension increases day by day in a dose-dependent manner. See Appendix-IV for the results of the ANOVA.

Under stiff boundaries with less than 0.5 ng/mL TGF-β1, tension decreases after 24 hours, but with TGF-β1 concentrations of 0.5 and 5 ng/mL, tension increases dramatically and keeps increasing until the end of the experiment at seven days. Under the stiffest boundary (k=1.05 nN/nm), 5 ng/mL TGF-β1 increases force per cell 8.6 fold compared to the no-TGF-β1 group under the same boundary stiffness. Boundary stiffness has no significant effect on cell forces in the absence of TGF-β1 (Figure 3.3, please see Appendix-IV for ANOVA results). Similarly, TGF-β1 does not alter cell-generated forces significantly under soft boundaries (k < 0.33 mN/mm, Figure 3.3).

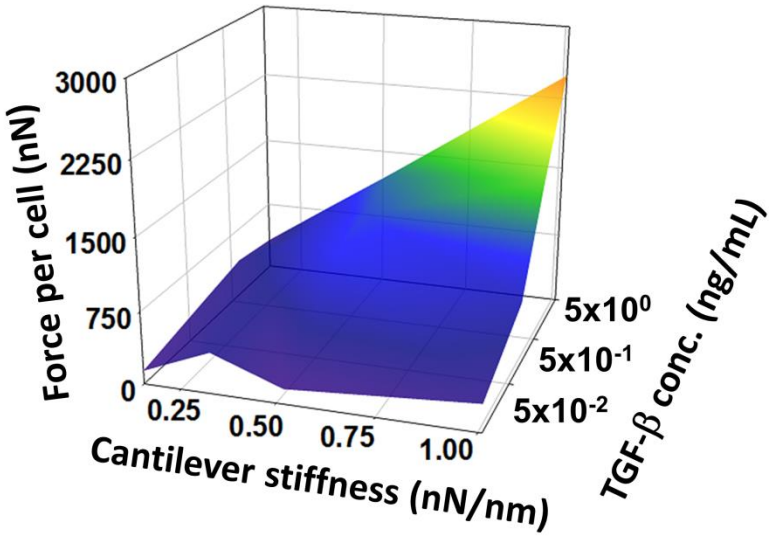

Figure 3. 3 Response surface of force-per-cellvalues on 7th day for all groups (n=8-12 per group).

Under the softest boundary (k = 0.15 nN/nm), increasing TGF-β1 concentration does not significantly affect homeostatic tension. Similarly, in the absence of TGF-β1, increasing boundary stiffness does not alter force-per-cell values. At higher levels, these factors interacted synergistically.

3.3.3 TGF-β1 and stiffness interaction model

The optimal form of the regression model determined utilizing DOE software fit the complete stiffness-TGF-β1-force data set with high correlation with only four parameters. The statistical analysis indicates that each parameter has significant impact with little interaction between parameters (Table 1). Strong interaction between TGF-β1 and boundary stiffness is quantitatively demonstrated by the model ($p < 0.0001$), and the interaction term provided substantially higher correlation with the data ($r^2 = 0.92$ with the interaction term compared to $r^2 = 0.69$ without the interaction term).

Table 2. 1 Model parameters for the regression model (Eqn 1); ANOVA results indicate that each parameter has significant impact on the fit to the dataset.

c_1	2140 (nN)
c_2	780 (nN)
c_3	1660 (nm)
c_4	710 (nm)

	F value	P value
Model	48	<0.0001
k	73	0.0001
TGFβ1	64	<0.0001
Interaction	36	<0.0001

3.3.4 Active isometric cell force, stimulated contraction and residual tension

Active isometric cell force (F_{CELL}), stimulated contraction by activation of VICs with 90 mM KCl ($F_{STIMULATED}$), and residual tension per cell in the matrix after Cyto-D treatment ($F_{RESIDUAL}$) are shown in Figure 3.4. The active isometric cell force is significantly higher under stiff boundaries with TGF-β1 than any other group. Stimulated contraction as a response to KCl, on the other hand, is significantly lower in TGF-β1+ groups, either under soft or stiff boundaries, and it is the highest under stiff boundary without TGF-β1. Increasing boundary stiffness increases $F_{STIMULATED}$ significantly without TGF-β1 treatment.

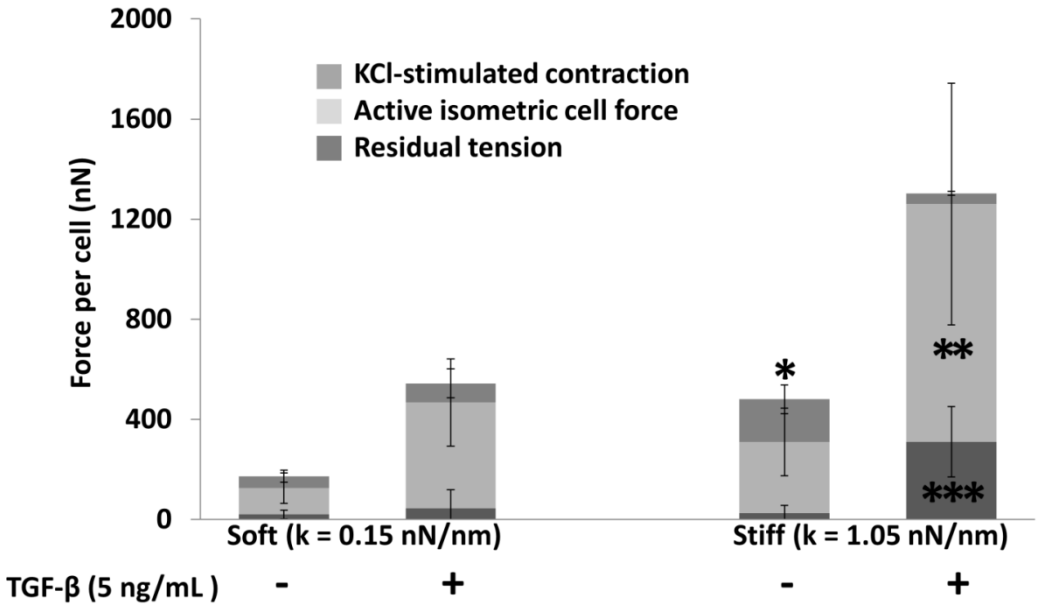

Figure 3. 4 Active isometric cell force, KCl-stimulated contraction, and residual tension in micro-tissuescultured against soft (0.15 nN/nm) or stiff(1.05 nN/m) posts with or without TGF-β1 (5 ng/mL) after four days of culture ($n \geq 3$). Against the stiff boundary with TGF-β1, cells are in a state of high static contraction and produce negligible additional force in response to KCl stimulation but generate large residual tension in the matrix compared to other groups. Cells cultured against stiff boundaries without TGF-β1 provide a stronger response to KCl than the other groups. Two-way ANOVA $p<0.05$:∗: significantly higher KCl-stimulated contraction from all other groups, ∗∗: significantly higher active isometric cell force from all other groups. ∗∗∗: Significantly higher residual tension from all other groups.

3.3.5 α-SMA expression

TGF-β1 and boundary stiffness do not alter the total amount of staining or brightness of α-SMA staining. However, the distribution is dramatically different between TGF-β1- and TGF-β1+ groups. In TGF-β1+ groups, α-SMA is incorporated in stress fibers, while in TGF-β1+ groups α-SMA staining is punctate and in a short rod-like shape (Figure 3.5).

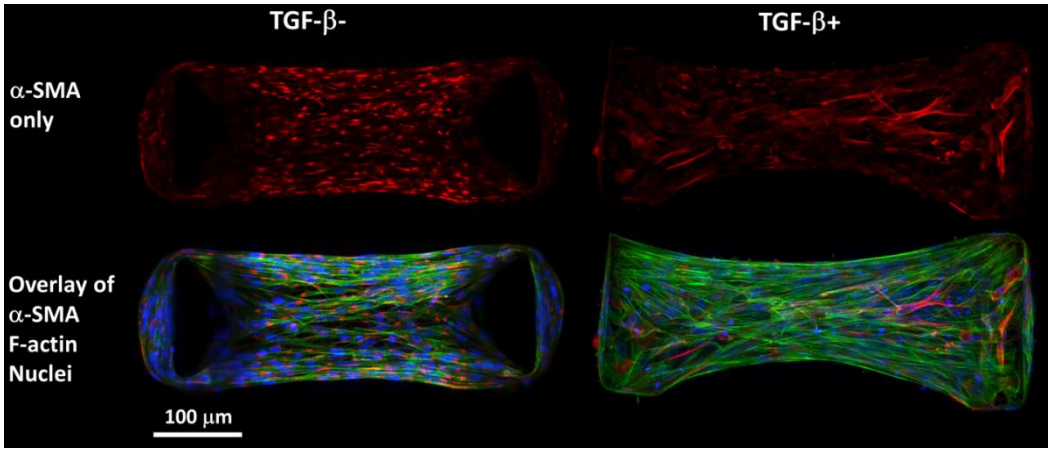

Figure 3. 5 In fibrin gels cultured between stiff posts in chemically defined media for four days,α-SMA staining is punctate and not localized on stress fibers in the absence of TGF-β1 (left), whereas ,α-SMA staining is bright and co-localized with stress fibers in the presence of 5 ng/ml TGF-β1 (right) indicating the myofibroblast phenotype.

3.3.6 Effect of tension on collagen accumulation stimulated by TGF-β1 and EGF

Figure 3.6A shows representative images of collagen staining in micro-tissues. TGF-β1 increases the mean collagen intensity per cell significantly for both soft and stiff boundaries. EGF causes a significant increase in mean collagen intensity only for the soft boundary (Figure 3.6B). TGF-β1 increases force-per-cell in the case of stiff boundaries, but not soft boundaries; whereas EGF does not significantly affect force-per-cell values at any concentration tested regardless of boundary stiffness (Figure 3.6C).

When cell-generated forces are inhibited with 5 μM Blebbistatin, TGF-β1 still increases total *de novo* collagen intensity in micro-tissues; however, enhancement of collagen production with TGF-β1 is attenuated (Figure 3.7A).

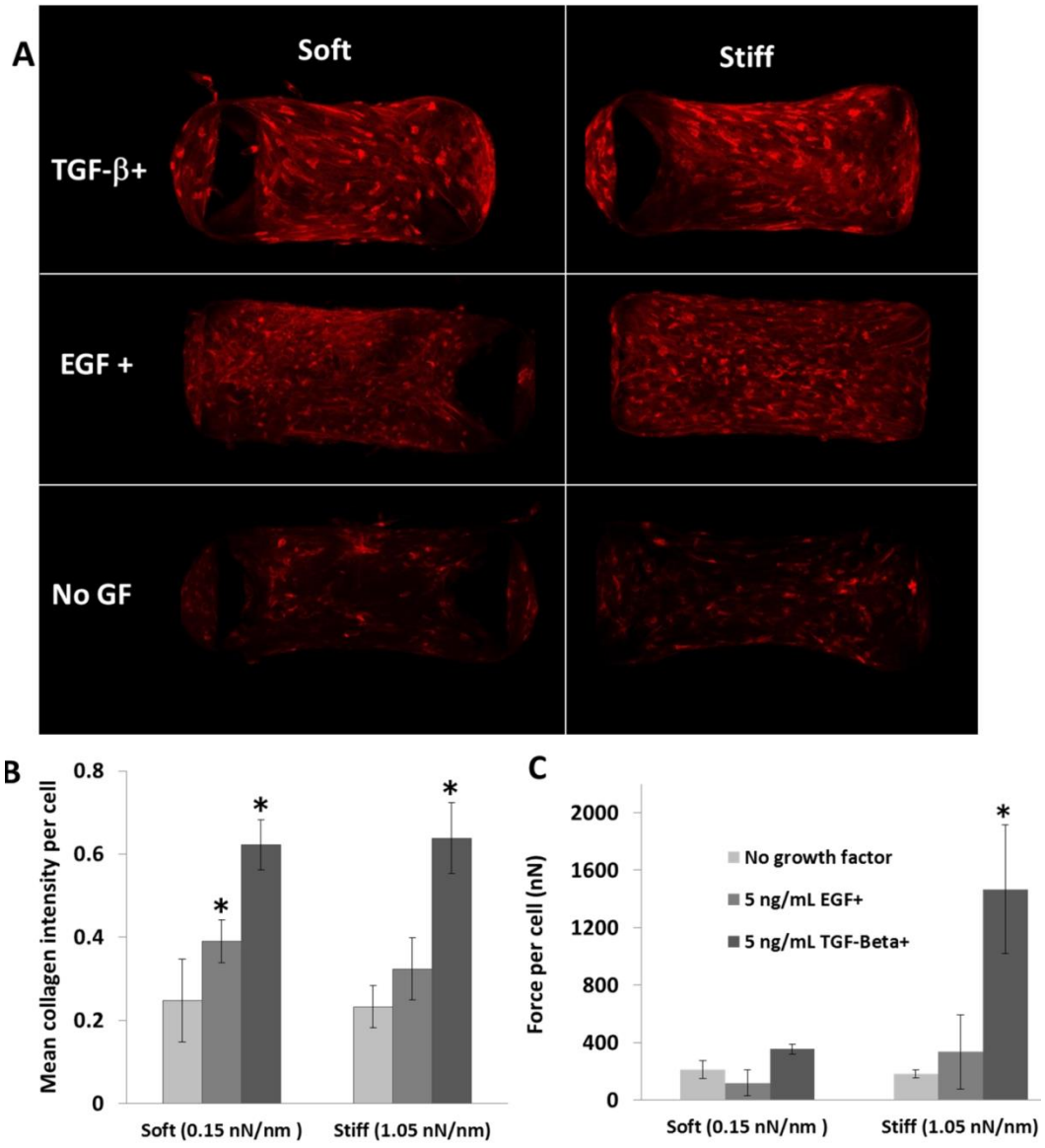

Figure 3. 6 A) De novo collagen stained in micro-tissues after five days in culture against soft (0.15 nN/nm) and stiff (1.05 nN/nm) boundaries.B) TGF-β1 increases collagen production per cell equally under soft and stiff boundaries. EGF increases collagen intensity significantly only under soft boundary. Two-way ANOVA, $p<0.05$:∗: Significantly higher than control groups ($p<0.05$) (n=3). C) Force-per-cell values after four days of culture. EGF does not alter isometric cell force significantly. ∗: Significantly higher force per cell than all other groups (n=4).

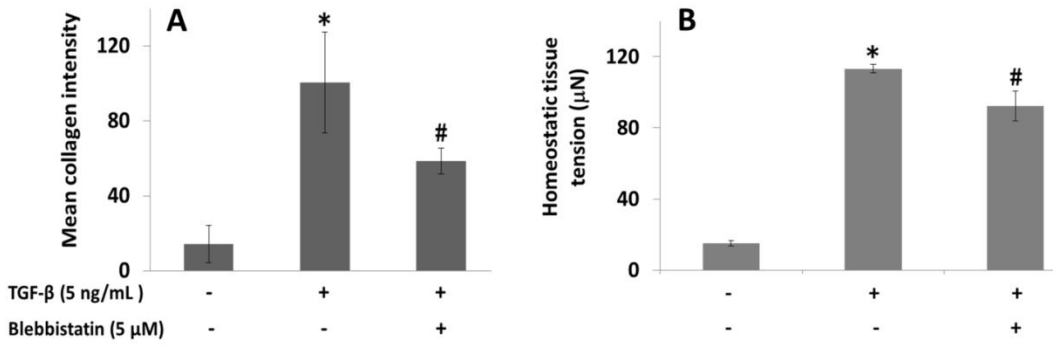

Figure 3. 7 A) Mean collagen intensity in equal ROIs on day 6 and B) mean homeostatic tissue tension in micro-tissues cultured with either 0 or 5 ng/mL TGF-β1 and either 0 or5 μM Blebbistatin against stiff boundaries (1.05 nN/nm). Enhancement of tension and collagen production with TGF-β1 are attenuated by Blebbistatin. One-way ANOVA, $p<0.005$:∗: Significantly higher from all other groups, #: Significantly higher from control (no-TGF-β1/no-Blebbistatin) group.

3.4 Discussion

This study represents the first quantitative characterization of the combined effects of stiffness and TGF-β1 on myofibroblast activation in a 3D tissue model. Our regression analysis indicates that TGF-β1 and boundary stiffness increase the homeostatic level of tension in VIC-populated fibrin gels both independently and synergistically. However, increasing only one of these factors with minimal levels of the other does not increase the cell-generated forces significantly. We also found that when cultured with a high concentration of TGF-β1 against stiff boundaries, VICs are in a state of nearly maximal contraction and impart significant residual tension on the matrix during remodeling. Finally, we observed that collagen production is stimulated by TGF-β1 treatment in a tension-dependent manner, yet collagen accumulation is significant even under low tension with TGF-β1 but not EGF supplementation. Taken together, the results indicate the possibility of generating collagen-rich engineered tissues under a low tension environment to produce TEHV leaflets with minimal retraction.

3.4.1 TGF-β1 and stiffness are strongly synergistic, but moderate levels of both are required

Although it is clear from the literature that both TGF-β1 and resistance to cell-generated tension (i.e., stiffness) of the 2D substrate or 3D matrix are necessary factors for myofibroblast activation [5, 15, 16], quantitative relationships between these parameters have not been developed. It is generally accepted that with increasing TGF-β1 concentration (4 levels), α-SMA protein levels increase in VICs cultured on rigid tissue culture plastic or glass [30, 57]. In our previous study utilizing compliant 2D substrates (15 different moduli spanning a large range), we observed a sigmoidal relationship between substrate modulus and α-SMA-positive stress fibers, and we also observed synergy with TGF-β1 (0 or 5 ng/mL) [17]. It appears that α-SMA-positive stress fibers are formed only over a threshold substrate modulus (5-9 kPa for VICs [17] and 20 kPa for dermal fibroblasts [22]). Further, Anseth et al. found that decreasing substrate modulus in real time decreases the number of α-SMA positive VICs, which implies that myofibroblast differentiation is reversible under a threshold of stiffness [23]. In anchored collagen gels that are released from their rigid boundaries, TGF-β1 significantly increases both gel compaction rate and α-SMA expression in a dose dependent manner [24, 28, 30]. In contrast, in free floating gels (not cultured against rigid anchors then released) where high tension cannot be generated by the cells, α-SMA is not expressed. Combined these findings clearly demonstrate an interaction between stiffness and TGF-β1 in terms of myofibroblast activation, yet it is not possible to identify the functional relationship between these factors since only one stimulus was tested at multiple levels in each study and cell forces have not been directly measured.

High force generation is a powerful functional measure of the myofibroblast phenotype [18]. Traction force microscopy studies demonstrate that increasing stiffness increases

traction forces applied to the substrate by fibroblasts [20-22]. Hinz and colleagues report that a minimum force per focal adhesion (125 nN) is required for recruitment of α-SMA into stress fibers [22], implying a minimum stiffness for myofibroblast differentiation. Tschumperlin and colleagues [21] found that TGF-β1 does not affect lung fibroblast-generated forces when substrate modulus is less than 13 kPa, while it causes a dramatic stiffness-dependent increase over this stiffness. Here we observed a similar trend in cell-generated forces in our 3D culture system in that TGF-β1 has no significant effect under soft boundaries ($k < 0.33$ N/m) but has a strong dose-dependent effect for higher stiffness posts. For the first time, by using graded levels of both stiffness and TGF-β1 simultaneously, we obtained complete force response surface as a function of these factors in 3D which can be used to determine scaffold and culture parameters to obtain a desired level of tension.

In the present study, we utilized a limited range of boundary stiffness (0.15-1.05 nN/nm) and TGF-β (0-5 ng/mL) concentrations. Higher post stiffness values or TGF-β concentrations (up to 10 ng/mL) can be used to mimic the pathological conditions and determine the saturation of cell response to these factors.

3.4.2 Stiffness effects on cell force in the absence of exogenous TGF-β1 may be due to serum

Previous studies utilizing the micro-tissue system report increases in the forces generated by fibroblasts [42, 46] and cardiomyocytes [43] with increasing post stiffness in the absence of exogenous TGF-β1. In contrast, our findings indicate that stiffness only has a strong dose-dependent effect at concentrations of TGF-β1 higher than 0.05 ng/mL. Further, in the absence of TGF-β1, the α-SMA distribution is diffuse in the cytoplasm of ours cells, even under the stiffest boundary where the force per cell is approximately 300 nN. The sensitivity to stiffness observed in previous investigations without explicit

growth factor supplementation may be due to the presence of growth factors in serum [58]. In this study, we utilize chemically defined medium to avoid growth factors contained in serum without "starving" the cells of other essential components in serum.

3.4.3 VICs generate high force per cell which can lead to failure to form micro-tissues

The force-per-cell values obtained in the present study (130-2500 nN) are significantly higher than values reported in previous studies using μTUG system (15-25 nN for per 3T3 fibroblast) [46, 56] and culture force monitors (50-200 nN per fibroblast) [20]. This discrepancy is mainly due to differences in how the force-per-cell is calculated. In previous studies, the force per cell is generally determined by dividing the force by the total number of cells in the gel (i.e., assuming all cells act in parallel), which is an oversimplification. Alternatively, as we have previously described [42, 47] we divide the total tension applied to one post by the average number of representative volume elements (RVEs) parallel to each other in the central portion of the tissue which assumes that the representative number of cells in a given cross-section of the tissue act in parallel [47] (Figure S2, Appendix-II). When calculated using the standard method of dividing the force by the total number of cells in the gel, the force-per-cell values in the present study range from 19-422 nN. These values similar to previously reported, but are slightly higher possibly due to the contractility of the VIC cell type, a soluble factor in the chemically defined medium (especially the high concentration of TGF-β1), and/or our use of higher boundary stiffness than previous μTUG systems (but lower than the isometric CFM systems).

The high force per cell relative to the amount of ECM production by the cells was one of the main reasons for tissue failures in the device, especially with high post stiffness and TGF-β1 concentration. Many tissues slipped of the soft posts under high tension

conditions (Appendix-V, Figure S3A), and tissue thinning due to fibrinolysis and/or low ECM production in the absence of growth factors lead to ripping of the tissues (Figure S3B). To prevent micro-tissues from slipping off of the posts, the cell density was decreased to reduce tension, and in turn, post deflection; however, lower cell numbers limit the maximum stiffness of posts that can be utilized. To minimize tissue thinning and breaking, aminocaproic acid was added to culture media, but it did not prevent tissue breaking. Adding aprotinin decreased tissue breaking significantly. Tissues also stuck to the PDMS walls due to the adhesive nature of fibrin and lead to failure (Figure S3C). Increasing Pluronic concentration was utilized to prevent fibrin from sticking to the PDMS, but too high concentration led to tissues popping out from the wells. Due to this limitation, Pluronic concentration was kept under 2% for all groups.

3.4.4 TGF-β1-supplemented cells exist in a nearly maximally contracted state

To separate the cells' ability to generate and hold isometric force against the posts from their ability to actively contract in response to an agonist (i.e., contractility), we stimulated the cells with KCl following four days of culture. One of the most striking findings of this analysis is that the cells cultured against stiff posts with TGF-β1, identified as myofibroblasts by their α-SMA-positive stress fibers (Figure 3.5), are the least contractile of all groups (3.3 % increase in force over homeostatic tension with KCl stimulation, Figure 3.4). In the absence of TGF-β1, the cells generated lower total forces against stiff posts than with the growth factor but were significantly more contractile than all other groups (54 % increase in force over homeostatic tension with KCl stimulation), even greater than TGF-β1-treated cells cultured against soft posts. Recently, it was reported that cyclic distension of fibroblast-populated fibrin constructs does not alter the effect of TGF-β1 on KCl-stimulated contraction or number of α-SMA positive cells [39]. We speculate that cells are already able generate substantial tension against stiff

boundaries and differentiate into myofibroblasts, thus additional mechanical conditioning has little additional effect on their contractile ability. Grinnell and colleagues [28] have also found that, in anchored fibroblast-populated collagen gels, cells pretreated with TGF-β1 for five days appear to be unable to contract in response to agonists (lysophosphatidic acid (LPA) or additional TGF-β1) when released from the rigid boundary. Taken together, myofibroblasts appear to exist in a nearly maximally contracted state - they apply high isometric force to the matrix yet have little additional ability to contract in response to external stimulation.

We did the activated contraction and residual tension measurements at room temperature. Although temperature may affect cell response to KCl or Cytochalasin-D, we assumed that this effect to be negligible since we kept imaging period after each treatment under ten minutes.

3.4.5 Residual tension is enhanced by TGF-β1 only with high post stiffness

The other striking result from our analysis of the components of the total force applied to the posts is that the residual tension in the matrix is much higher under stiff boundaries with TGF-β1 than other groups (7-15 fold over other groups). This result indicates that myofibroblasts remodel the tissue much more extensively than non-activated fibroblasts. The effect of residual tension on tissue retraction has been investigated in previous studies utilizing fibroblast-populated protein gels [51] and polymer scaffolds [4] by eliminating active cell contraction with Cyto-D or Rho-associated protein kinase (ROCK) inhibitors prior to release of anchored matrices. When active cell force is inhibited, total retraction upon release is decreased by 75% in fibrin gels [51], 80% in collagen gels [59] and 40% in PGA/P4HB scaffolds [4]. To decrease retraction of fibrin-based TE heart valve leaflets, Tranquillo and colleagues treated the engineered tissues with Blebbistatin

(Myosin II inhibitor) 2-4 days prior to implantation at the end of a 3-week static culture period [3]. The treatment provided a transient retraction and the valves were functional initially; however, after four weeks *in vivo* regurgitation due to tissue shrinkage caused valve failure. More recently, the cells have been removed from TEHVs altogether in an attempt to eliminate retraction, and decellularized TEHVs have been repopulated with non-contractile cells [60, 61], but these valves also retracted after *in vivo* remodeling [61].

Taken together, these results imply that cell-generated forces must be reduced throughout the remodeling period to eliminate residual tension (and thus passive retraction) rather than simply blocking cell contractile activity immediately prior to implant. Yet it remains unclear whether robust TE constructs rich in organized collagen can be created under low tension since tension is needed to stabilize collagen against enzymatic degradation [62, 63] and the effect of tension on collagen production of VICs is not known. To explore the feasibility of generating collagenous tissues under low tension, we investigated the effects of boundary stiffness and growth factors on collagen accumulation in our fibrin gel micro-tissues.

To eliminate cell-generated tension and isolate the residual tension in the matrix, we used Cytochalasin-D. Since Cytochalasin-D inhibits cytoplasmic actin polymerization, it not only removes cell force but also damages cell-cell adhesion and causes loss of tissue integrity. In the videos showing response to Cytochalasin-D treatment, following tissue relaxation, tissue disintegration is observed [64]. Therefore, residual tensions values reported here can be lower than actual. Blebbistatin (myosin II inhibitor) can be a better option to isolate residual tension in the future studies.

3.4.6 TGF-β1 stimulates substantial collagen production - even under low tension

Our data indicate that boundary stiffness alone, in the absence of growth factors (and serum), does not significantly affect collagen accumulation (Figure 3.6A, B). This result parallels the lack of difference in homeostatic tension between stiffness groups in the absence of TGF-β1 (Figure 3.6 C). These data are consistent with previous studies which show that cyclic stretching alone, in the absence of serum or growth factors, does not affect procollagen synthesis in fibroblasts [36]. With the addition of 5 ng/mL TGF-β1, however, we observed a similar (approximately 2.5-fold) increase in collagen staining under both stiff and soft boundaries even though the growth factor does not stimulate a significant increase in tension against soft posts. This lack of mechanical effect is in contrast to studies which show that dynamic stretch enhances the stimulation of procollagen synthesis by serum or TGF-β1 [36, 65]. When we decreased the cell-generated tension with a low concentration of Blebbistatin, as an alternative to utilizing low boundary stiffness, the augmentation of collagen production with TGF-β1 was significantly attenuated. Taken together, these findings indicate that both mechanical forces and growth factors are necessary for stimulation of collagen production, but there may be particular combinations (e.g., TGF-β1 stimulation under low mechanical loading) which stimulate sufficient collagen accumulation without inducing unwanted tension in the tissue. Although our results are promising, our collagen accumulation measurements were based on optical evaluations after only five days in culture, an early stage for tissue remodeling. The effects of cell generated forces on ECM synthesis and *de novo* tissue integrity must be elucidated in long-term studies.

EGF also increases collagen accumulation under our experimental conditions, but the increase is significantly less than for TGF-β1 supplementation. Surprisingly, EGF has less of an effect on collagen accumulation for cells cultured against stiff posts (1.4-fold)

than soft posts (1.6-fold). Previously, we showed that EGF increases collagen accumulation in fibroblast-populated fibrin gels cultured against rigid boundaries to the same extent as an equivalent concentration of TGF-β1 (5 ng/mL) [50, 51]. In the aforementioned study, the EGF-treated samples retracted significantly less than both TGF-treated and serum-fed control samples suggesting lower cell-generated forces in the EGF group. However, in the retraction assay, the isometric force is not measured prior to release and the total retraction is affected by residual matrix stress, stiffness of matrix, and cell contractility. Data from the current study indicate that EGF likely stimulated lower cell-generated force than TGF-β1 in the rigidly anchored fibrin gels. Assuming that the tension was lower throughout the culture duration, it is unclear why collagen accumulation was equivalent with EGF and TGF-β1 supplementation in the previous study whereas it is much lower in this study. It is possible that the balance between collagen production and degradation changes in its tension dependency over long-term culture (21 days in the previous study compared to five days in this study).

Overall, when comparing the force and collagen per cell, it is clear that the level of tension in the gel modulates collagen accumulation, but that these parameters can be uncoupled with the use of different growth factors. For example, the average force per cell in the EGF/stiff group is approximately the same as for the TGF-β1/soft group (Figures 3.6 B & C), yet the collagen accumulation is dramatically lower for the EFG/stiff group.

Here, we semi-quantified *de novo* collagen accumulation by measuring average fluorophore intensity. Combined effect of stiffness and growth factors on ECM production needs to be elucidated by quantifying *de novo* collagen content with hydroxiproline assays. In addition to proteins providing mechanical strength, such as

collagen, key components maintaining stability like elastin and GAGs needs to be quantified with suitable assays [66].

3.5 Summary and Conclusions

In the present study, we quantified the interaction between the boundary stiffness and TGF-β1 on VIC-generated forces in a 3D tissue model. We showed that higher active isometric-cell force leads to larger residual tension in the tissues, which implies that to prevent built-up of large residual tension, cell contractility must be regulated through entire culture period. We also observed that collagen accumulation per cell can be stimulated in similar rates under significantly different tension levels. The ability to increase collagen production under low tension is promising for TE applications; since increasing ECM production without inducing myofibroblast activation will likely decrease retraction. Obtaining robust tissues without excessive tissue tension might be possible by augmenting ECM synthesis by growth factors together with regulation of cell-generated forces by drugs. More research is needed to determine optimum tension levels in the tissue, suitable drugs to regulate cell-generated forces and collagen degradation through entire culture period, and optimum growth factor concentrations. High throughput experiments by using micro-tissue systems can be used to determine these optimum conditions, and, these conditions can be tried for organ-size constructs.

References

[1] Pedersen JA, Swartz MA. Mechanobiology in the third dimension. Ann Biomed Eng. 2005;33:1469-90.
[2] Kural MH, Billiar KL. Regulating tension in three-dimensional culture environments. Experimental Cell Research. 2013;319:2447-59.
[3] Syedain ZH, Lahti MT, Johnso SL, Robinson PS, Ruth GR, Bianco RW, et al. Implantation of a tissue-engineered heart valve from human fibroblasts exhibiting short term function in the sheep pulmonary artery. Cardiovasc Eng Technol. 2011;2:101-12.
[4] van Vlimmeren MA, Driessen-Mol A, Oomens CW, Baaijens FP. Passive and active contributions to generated force and retraction in heart valve tissue engineering. Biomech Model Mechanobiol. 2012;11:1015-27.
[5] Tomasek JJ, Gabbiani G, Hinz B, Chaponnier C, Brown RA. Myofibroblasts and mechano-regulation of connective tissue remodelling. Nat Rev Mol Cell Biol. 2002;3:349-63.
[6] Lundberg MS. Cardiovascular tissue engineering research support at the National Heart, Lung, and Blood Institute. Circ Res. 2013;112:1097-103.
[7] Hoenig MR, Campbell GR, Rolfe BE, Campbell JH. Tissue-engineered blood vessels: alternative to autologous grafts? Arteriocler Thromb Vacs Biol. 2005;25:1128-34.
[8] Gauvin R, Larouche D, Marcoux H, Guignard R, Auger FA, Germain L. Minimal contraction for tissue-engineered skin substitutes when matured at the air-liquid interface. J Tissue Eng Regen Med. 2013;7:452-60.
[9] Roy-Chaudhury P, Kelly BS, Miller MA, Reaves A, Armstrong J, Nanayakkara N, et al. Venous neointimal hyperplasia in polytetrafluoroethylene dialysis grafts. Kidney Int. 2001;59:2325-34.
[10] van Vlimmeren MA, Driessen-Mol A, Oomens CW, Baaijens FP. An in vitro model system to quantify stress generation, compaction, and retraction in engineered heart valve tissue. Tissue Eng Part C Methods. 2011;17:983-91.
[11] Schmidt D, Dijkman PE, Driessen-Mol A, Stenger R, Mariani C, Puolakka A, et al. Minimally-invasive implantation of living tissue engineered heart valves: a comprehensive approach from autologous vascular cells to stem cells. J Am Coll Cardiol. 2010;56:510-20.
[12] Rabkin E, Aikawa M, Stone JR, Fukumoto Y, Libby P, Schoen FJ. Activated interstitial myofibroblasts express catabolic enzymes and mediate matrix remodeling in myxomatous heart valves. Circulation. 2001;104:2525-32.
[13] Hoerstrup SP, Kadner A, Melnitchouk S, Trojan A, Eid K, Tracy J, et al. Tissue engineering of functional trileaflet heart valves from human marrow stromal cells. Circulation. 2002;106:I143-50.
[14] Schoen FJ. Evolving concepts of cardiac valve dynamics: the continuum of development, functional structure, pathobiology, and tissue engineering. Circulation. 2008;118:1864-80.
[15] Hinz B. Formation and function of the myofibroblast during tissue repair. J Invest Dermatol. 2007;127:526-37.
[16] Hinz B, Mastrangelo D, Iselin CE, Chaponnier C, Gabbiani G. Mechanical tension controls granulation tissue contractile activity and myofibroblast differentiation. Am J Pathol. 2001;159:1009-20.
[17] Quinlan AM, Billiar KL. Investigating the role of substrate stiffness in the persistence of valvular interstitial cell activation. J Biomed Mater Res A. 2012;100:2474-82.

[18] Hinz B, Celetta G, Tomasek JJ, Gabbiani G, Chaponnier C. Alpha-smooth muscle actin expression upregulates fibroblast contractile activity. Mol Biol Cell. 2001;12:2730–41.
[19] Chen J, Li H, SundarRaj N, Wang JH. Alpha-smooth muscle actin expression enhances cell traction force. Cell Motil Cytoskeleton. 2007;64:248-57.
[20] Han SJ, Bielawski KS, Ting LH, Rodriguez ML, Sniadecki NJ. Decoupling substrate stiffness, spread area, and micropost density: a close spatial relationship between traction forces and focal adhesions. Biophys J. 2012;103:640-8.
[21] Marinkovic A, Mih JD, Park JA, Liu F, Tschumperlin DJ. Improved throughput traction microscopy reveals pivotal role for matrix stiffness in fibroblast contractility and TGF-beta responsiveness. Am J Physiol Lung Cell Mol Physiol. 2012;303:L169-80.
[22] Goffin JM, Pittet P, Csucs G, Lussi JW, Meister JJ, Hinz B. Focal adhesion size controls tension-dependent recruitment of alpha-smooth muscle actin to stress fibers. J Cell Biol. 2006;172:259-68.
[23] Kloxin AM, Benton JA, Anseth KS. In situ elasticity modulation with dynamic substrates to direct cell phenotype. Biomaterials. 2010;31:1-8.
[24] Arora PD, Narani N, McCulloch CA. The compliance of collagen gels regulates transforming growth factor-beta induction of alpha-smooth muscle actin in fibroblasts. Am J Pathol. 1999;154:871-82.
[25] Vaughan MB, Howard EW, Tomasek JJ. Transforming growth factor-beta1 promotes the morphological and functional differentiation of the myofibroblast. Exp Cell Res. 2000;257:180-9.
[26] Inoue M, Ono I, Tateshita T, Kuroyanagi Y, Shioya N. Effect of a collagen matrix containing epidermal growth factor on wound contraction. Wound Repair Regen. 1998;6:213-22.
[27] Murray MM, Rice K, Wright RJ, Spector M. The effect of selected growth factors on human anterior cruciate ligament cell interactions with a three-dimensional collagen-GAG scaffold. J Orthop Res. 2003;21:238-44.
[28] Grinnell F, Ho CH. Transforming growth factor beta stimulates fibroblast-collagen matrix contraction by different mechanisms in mechanically loaded and unloaded matrices. Exp Cell Res. 2002;273:248-55.
[29] Tuan T, Song A, Chang A, Younai S, Nimni ME. In vitro fibroplasia: Matrix contraction, cell growth, and collagen production of fibroblasts cultured in fibrin gels. Exp Cell Res. 1996;223:127–34.
[30] Walker GA, Masters KS, Shah DN, Anseth KS, Leinwand LA. Valvular myofibroblast activation by transforming growth factor-beta: implications for pathological extracellular matrix remodeling in heart valve disease. Circ Res. 2004;95:253-60.
[31] Yao L, Swartz DD, Gugino SF, Russell JA, Andreadis ST. Fibrin-based tissue-engineered blood vessels: differential effects of biomaterial and culture parameters on mechanical strength and vascular reactivity. Tissue Eng. 2005;11:991-1003.
[32] Roberts AB, Sporn MB, Assoian RK, Smith JM, Roche NS, Wakefield LM, et al. Transforming growth factor type beta: rapid induction of fibrosis and angiogenesis in vivo and stimulation of collagen formation in vitro. PNAS. 1986;83:4167-71.
[33] Neidert MR, Lee ES, Oegema TR, Tranquillo RT. Enhanced fibrin remodeling in vitro with TGF-beta1, insulin and plasmin for improved tissue-equivalents. Biomaterials. 2002;23:3717-31.
[34] Grassl ED, Oegema TR, Tranquillo RT. A fibrin-based arterial media equivalent. Journal of biomedical materials research Part A. 2003;66:550-61.

[35] Breen EC. Mechanical strain increases type I collagen expression in pulmonary fibroblasts in vitro. J Appl Physiol. 2000;88:203-9.
[36] Parsons M, Kessler E, Laurent GJ, Brown RA, Bishop JE. Mechanical load enhances procollagen processing in dermal fibroblasts by regulating levels of procollagen C-proteinase. Exp Cell Res. 1999;252:319-31.
[37] Yang G, Crawford RC, Wang JH. Proliferation and collagen production of human patellar tendon fibroblasts in response to cyclic uniaxial stretching in serum-free conditions. J Biomech. 2004;37:1543-50.
[38] Hinz B, Gabbiani G, Chaponnier C. The NH2-terminal peptide of alpha-smooth muscle actin inhibits force generation by the myofibroblast in vitro and in vivo. J Cell Biol. 2002;157:657-63.
[39] Hall MS, Long R, Feng X, Huang Y, Hui C-Y, Wu M. Toward single cell traction microscopy within 3D collagen matrices. Experimental Cell Research. 2013;319:2396-408.
[40] Delvoye P, Wiliquet P, Leveque JL, Nusgens BV, Lapiere CM. Measurement of mechanical forces generated by skin fibroblasts embedded in a three-dimensional collagen gel. J Invest Dermatol. 1991;97:898-902.
[41] Kolodney MS, Wysolmerski RB. Isometric contraction by fibroblasts and endothelial cells in tissue culture: a quantitative study. J Cell Biol. 1992;117:73-82.
[42] John J, Quinlan AT, Silvestri C, Billiar K. Boundary stiffness regulates fibroblast behavior in collagen gels. Ann Biomed Eng. 2010;38:658-73.
[43] Boudou T, Legant WR, Mu A, Borochin MA, Thavandiran N, Radisic M, et al. A microfabricated platform to measure and manipulate the mechanics of engineered cardiac microtissues. Tissue Eng Part A. 2012;18:910-9.
[44] Freyman TM, Yannas IV, Yokoo R, Gibson LJ. Fibroblast contraction of a collagen–GAG matrix. Biomaterials. 2001;22:2883-91.
[45] Throm Quinlan AM, Sierad LN, Capulli AK, Firstenberg LE, Billiar KL. Combining dynamic stretch and tunable stiffness to probe cell mechanobiology in vitro. PLoS One. 2011;6:e23272.
[46] Legant WR, Pathak A, Yang MT, Deshpande VS, McMeeking RM, Chen CS. Microfabricated tissue gauges to measure and manipulate forces from 3D microtissues. PNAS. 2009;106:10097-102.
[47] Kural MH, Billiar K. Regulating tension in three-dimensional culture environments. Exp Cell Res. 2013;10.1016/j.yexcr.2013.06.019.
[48] Ahlfors JE, Billiar KL. Biomechanical and biochemical characteristics of a human fibroblast-produced and remodeled matrix. Biomaterials. 2007;28:2183-91.
[49] Tranquillo R, Isenberg B. Artificial Soft Tissue Fabrication from Cell-Contracted Biopolymers. In: Guilak F, Butler D, Goldstein S, Mooney D, editors. Functional Tissue Engineering: Springer New York; 2003. p. 305-17.
[50] Throm AM, Liu WC, Lock CH, Billiar KL. Development of a cell-derived matrix: effects of epidermal growth factor in chemically defined culture. J Biomed Mater Res A. 2010;92:533-41.
[51] Grouf JL, Throm AM, Balestrini JL, Bush KA, Billiar KL. Differential effects of EGF and TGF-beta1 on fibroblast activity in fibrin-based tissue equivalents. Tissue Eng. 2007;13:799-807.
[52] Kershaw JD, Misfeld M, Sievers HH, Yacoub M. H., Chester AH. Specific regional and directional contractile responses of aortic cusp tissue. J Heart Valve Dis. 2004;13:798-803.

[53] Merryman DW, Shadow HS, Schoen FJ, Sacks MS. The effects of cellular contraction on aortic valve leaflet flexural stiffness. J Biomech. 2006;39:88-96.
[54] Ingber DE, Prusty D, Sun Z, Betensky H, Wang N. Cell shape, cytoskeletal mechanics, and cell cycle control in angiogenesis. J Biomech. 1995;28:1471-84.
[55] Tamariz E, Grinnell F. Modulation of fibroblast morphology and adhesion during collagen matrix remodeling. Mol Biol Cell. 2002;13:3915-29.
[56] West AR, Zaman N, Cole DJ, Walker MJ, Legant WR, Boudou T, et al. Development and characterization of a 3D multicell microtissue culture model of airway smooth muscle. Am J Physiol Lung Cell Mol Physiol. 2013;304:L4-16.
[57] Cushing MC, Liao J-T, Anseth KS. Activation of valvular interstitial cells is mediated by transforming growth factor-β1 interactions with matrix molecules. Matrix Biol. 2005;24:428-37.
[58] Sundararaghavan HG, Monteiro GA, Lapin NA, Chabal YJ, Miksan JR, Shreiber DI. Genipin-induced changes in collagen gels: correlation of mechanical properties to fluorescence. J Biomed Mater Res A. 2008;87:308-20.
[59] Tomasek JJ, Haaksma CJ, Eddy RJ, Vaughan MB. Fibroblast contraction occurs on release of tension in attached collagen lattices: dependency on an organized actin cytoskeleton and serum. Anat Rec. 1992;232:359-68.
[60] Dijkman PE, Driessen-Mol A, Frese L, Hoerstrup SP, Baaijens FPT. Decellularized homologous tissue-engineered heart valves as off-the-shelf alternatives to xeno- and homografts. Biomaterials. 2012;33:4545-54.
[61] Weber B, Dijkman PE, Scherman J, Sanders B, Emmert MY, Grünenfelder J, et al. Off-the-shelf human decellularized tissue-engineered heart valves in a non-human primate model. Biomaterials. 2013;34:7269-80.
[62] Flynn BP, Bhole AP, Saeidi N, Liles M, DiMarzio CA, Ruberti JW. Mechanical strain stabilizes reconstituted collagen fibrils against enzymatic degradation by mammalian collagenase matrix metalloproteinase 8 (MMP-8). PLoS ONE. 2010;5:e12337.
[63] Chiquet M. Regulation of extracellular matrix gene expression by mechanical stress. Matrix Biol. 1999;18:417-26.
[64] Kural MH, Billiar KL. Mechanoregulation of valvular interstitial cell phenotype in the third dimension. Biomaterials. 2014;35:1128-37.
[65] Butt RP, Bishop JE. Mechanical load enhances the stimulatory effect of serum growth factors on cardiac fibroblast procollagen synthesis. J Mol Cell Cardiol. 1997;29:1141-51.
[66] Tripi DR, Vyavahare NR. Neomycin and pentagalloyl glucose enhanced cross-linking for elastin and glycosaminoglycans preservation in bioprosthetic heart valves. Journal of biomaterials applications. 2014;28:757-66.

CHAPTER 4: Effect of Boundary Stiffness on Myofibroblast Persistence in 3D

4.1 Introduction

Myofibroblasts play a key role in tissue remodeling and wound healing [1, 2]. Being able to generate high traction forces and secrete abundant extracellular matrix (ECM) proteins, myofibroblasts can reorganize their surrounding matrix, rapidly close wounds and repair matrix damage [3]. However, prolonged presence of myofibroblasts due to excessive activation of fibroblasts and/or insufficient myofibroblast apoptosis leads to fibrocontractive remodeling and scar tissue [3-5]. By compacting surrounding matrix, digesting native ECM and secreting excessive amounts of stiff collagen, myofibroblasts contribute to diseases of many different organs [6-8].

In heart valves, activation of a large proportion of valvular interstitial cells (VICs) to the myofibroblast phenotype (more than 60% of the total cell population) is associated with valve fibrosis [9]. Moreover, in 82% of calcified aortic valves, myofibroblasts are colocalized with calcified regions and apoptotic cells [9]. In addition to being associated with heart valve disease, myofibroblasts are responsible for tissue thickening and retraction in engineered heart valves [10, 11]. Thus, being able to reverse the myofibroblast phenotype (i.e., de-differentiate VICs back to the quiescent state) and/or control the rate of clearing of myofibroblasts from the tissue via apoptosis would be of great benefit for therapeutic applications.

High substrate modulus and transforming growth factor-beta (TGF-β) have been shown to be key activators of fibroblasts and VICs to myofibroblast [12-14]. Specifically, on high modulus substrates in the presence of TGF-β, fibroblastic cells form α-SMA-rich stress fibers – the defining visual hallmark of the myofibroblast phenotype – and generate high intracellular tension. We recently demonstrated quantitatively that this synergistic

relationship between stiffness and TGF-β in modulating VIC-generated forces also applies in three-dimensional (3D) ECM [15].

Although, the mechanical environment is clearly critical for triggering myofibroblast activation, there is little known about mechanical reversibility of this phenotype. Early *in vivo* data indicated that myofibroblasts are cleared following wound closure by apoptosis (programmed cell death) rather than de-differentiation [16]. More recently, reducing the resistance to cell contraction has also been shown to trigger apoptosis; releasing a stiff splint holding the edges of an excisional wound caused apoptosis in 8% of the total cell population [17]. In an analogous *in vitro* 3D system where collagen gels seeded with dermal myofibroblasts were detached from rigid boundaries, apoptosis was triggered in 15% of the cells [18]. A similar study utilizing fibroblasts isolated from scar tissue [19] reported 40% apoptosis following the release of anchored collagen gels.

In contrast, there is recent evidence that myofibroblasts may de-differentiate with changes in the mechanical environment. Anseth and her group seeded VICs on light-responsive gel substrates for three days then decreased gel Young's modulus dynamically [20, 21]. They observed a significant decrease in number of cells expressing α-SMA, indicating phenotypic reversion after two additional days of culture at the lower modulus. However, when they cultured VICs on stiff gels for a longer time period (seven days), reduction of substrate modulus did not result in de-differentiation [21]. The cells on the real-time softened gels had higher apoptosis proportions than cells on gels that remained stiff, but the proportions were not significantly different than control cells cultured on low modulus substrates. In the aforementioned 2D and 3D studies, the experimental manipulations reduce the mechanical tension able to be generated by the cells, but in

none of the studies is the tension quantified, thus it is unclear if the magnitude of tension is a key parameter regulating de-differentiation and apoptosis.

We hypothesize that a reduction of the ability of myofibroblasts to generate tension due to alteration of the mechanical environment triggers de-differentiation and, for a large decrease in tension, apoptosis. To test this hypothesis, we cultured VICs in 3D fibrin micro-tissues suspended between flexible posts the deflection of which can be used to quantify the tissue tension. To determine the effect of mechanical tension drop on myofibroblast phenotype, we cultured micro-tissues under high tension by holding one of the micro-posts rigidly with magnetic force applied to a nickel bead glued onto the post; the post was then released by removing the permanent magnet. To create a more severe tension drop, we released tissues completely from the micro-posts and cultured them free-floating. The findings of the present study provide insight for future studies aimed at directing myofibroblast fate in diseased or engineered tissues.

4.2 Methods

4.2.1 Cell Culture

Pig hearts were obtained from a local slaughter house (Blood Farm, Groton, MA). Aortic valves were excised within 2 hours after animals were killed. VICs were isolated according to a previously published protocol [22]. Briefly, aortic valve leaflets were rinsed with cold Dulbecco's phosphate buffered saline (DPBS, Cellgro, Manassas, VA), and submerged in 600 U/ml solution of Type II collagenase (Worthington Biochemical, Lakewood, NJ) in Dulbecco's Modified Eagle's Medium (DMEM, Life Technologies, Grand Island, NewYork) with 1% penicillin / streptomycin / amphotericin B (PSA, Life Technologies, Grand Island, New York) and 10% fetal bovine serum (FBS, Life

Technologies, Grand Island, New York). Both surfaces of the leaflets were rubbed by a sterile cotton swab to remove the valvular endothelial cells (VECs) in the collagenase solution. Next, leaflets were rinsed and incubated in 12 ml of collagenase solution at 37°C for 12 hours for enzymatic digestion. Finally, VICs were plated to tissue culture plastic flasks in DMEM with 1% PSA and 10% FBS. Cell with passage number 3 to 8 were used in all of the experiments. Two types of different pre-treatments were utilized in the current study: the first group was was pre-treated with low serum media containing 1% FBS for four days to have a more quiescent population initially and the second group was pre-treated with 10% FBS and 5 ng/mL TGF-β1 for four days to activate all cells to the myofibroblast phenotype.

4.2.2 Force Calculations with Micro-tissue Gauges (μ-TUGs)

As described in the previous chapter, to measure and regulate the cell-generated forces, micro-tissues were cultured in micro-wells containing two flexible posts made of poly(dimethylsiloxane) (PDMS, Dow Corning, Midland, MI). As cells compact the fibrin gel and form dog-bone shaped tissues around the posts, forces applied to posts can be calculated by measuring the posts deflection and using beam bending equations. Post deflections were measured at different time points and under different boundary conditions: right before applying the magnet (~1.5 day), ~10 hours following applying the magnet, right before removing magnet (2 or 3 days of culture), right after removing magnet, 7-12 hours after removing magnet, and 3 to 4 days after removing the magnet (Figure 4.1). Force measurements were taken right before and right after applying or removing magnet to evaluate the immediate cell-generated force response to real-time stiffening of the boundary. Force measurements at the intermediate time points were taken to have a better knowledge about the trend in myofibroblasts activation or de-differentiation (if any). The average force per cell was calculated by dividing the total

force applied to one of the posts by the average number of representative volume elements (RVEs) spanning a cross-sectional area in the middle of the micro-tissue (Appendix-II).

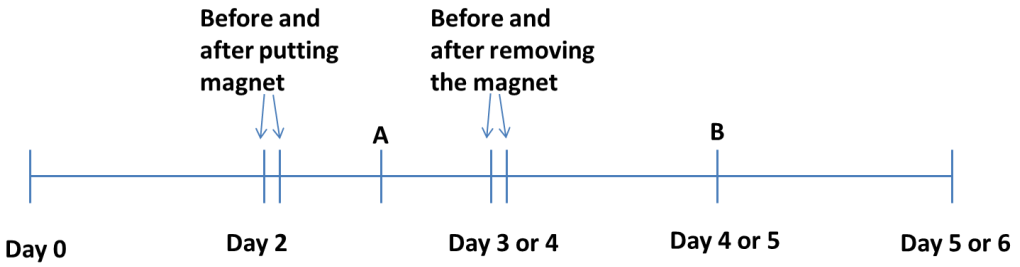

Figure 4. 1 Time points for force measurements.To evaluate immediate cell response to real-time changes in boundary stiffness, force measurements were taken right before and after putting and removing magnet. Measurements were taken at intermediate time points (A and B) to understand the time course of possible changes in cell phenotype.

4.2.3 VIC-Populated Fibrin Micro-Tissues

Empty µ-TUGs were treated with 3.5 % Pluronic F-127 (Invitrogen, Eugene, Oregon) to prevent cell attachment to the PDMS. VICs (160,000 cell/mL) were re-suspended in fibrin gels solution containing 3.3 mg/mi fibrinogen from bovine plasma (Sigma, St. Louis, MO) and 0.22 U/ml thrombin (Sigma, St. Louis, MO). The cell-gel mixture was centrifuged into the micro wells and the excess gel solution remained out of the wells was aspirated. Following one hour of incubation at 37 C to allow gel polymerization, culture media containing DMEM with 1% PSA, 33.3 µg/ml aprotinin (Sigma, St. Louis, MO) and 50 µg/ml L-ascorbic acid phosphate magnesium salt n-hydrate and with two different serum and growth factor concentrations was added to µ-TUG dishes: first one is 1 ng/mL TGF-β1 and 10% FBS abd the second one is 1% FBS with no TGF-β. Different micro-post stiffness levels were obtained by using different PDMS monomer-to-curing agent ratios and different baking temperatures as described in previous chapter.

4.2.4 Changing Boundary Stiffness in Real Time

Micro-posts with stiffness of 0.33 nN/nm were chosen as the low boundary stiffness level since, based on the force-per-cell measurements obtained for our previous study [15], at this level cell-generated forces remain constant after two days. In contrast, cell-generated forces keep increasing for seven days when cultured against 0.56 nN/nm posts in the presence of TGF-β1 (Appendix-VI) [15]. Therefore, increasing effective boundary stiffness ($k_{eff}^{-1} = k_1^{-1}+k_2^{-1}$) in real time from k_{eff} = 0.165 nN/nm to k_{eff} = 0.33 nN/nm by holding one post rigidly was expected to provide a transition between the two phonotypic states (Figure 4.2-B). The response of cell-generated forces to a dynamic change in boundary stiffness was predicted based on our previously quantified force-stiffness-TGF-β relationship (Figure 4.3). The changes in cell-generated forces obtained with different post stiffness (k = 0.15 nN/nm and 0.56 nN/nm) are given in Appendix-VII. To obtain an initially-stiff boundary condition, one of the micro-posts in each well was held rigidly by applying magnetic force to a nickel sphere (Alfa Asear 200 mesh, diameter = 100-150 μm, Ward Hill, Massachusetts) glued on top of the post as shown in Figure 4.2. Considering that two micro-posts create a resistance to cell-generated tension in series, the effective boundary stiffness was calculated as shown in Figure 4.2-B. Micro-tissues 2were cultured with one post rigidly held for one or two days to increase the effective stiffness, then the magnet was removed and the post was released to decrease the effective stiffness in real time.

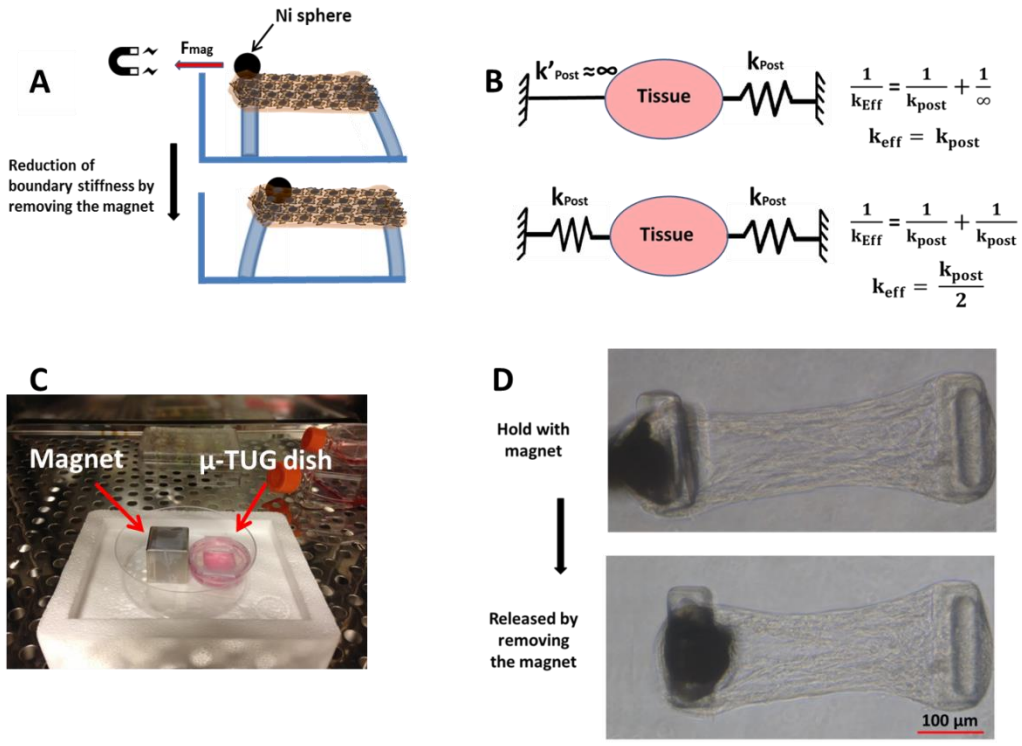

Figure 4. 2 A: Nickel particle glued onto the micro-post is held rigidly by a permanent magnet for one or two days. Stiffness is reduced in real time by removing the magnet. B: Calculation of estimated effective boundary stiffness as a result of holding one of the posts. C: A μ-TUG dish with permanent magnet in the incubator. D: Phase images of micro-tissue before and after removing the magnet.

To create a more severe reduction of boundary stiffness, we fully released the micro-tissues from one of the posts as shown in Figure 4.4, after two days of culture suspended between two posts.

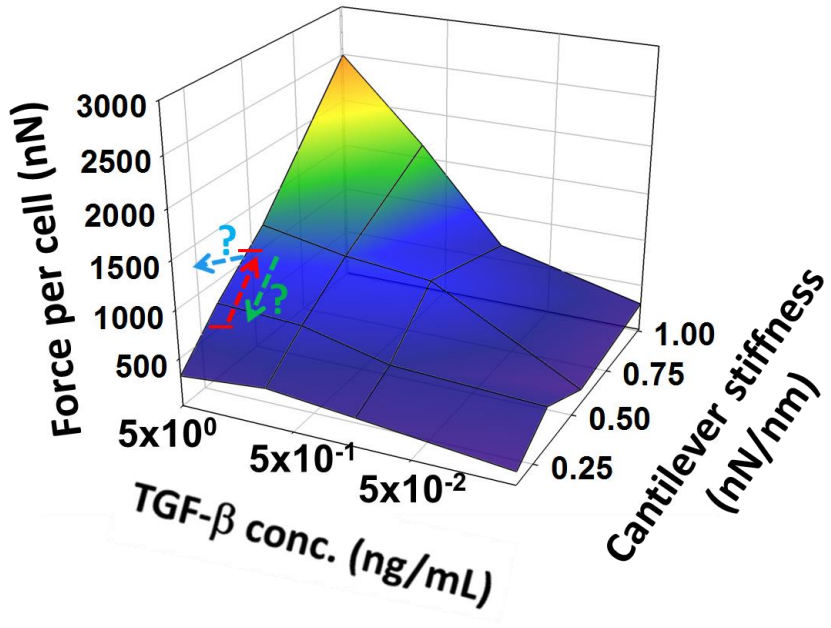

Figure 4. 3 Red arrow shows the predicted response of cell-generated forces to increasing boundary stiffness in real time when post stiffness was k = 0.33 nN/nm posts. Blue and green arrows show two of possible responses to boundary stiffness reduction. Modified plotting of data from previous chapter.

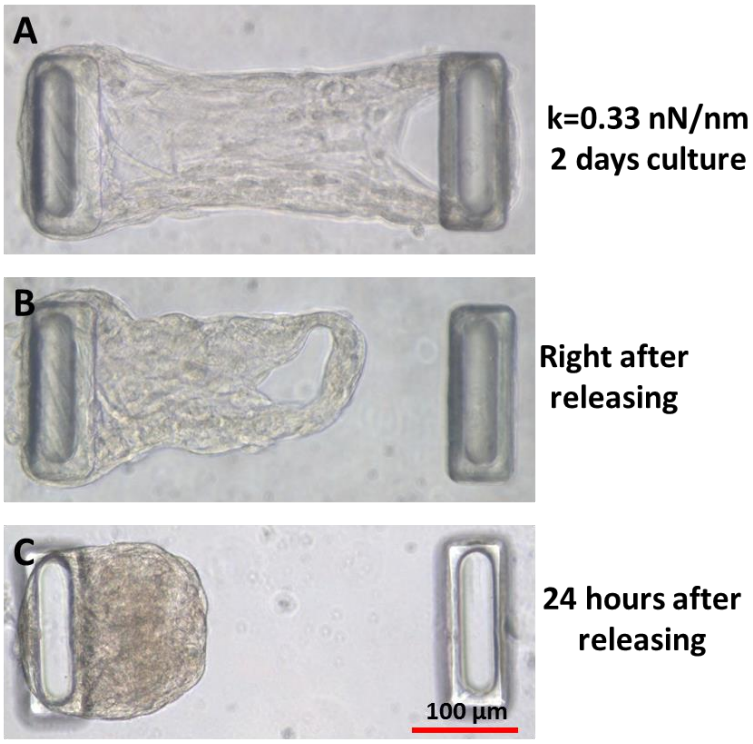

Figure 4. 4 Phase images of fully-released micro-tissues (k = 0.33 nN/nm posts). A: Before release (2 days culture). B: Right after releasing the tissue. C: 24 hours after release.

4.2.5 Evaluating α-SMA and Apoptosis

To detect apoptotic cells, 5μM NucView 488 Caspase-3 assay substrate (Biotum, Hayward, CA) was applied to micro-tissues for 30 minutes prior to fixing the tissues. This initially non-fluorescent assay substrate consists of fluorogenic DNA dye coupled to the caspase-3/7 DEVD recognition sequence and when caspase3/7 cleaves the substrate in apoptotic cells, a high-affinity DNA dye with bright green fluorescence is released. As a positive control for caspase-3 expression, 5 uM Staurosporin was applied to micro-tissues for 5 hours in a separate dish. Micro-tissues were fixed in 4% paraformaldehyde and permeabilized with 0.25% Triton X-100 (Sigma, St. Louis, MO), stained, and analyzed using imaging. Total number of nuclei and the total number of apoptotic cells were counted in each micro-tissue. To visualize α-SMA, tissues were blocked with 1.5% normal goat serum in PBS for 30 min, and incubated with primary anti-α-SMA (Sigma, St. Louis, MO) antibody for 1 h. Fluorescently labeled secondary antibody (Alexa-546, Invitrogen, Carlsbad, CA) was then applied and imaged with Leica SP5 point scanning confocal/DMI6000 inverted microscope. Fixed mouse brain and rat carotid tissues were stained in parallel as negative and positive controls, respectively.

4.2.6 Statistical Analysis

All data points are reported as mean ± standard deviation. Statistical comparisons were made using either t-test or two-way analysis of variance (ANOVA) depending upon the number of groups, with $p < 0.05$ considered significant. When a significant difference was found with two-way ANOVA, pairwise comparisons were completed with the Holm-Sidak method (Sigmaplot 11.0, Systat Software).

4.3 Results

4.3.1 Effects of Changing Boundary Stiffness in Real Time on Cell-Generated Forces

When cultured against medium soft boundaries (k_{eff} = 0.165 nN/nm), the cell-generated forces increase for approximately two days, then level off at a homeostatic level of tension. In contrast, when one post is held rigidly by placing the magnet close to the culture dish (k_{eff} = 0.33 nN/nm), cell-generated forces start to increase rapidly and continue to increase until the magnet is removed. When the magnet is removed (after 24 or 60 hours depending upon the experimental group), the tissue tension drops abruptly but then begins to steadily increase. In the 24-hour-held group (stiffened to k_{eff} = 0.33 nN/nm and softened back to k_{eff} = 0.165 nN/nm in real time), the cell-generated forces rebound to the peak values within two days of additional culture (Figure 4.5).

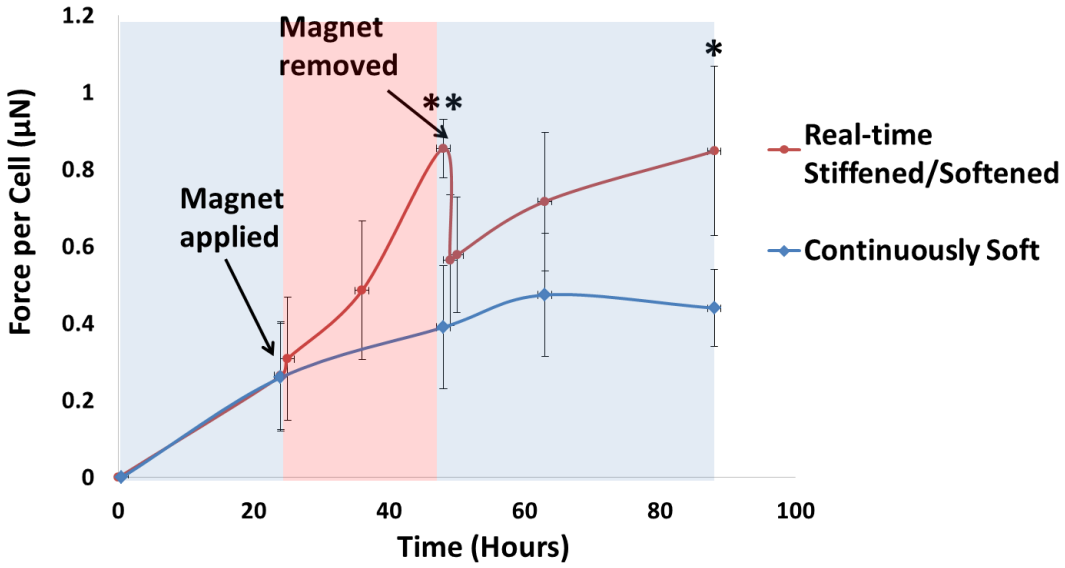

Figure 4. 5 Initially k_{eff} = 0.165 nN/nm for both groups (blue region on the left). In the real-time stiffened/softened group, k_{eff} is increased to 0.33 nN/nm by application of magnetic force (pink region). Removing the magnet decreased keff to its initial value in real-time stiffened/softened group (blue region on the right). Holding one post rigidly increased cell generated forces (**: Significantly higher force per cell than continuously soft group (t-test, p=0.001)). Removal of the magnet caused an abrupt drop in tissue tension, but tension rebounded and continued to increase the force (*: Significantly higher force per cell than

continuously soft group (t-test, $p<0.05$) For all groups TGF-β: 1 ng/mL and the individual post stiffness = 0.33 nN/nm).

4.3.2 Effect of Boundary Stiffness Reduction on α-SMA Distribution

No change in α-SMA distribution was observed as a result of changing the boundary stiffness in real time by removing the magnetic force (Figure 4.6). All of the cells have α-SMA incorporation into stress fibers, except when cultured against very soft micro-posts where neither the control nor stiffened group showed α-SMA+ stress fibers (Appendix-VIII). Less α-SMA staining was observed in the inner regions of doge-bone tissues and no stain was observed in the core of the completely released tissues (balled-up tissues) (Figure 4.7). Yet the cells on the outer surface of the retracted tissues still stained positive for α-SMA indicating the persistence of myofibroblast markers in those cells. The lack of staining of the internal cells may be due to hindered diffusion of secondary antibody rather than de-differentiation (see Discussion).

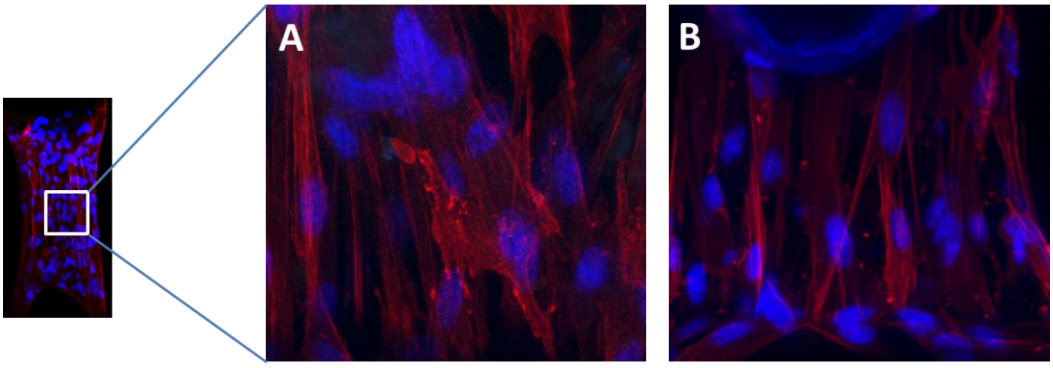

Figure 4. 6 A: α-SMA (red) and cell nuclei (blue) in micro-tissue with one post hold rigidly (higher boundary stiffness). B: Micro-tissue between continuously soft posts (lower boundary stiffness). The sequestration of α-SMA into the stress fibers in these images indicates that the VICs in both groups are myofibroblasts.

4.3.3 Effect of Boundary Stiffness Reduction on Apoptosis

In all cases, apoptosis was observed only when VICs were pretreated with 5 ng/mL TGF-β before seeding into the micro-tissues (Figure 4.8). The proportion of apoptotic cells does not increase significantly when the effective boundary stiffness is reduced by

releasing the rigidly held post (5.7±2.04% in real-time stiffened/softened group, 4.07±2.67 in continuously soft group). Releasing micro-tissues from posts completely and letting them contract into a ball increases the proportion of apoptotic cells significantly (31.4±21.1%), but apoptosis was not observed when cells are pre-treated and cultured with low serum (1% FBS) (Figure 4.9).

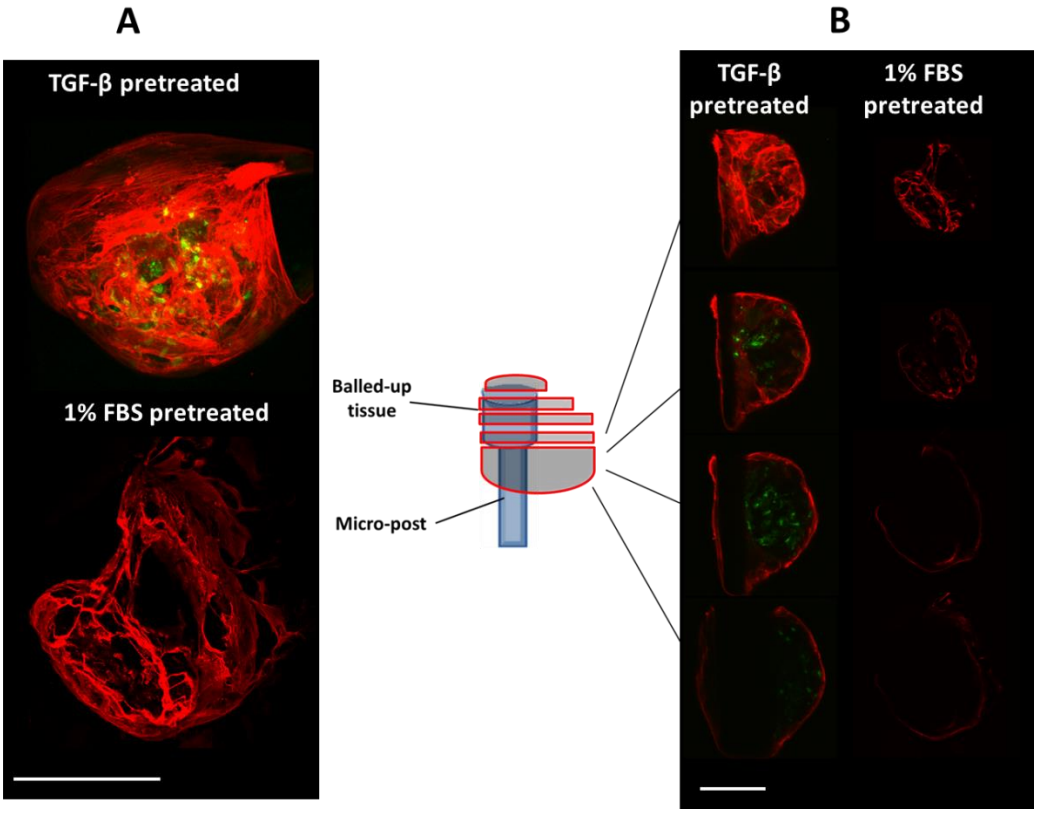

Figure 4. 7 A: Maximum projections of confocal images of a fully released micro-tissue two days after release. B: Z-stack slices at different levels of the micro-tissues (Red: α-SMA, Green: Caspase-3). Only cells on the surface of the completely released (balled-up) tissues stain positive for α-SMA, while only the cells in the inner regions of TGF-β pretreated group stain positive for the apoptotic marker (scale bars: 100 μm).

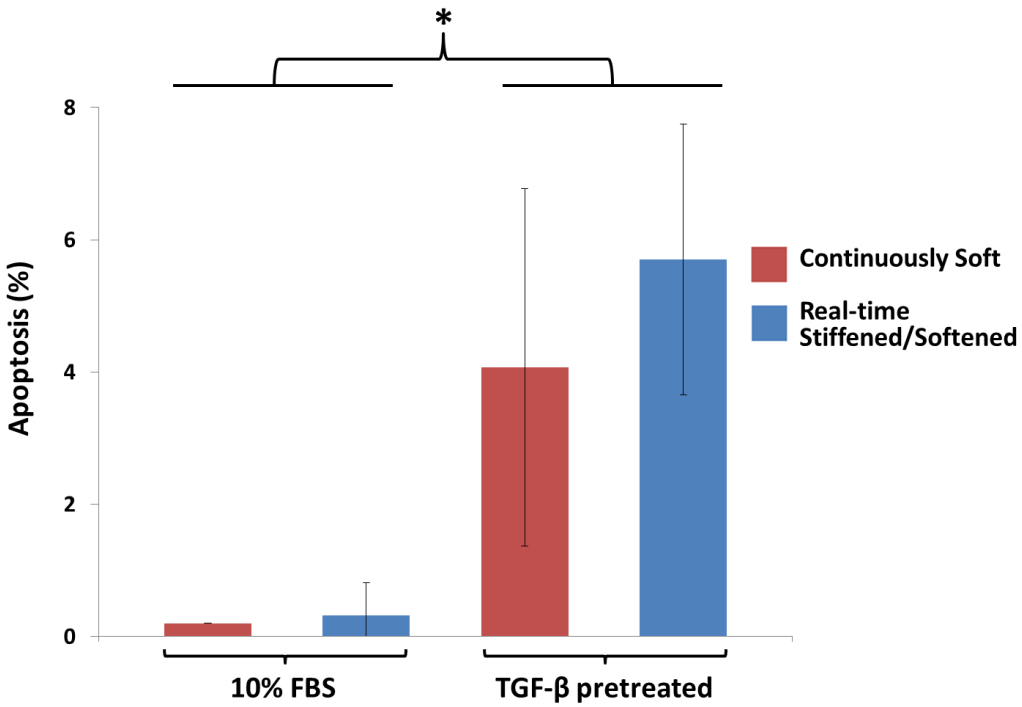

Figure 4. 8 5 ng/mL TGF-β pretreatment increases apoptosis in micro-tissues (n=4-6, *: p<0.001, Two-way ANOVA).

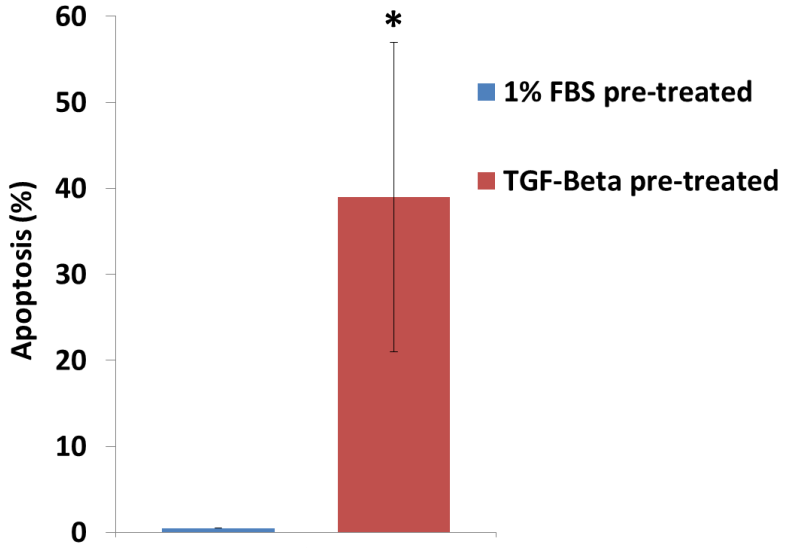

Figure 4. 9 Releasing micro-tissues, completely, triggers apoptosis in TGF-β pre-treated groups tissues (n=3, *: p<0.05, t-test).

4.4 Discussion

This study is the first quantitative investigation of the effects of dynamic changes in stiffness on cell phenotype in a 3D protein matrix. Our novel method utilizing magnetic force to constrain the motion of one of two flexible posts between which VIC-populated micro-tissues were cultured effectively doubled the boundary stiffness and resulted in a significant increase in cell-generated forces. When the magnetic force was removed, the effective boundary stiffness was halved, and the tissue tension dropped to 65-87% of the peak value. Surprisingly, following release the cell-generated forces continued to increase for the next two days rather than reducing down to the homeostatic tension level of the control group with identical (but constant) boundary stiffness. The rapid release of tension with the return to baseline boundary stiffness did not result in a decrease in number of cells with α-SMA positive stress fibers or an increase in apoptosis. In contrast, when samples were entirely released from the boundaries and cultured free floating (where tension is minimal but cannot be measured), cells on the outer surface of the tissues remained positive for α-SMA, but the proportion of apoptotic cells increased more than five-fold (31%) in the central region. Together, these data indicate that modest temporary changes in boundary stiffness can have lasting effects on myofibroblast activation and persistence in 3D matrices, and that a large decrease in the ability of the cells to generate tension is required to trigger de-differentiation and apoptosis.

It has been reported that static magnetic field has no significant effect on cell growth or survival under normal culture conditions regardless of magnetic density [23]. Additionally, unless cells are pre-treated with X-irradiation or ferrous ions, static magnetic field does not cause significant DNA damage up to a maximum of 10 T. The magnetic field created by the permanent magnet utilized in this study is less the 0.7 T in

the present study (Appendix-IX). Moreover, all micro-tissues are exposed to the magnetic field, since both tissues with magnetically-held posts and tissues without Ni particle (continuously soft boundary group) were in the same dish. Therefore, we attribute the change in cell behavior to real-time change in boundary stiffness (holding or releasing the post). However, future experiments can be done with more rigorous controls, e.g., holding posts by gluing glass rods affixed to well wall instead of magnets to rigidly hold the posts. In addition, using nickel particles glued onto posts in the absence of magnetic field can be suggested as a control for the effect of the Ni particles.

Previously, by utilizing graded levels of boundary stiffness and TGF-β concentrations, we showed that these two factors increase cell-generated forces in a synergistic way, and that increasing one of the factors without a moderate level of the other factor does not affect cell-generated forces significantly [15]. Under soft boundaries and/or low TGF-β concentration, cell-generated forces reach a plateau after 2 days, while they keep increasing if the post stiffness is greater than 0.33 nN/nm and TGF-β is greater than 0.05 ng/mL [15]. Despite differences of culture media (FBS in this study rather than chemically defined) and the pre-treatment with TGF-β in this study, the force-per-cell values in the present study are comparable with our previous results for similar boundary stiffness and TGF-β level. Moreover, increasing boundary stiffness via magnetic force affects the cell-generated-forces in the same fashion.

When the boundary stiffness is decreased in real time by releasing the magnetically held post, cell-generated forces keep increasing as if they are still at the higher boundary stiffness level when cells are pretreated and cultured with 10% FBS and 5 ng/mL TGF-β. These observations indicate that culturing cells under higher stiffness for just one or two days results in an irreversible transformation in cell phenotype. In contrast to our

findings in 3D, using tunable stiffness 2D substrates with photodegradable chemistry, Anseth and colleagues have demonstrated that reducing substrate modulus in real time results in de-differentiation of activated VICs [24]. In their initial study, after three days of culture on stiff (32 kPa) substrates, they reduced the modulus to 7 kPa and observed a substantial decrease in α-SMA-positive stained cells after two days. The same group more recently reported that culturing cells on stiff substrates for seven days and then reducing the modulus in real time does not result in the myofibroblast de-differentiation and the concluded that there is a time or dose limit for lineage plasticity for myofibroblast-to-fibroblast transition [21]. In the present study, the dose limit for myofibroblasts de-differentiation might have been exceeded due to the pretreatment of the cells with TGF-β1 for four days. Moreover, cell-matrix interactions in 3D may have an irreversible upregulation of pathways increasing force generation, which can explain the increase in cell-generated forces even when the boundary stiffness is reduced in the present study. Alternatively, in 3D, a positive feedback due to local stiffening can promote higher contractile forces, whereas, in 2D, this dynamic reciprocity between the cells and matrix does not exist – when the substrate modulus is decreased, there is no lingering feedback on the cells.

Intrinsic mechanical properties of the remodeled matrix can affect the cell sensitivity to changes in global environment. Recently, by using the μ-TUG system, Zhao et al. [25] showed that the modulus of the micro-tissues correlates positively with post stiffness. Similar to that study, here we used incremental strain instead of taking the non-deformed length of the micro-tissues, since tissues initially under stress by cell force [25]. In the present study, when we increased the boundary stiffness for one day, the average matrix modulus of the fibrin micro-tissues increased (from 37 kPa to 82 kPa); however, the difference was not statistically significant (Appendix-X) ($p < 0.05$; power = 0.141).

Factors which may have contributed to the large variability in matrix stiffness values include the low number of tissues (n = 3), the broad range of cells-per-tissue in the group with stiffened boundary (held for 1 day), and the fact that one of the tissues which was close to failure in this group. Further, the matrix moduli of our micro-tissues are dramatically higher than that of reported by Zhao et al, for similar boundary stiffness [25]. This difference may be due to different gel proteins (fibrin v. collagen), cell types (VICs v. NIH 3T3 cells), and TGF-β concentrations (5 ng/ml v. none) used in two studies. We attempted to repeat this experiment with higher number of samples but experiment failed due to excessive cell death determined in the tissues (~50%). Limitations of the μ-tissue gauge method including cell death are discussed in the next chapter.

In addition to intrinsic matrix stiffness, cell-cell and cell-matrix connections are also key factors increasing contractile ability and activating myofibroblast phenotype. Studies utilizing 2D substrates show that "supermature" focal adhesions (FA) with 6-30 μm sizes are required to generate threshold intracellular tension necessary for recruitment of α-SMA in stress fibers [26, 27]. Supermature FAs are recognized by expressing ECM fibronectin splice variant ED-A and α5β1 integrin. Unlike normal fibroblasts, myofibroblasts express OB-cadherin in cell-cell junctions, and inhibition of OB-cadherin decreases contractile ability and down regulates myofibroblast markers [27, 28]. In our case, supermature FAs and/or OB-cadherin rich cell-cell contacts formed during high-tension-culture period might be sustaining the ability of the cells to generate force even after reduction of the tissue tension. However, FAs and cadherin were not evaluated in the present study. Further research is needed to compare FA sizes or OB-cadherin staining under different mechanical tension levels and following tension reduction.

As a preliminary study, we treated micro-tissues with a conical Wnt pathway inhibitor which also degrades active β-catenin (JW-67, R&D Systems, MN) to weaken cell-cell contacts. Cell-generated forces remained almost flat or increased by time even under real-time stiffened boundary with JW-67 treatment while they increased in control group. However, this experiment needs to be repeated because of high cell-death proportion in micro-tissues. Although the Wnt pathway plays roles in important cell functions such as proliferation and migration, if it reduces the sensitivity of cell-generated forces to boundary stiffness, as our preliminary results imply, targeting β-catenin may be considered a therapeutic option for valve diseases. Yet, more research is needed to clearly understand the effect of β-catenin degradation on myofibroblast activation in 3D.

We observed persistence of α-SMA incorporation in stress fibers on the tissue surface following complete release of the boundary, but no α-SMA stain in the inner regions of the balled-up tissues. This result may be interpreted as complete diminishment of α-SMA in the middle regions of the tissue as a result of re-distribution of stress throughout the tissue. Intracellular tension may be maintained on the surface but decreased to levels at which α-SMA is not sequestered in the stress fibers in the inner regions. Alternatively, the lack of stain in the tissue core may be due to insufficient penetration of the secondary antibody into the tissues. Minimal collagen staining, which utilizes the same secondary antibody, was observed in the inner regions of the dog-bone shaped tissues in our previous study. To better analyze the α-SMA distribution in the middle regions of the tissues, the tissues need to be sectioned and analyzed with histology.

Upon complete release from the posts, apoptotic markers were observed in the TGF-β-pretreated group, but not in the non-TGF-β-pretreated group (note that the caspase stain does not use a secondary antibody and may penetrate further than the α-SMA and

collagen stain). It has been reported that releasing rigidly anchored myofibroblast-populated collagen gels and letting them contract or releasing splints holding wound edges triggers apoptosis [17-19]. Although the actual force values cannot be measured in samples fully freed from the boundaries, a rough correlation between the severity of the tension drop and the proportion of apoptotic cells appears to be emerging. In order of increasing severity of tension drop (estimated but not quantified): releasing splinted wound likely reduces the tension from a high level to a moderate level and results in 8% apoptosis, completely releasing myofibroblast-populated collagen gels from high tension to very low (zero boundary stiffness) results in 15% apoptosis, and completely releasing scar myofibroblast-populated collagen gels from very high tension to low (zero boundary stiffness) results in 40% apoptosis. In contrast, when myofibroblasts were isolated from hypertrophic scar tissues, apoptosis was not triggered upon release of rigidly anchored collagen gels [19]. Hypertrophic scar myofibroblasts secrete tissue transglutaminase enzyme which prevents collagen matrix degradation by both collagenase D and matrix metalloproteinase-2 [19], likely leading to a stiffer local matrix.

In the present study, we observed apoptosis in 38% of VICs pretreated with 5 ng/mL TGF-β for four days but less than 0.1% apoptosis in non-TGF-β -pretreated VICs upon complete release. Releasing rigidly anchored gels to a zero-boundary condition may cause a temporal imbalance between intracellular and extracellular tension which triggers apoptosis. Anseth and colleagues did not evaluate apoptosis in persistent myofibroblasts upon softening of the substrate [21]. Here we show that, apoptosis occurs only in TGF-β pre-treated group, where the initial cell-generated tension is higher (Appendix-XI). These findings can be interpreted as there is a threshold for intracellular tension above which decreasing stiffness –in turn tension- triggers apoptosis due to abrupt temporal imbalance between intracellular and extracellular tension.

4.5. Conclusion

The results of this study demonstrate that with only a temporary increase in boundary stiffness (1-2 days), cell-generated forces continue to increase as if the stiffness is permanently increased. Reasons for the continued high generation of force-per-cell are unclear at this time. The lack of phenotypic reversion could be due to increased cell density or cell-cell contact with increased compaction during the dynamically stiffened phase of culture, or possibly due to an increase in intrinsic stiffness of the ECM due to enhanced remodeling during the time the post was held magnetically.

Here we also demonstrate that the magnitude of the tension reduction plays an important role in myofibroblast persistence and apoptosis. In the present study, the myofibroblast phenotype was shown to be persistent (at least on the outer surface of the micro-tissues) regardless of the drop in tension, and apoptosis is only observed only with TGF-β1 pretreatment and a large drop in tension. These findings imply that it is very difficult to de-activate the myofibroblast phenotype once it reaches a certain severity, without causing tissue collapse in tissue engineered structures. To prevent the development of this irreversible situation, cell-generated forces and phenotype should be regulated throughout the entire *in vitro* culture period. Preventing excessive myofibroblasts activation and tissue stiffening could be helpful in creating functional tissue equivalents without fibrocontractive remodeling.

References

[1] Hinz B. Formation and function of the myofibroblast during tissue repair. The Jounal of Investigative Dermatology. 2007;127:526-37.
[2] Desmouliere A, Geinoz A, Gabbiani F, Gabbiani G. Transforming growth factor-beta 1 induces alpha-smooth muscle actin expression in granulation tissue myofibroblasts and in quiescent and growing cultured fibroblasts. J Cell Biol. 1993;122:103-11.
[3] Hinz B, Phan SH, Thannickal VJ, Galli A, Bochaton-Piallat ML, Gabbiani G. The myofibroblast: one function, multiple origins. Am J Pathol. 2007;170:1807-16.
[4] Tomasek JJ, Gabbiani G, Hinz B, Chaponnier C, Brown RA. Myofibroblasts and mechano-regulation of connective tissue remodelling. Nature reviews Molecular cell biology. 2002;3:349-63.
[5] Sarrazy V, Billet F, Micallef L, Coulomb B, Desmouliere A. Mechanisms of pathological scarring: role of myofibroblasts and current developments. Wound repair and regeneration : official publication of the Wound Healing Society [and] the European Tissue Repair Society. 2011;19 Suppl 1:s10-5.
[6] Henderson NC, Iredale JP. Liver fibrosis: cellular mechanisms of progression and resolution. Clinical Science. 2007;112:265-80.
[7] Dussaule JC, Guerrot D, Huby AC, Chadjichristos C, Shweke N, Boffa JJ, et al. The role of cell plasticity in progression and reversal of renal fibrosis. International journal of experimental pathology. 2011;92:151-7.
[8] Wallach-Dayan SB, Golan-Gerstl R, Breuer R. Evasion of myofibroblasts from immune surveillance: a mechanism for tissue fibrosis. Proc Natl Acad Sci U S A. 2007;104:20460-5.
[9] Mohler ER, 3rd, Gannon F, Reynolds C, Zimmerman R, Keane MG, Kaplan FS. Bone formation and inflammation in cardiac valves. Circulation. 2001;103:1522-8.
[10] Syedain ZH, Lahti MT, Johnso SL, Robinson PS, Ruth GR, Bianco RW, et al. Implantation of a tissue-engineered heart valve from human fibroblasts exhibiting short term function in the sheep pulmonary artery. Cardiovasc Eng Technol. 2011;2:101-12.
[11] Schmidt D, Dijkman PE, Driessen-Mol A, Stenger R, Mariani C, Puolakka A, et al. Minimally-invasive implantation of living tissue engineered heart valves: a comprehensive approach from autologous vascular cells to stem cells. Journal of the American College of Cardiology. 2010;56:510-20.
[12] Hinz B. Tissue stiffness, latent TGF-beta1 activation, and mechanical signal transduction: implications for the pathogenesis and treatment of fibrosis. Current rheumatology reports. 2009;11:120-6.
[13] Quinlan AM, Billiar KL. Investigating the role of substrate stiffness in the persistence of valvular interstitial cell activation. Journal of biomedical materials research Part A. 2012;100:2474-82.
[14] Walker GA, Masters KS, Shah DN, Anseth KS, Leinwand LA. Valvular myofibroblast activation by transforming growth factor-beta: implications for pathological extracellular matrix remodeling in heart valve disease. Circulation research. 2004;95:253-60.
[15] Kural MH, Billiar KL. Mechanoregulation of valvular interstitial cell phenotype in the third dimension. Biomaterials. 2014;35:1128-37.
[16] Desmouliere A, Redard M, Darby I, Gabbiani G. Apoptosis mediates the decrease in cellularity during the transition between granulation tissue and scar. The American journal of pathology. 1995;146:56-66.
[17] Carlson MA, Longaker MT, Thompson JS. Wound splinting regulates granulation tissue survival. The Journal of surgical research. 2003;110:304-9.

[18] Grinnell F, Zhu M, Carlson MA, Abrams JM. Release of mechanical tension triggers apoptosis of human fibroblasts in a model of regressing granulation tissue. Experimental cell research. 1999;248:608-19.
[19] Linge C, Richardson J, Vigor C, Clayton E, Hardas B, Rolfe K. Hypertrophic scar cells fail to undergo a form of apoptosis specific to contractile collagen-the role of tissue transglutaminase. The Journal of investigative dermatology. 2005;125:72-82.
[20] Wang H, Haeger SM, Kloxin AM, Leinwand LA, Anseth KS. Redirecting Valvular Myofibroblasts into Dormant Fibroblasts through Light-mediated Reduction in Substrate Modulus. PLoS ONE. 2012;7:e39969.
[21] Wang H, Tibbitt MW, Langer SJ, Leinwand LA, Anseth KS. Hydrogels preserve native phenotypes of valvular fibroblasts through an elasticity-regulated PI3K/AKT pathway. Proceedings of the National Academy of Sciences. 2013;10.1073/pnas.1306369110.
[22] Quinlan AMT, Sierad LN, Capulli AK, Firstenberg LE, Billiar KL. Combining dynamic stretch and tunable stiffness to probe cell mechanobiology in vitro. PloS one. 2011;6:e23272.
[23] Miyakoshi J. Effects of static magnetic fields at the cellular level. Progress in Biophysics and Molecular Biology. 2005;87:213-23.
[24] Kloxin AM, Benton JA, Anseth KS. In situ elasticity modulation with dynamic substrates to direct cell phenotype. Biomaterials. 2010;31:1-8.
[25] Zhao R, Chen CS, Reich DH. Force-driven evolution of mesoscale structure in engineered 3D microtissues and the modulation of tissue stiffening. Biomaterials. 2014;35:5056-64.
[26] Goffin JM, Pittet P, Csucs G, Lussi JW, Meister JJ, Hinz B. Focal adhesion size controls tension-dependent recruitment of alpha-smooth muscle actin to stress fibers. J Cell Biol. 2006;172:259-68.
[27] Hinz B, Gabbiani G. Cell-matrix and cell-cell contacts of myofibroblasts: role in connective tissue remodeling. Thrombosis and haemostasis. 2003;90:993-1002.
[28] Verhoekx JS, Verjee LS, Izadi D, Chan JK, Nicolaidou V, Davidson D, et al. Isometric contraction of Dupuytren's myofibroblasts is inhibited by blocking intercellular junctions. The Journal of investigative dermatology. 2013;133:2664-71.

CHAPTER 5: Discussion

5.1 Overall Impact and Future Directions

The work presented in this thesis provides the first quantitative relationships between boundary stiffness, TGF-β and myofibroblast activation in 3D. Understanding how cells respond to mechanical and chemical signals and the ECM is essential for understanding cardiac physiology and pathology [1]. In particular, quantitative approaches are needed for understanding the interaction between these signals on cell behavior. This study reveals key relationships in the regulatory stimuli that may provide new insights into the fundamental processes of valve remodeling and fibrosis. Although the effects of completely freeing constrained fibroblast-populated collagen gels [2] or completely blocking TGF-β have been studied [3], the investigation of graded and controlled changes in stiffness and TGF-β concentration utilized herein represents a novel approach. This knowledge provides insight into ways in which VIC and other fibroblastic cell activation may be controlled in fibrotic and engineered tissues.

Controlling the fate of the myofibroblasts is desired to create functional engineered organs and to cure fibrotic diseases. In an engineered valve with living cells, for example, the design parameters are very complex since not only the passive stresses due to external loading need to be minimized, the cell-generated forces are also essential to control as they potentially lead to changes in the mechanics of the valve due to direct contraction [4] and by long-term phenotypic shifts and fibrotic remodeling. One possibility for developing a tissue engineered valve rapidly would involve culturing VICs under conditions that induce myofibroblast activation to maximize the rate of matrix synthesis (e.g., high stent stiffness) and then altering culture conditions (e.g., by increasing stent compliance) to reduce the myofibroblast activity to the level of a healthy valve for implantation. An understanding of how boundary stiffness affects VIC phenotype could

also provide the basis for developing new clinical treatments offering the possibility of reversing or even circumventing stenosis. For example, percutaneous valve repair methods involving removal of stiff tissue at the edges of a valve to halt or reverse valve fibrosis are conceivable. High-pressure water-stream scalpels [5] and thulium:YAG laser [6] have been used pre-clinically for percutaneous aortic valve resection and could potentially be utilized for removing fibrotic areas from a valve. However, as described in Chapter 4, the myofibroblast phenotype may be irreversible when the magnitude of tension reduction or boundary softening is limited while severe reduction of tension triggers apoptosis. The reasons for the persistent myofibroblast activation may include larger cell focal adhesion structures, stronger cell-cell contacts or stiffer local environment developed under initial stiff/high-tension condition. Quantifying and/or blocking, OB-cadherin, β-catenin or focal adhesions and quantifying the local matrix modulus at different stages of real-time changed stiffness conditions require further study. Therefore, research focusing on techniques to monitor and control cell phenotype during the entire remodeling period may facilitate further advancement in this area. It is possible that cell-generated forces and matrix stiffness can be prevented from reaching excessive levels where a phonotypic shift (de-differentiation) without apoptosis becomes impossible.

The focus of this thesis was the combinatorial effect of multiple myofibroblast activators on VIC phenotype. To be able to keep cell-generated tensions between “safe limits” where they are below myofibroblast activation thresholds and high enough to produce mechanically strong *de novo* tissues, the effect of tension on ECM remodeling needs to be elucidated quantitatively. Thus, research is needed to determine the optimal tension levels and growth factor combinations for robust tissue formation without excessive active and passive stresses built up in the tissue. In future work, the effects of growth

factors and boundary stiffness on the ECM components synthesized within the micro-tissues should be analyzed quantitatively; these include collagen, elastin, proteoglycans, and GAGs which are important not only for tissue mechanics, but also cell signaling.

Furthermore, the 3D culture model utilized in the present thesis can be used to study osteogenesis. Recently, it was shown that high glucose, elastin degradation products and TGF-β1 induces osteogenic differentiation synergistically in vascular smooth muscle cells [7]. The effect of tissue boundary stiffness on the interaction between these factors can be studied understand osteogenic differentiation more completely. In addition to differentiation, effect of calcification on tissue stiffness can be evaluated by using micro-tissue gauges to measure tissue modulus.

5.2 Limitations

Although the micro-tissue gauge system has the potential advantages of high-throughput experimentation, ease of microscopic eavalution, and minimal cell and material consumption, the method has limitations which cause frequent experimental failure (lack of micro-tissue formation). The most prevalent failure mechanisms include poor de-wetting (aspirating excess gel/cell solution to clear surface out of the micro-wells), tissue pop-outs (tissue floating upon addition of culture media after gel polymerization), tissue slipping off the posts and cell death in micro-tissues.

After resuspending cells in cold fibrin gel solution (fibrinogen and thrombin is reconstituted) it is added to micro-tissue gauge dishes and centrifuged into micro-wells. Immediately after centrifuge excess gel solution is aspirated by a glass Pasteur pipette so that gel solution is completely removed from the PDMS dish surface-out of the micro-wells. If gel starts to polymerize prematurely or the surface is not hydrophobic, gel-cell

mixture remains over the micro-wells and prevents formation of dog-bone tissues by keeping tissues attached to side walls of the wells. To avoid this problem; the Pluronic concentration can be increased to make surfaces more hydrophobic. However, too high of a Pluronic concentration may result in tissue pop-outs or tissue slipping from the posts. When micro-wells and posts become to hydrophobic, tissues can come out as soon as the culture media was added to dishes, or tissues can slip off the posts especially when posts are bent substantially due to TGF-β treatment or high cell number in the tissues. Maximum Pluronic concentrations were optimized as up to 2% in normal dishes and 4% in UV treated dishes (to cure UV activated glue for Ni particles on the posts). Nevertheless, PDMS aging and UV treatment increase the variability in PDMS hydrophobicity and may result in unexpected experiment failure. These problems narrow the range of available fibrinogen and thrombin concentrations, cell number and post stiffness in experiments.

Cell death in the micro-tissues was another major problem causing failure and making it difficult to reproduce results. Previously, the Chen group reported that in micro-tissues made of a collagen-fibrin mixture, cell death can reach up to 36% immediately after seeding and up to 54% in 7 days [8]. However, in some of our experiments all of the cells died after seeding. We determined two different reasons for cell deaths: first, in some cases, the gel may dry during incubation for polymerization prior to adding culture media (especially if the humidity level is low in the incubator). Second, we found more frequent cell death when cells are pre-treated with TGF-β or they are cultured longer on tissue culture plastic prior to seeding into micro-tissues. The reason for higher cell death frequency in pre-treated groups may be due to higher tension drop upon detaching from rigid cell culture plastic, which is in good agreement with our findings in Chapter 4. Cell cycle phase was not determined in any of our experiments. The relationship between

cycle phase, doubling-time and cell-death ratio needs to be elucidated in future studies. These limitations decreased the number of successful experiments and the number of samples in the present study.

Another limitation of the present studies is that we did not quantify the *de novo* ECM production. Collagen-I accumulation was semi-quantified by comparing fluorescent stain intensity under different boundary stiffness, but a quantitative analysis such as hydroxiproline assay was not utilized. As mentioned in the previous section, effect of cell-generated forces or stiffness on ECM secretion needs to be quantified in the future studies.

5.3 Conclusions

The studies presented in this thesis represent an important step forward understanding the effect of the mechanical environment on VIC phenotype and myofibroblast differentiation in general, in a 3D ECM environment. Our results imply that there may be optimum tissue tension and growth factor concentration levels at which ECM production can be promoted without excessive myofibroblast activation. Future studies focusing on the interactions between mechanical environment, growth factors and *de novo* ECM properties (both protein content and mechanical properties) will be helpful in creating robust engineered structures without fibrocontractive tissue remodeling. By regulating tension- in turn cell phenotype- with drugs and augmenting ECM secretion during *in vitro* culturing period, off-the-shelf TEHVs and other engineered organs without long-term complications such as retraction or tissue bulking can be produced. Moreover, 3D model presented here can be used for mechanosensitive drug studies to prevent or reverse heart valve fibrosis/calcification or other fibrocontractive diseases.

References

[1] Baudino TA, Carver W, Giles W, Borg TK. Cardiac fibroblasts: friend or foe? Am J Physiol Heart Circ Physiol. 2006;291:H1015-26.
[2] Grinnell F, Zhu M, Carlson MA, Abrams JM. Release of mechanical tension triggers apoptosis of human fibroblasts in a model of regressing granulation tissue. Exp Cell Res. 1999;248:608-19.
[3] Walker GA, Masters KS, Shah DN, Anseth KS, Leinwand LA. Valvular myofibroblast activation by transforming growth factor-beta: implications for pathological extracellular matrix remodeling in heart valve disease. Circulation research. 2004;95:253-60.
[4] Merryman WD, Huang HY, Schoen FJ, Sacks MS. The effects of cellular contraction on aortic valve leaflet flexural stiffness. J Biomech. 2006;39:88-96.
[5] Quaden R, Attmann T, Boening A, Cremer J, Lutter G. Percutaneous aortic valve replacement: resection before implantation. Eur J Cardiothorac Surg. 2005;27:836-40.
[6] Quaden R, Attmann T, Schunke M, Theisen-Kunde D, Cremer J, Lutter G. Percutaneous aortic valve replacement: endovascular resection of human aortic valves in situ. J Thorac Cardiovasc Surg. 2008;135:1081-6.
[7] Sinha A, Vyavahare NR. High-glucose levels and elastin degradation products accelerate osteogenesis in vascular smooth muscle cells. Diabetes and Vascular Disease Research. 2013;10:410-9.
[8] Boudou T, Legant WR, Mu A, Borochin MA, Thavandiran N, Radisic M, et al. A microfabricated platform to measure and manipulate the mechanics of engineered cardiac microtissues. Tissue Eng Part A. 2012;18:910-9.

APPENDICES

Apenndix-I: Permissions

ELSEVIER LICENSE
TERMS AND CONDITIONS

May 23, 2014

This is a License Agreement between Mehmet H Kural ("You") and Elsevier ("Elsevier") provided by Copyright Clearance Center ("CCC"). The license consists of your order details, the terms and conditions provided by Elsevier, and the payment terms and conditions.

All payments must be made in full to CCC. For payment instructions, please see information listed at the bottom of this form.

Supplier	Elsevier Limited The Boulevard,Langford Lane Kidlington,Oxford,OX5 1GB,UK
Registered Company Number	1982084
Customer name	Mehmet H Kural
Customer address	60 Prescott Street Worcester, MA 01605
License number	3394910387095
License date	May 23, 2014
Licensed content publisher	Elsevier
Licensed content publication	Experimental Cell Research
Licensed content title	Regulating tension in three-dimensional culture environments
Licensed content author	Mehmet Hamdi Kural,Kristen Lawrence Billiar
Licensed content date	1 October 2013
Licensed content volume number	319
Licensed content issue number	16
Number of pages	13
Start Page	2447
End Page	2459
Type of Use	reuse in a thesis/dissertation
Portion	full article
Format	both print and electronic
Are you the author of this Elsevier article?	Yes
Will you be translating?	No
Title of your thesis/dissertation	REGULATING VALVULAR INTERSTITIAL CELL PHENOTYPE BY BOUNDARY STIFFNESS
Expected completion date	Jun 2014
Estimated size (number of pages)	120

Appendix-II: Force calculation in micro-tissue gauges

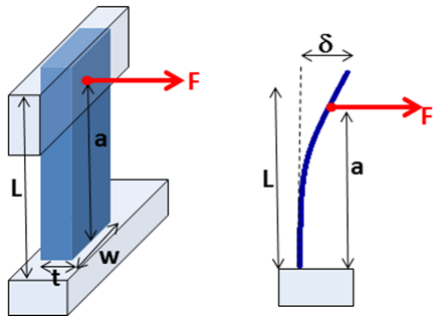

Beam bending equation: $\boldsymbol{I = \frac{wt^3}{12}}$ $\boldsymbol{F = \frac{\delta * 6EI}{a^2 * (3L - a)}}$ (Suppl. Eqn-1)

In the beam bending equation, E is theYoung's modulus of PDMS, δ is the post deflection, and a, L, t and w are geometric terms.

Representative volume elements (RVEs)

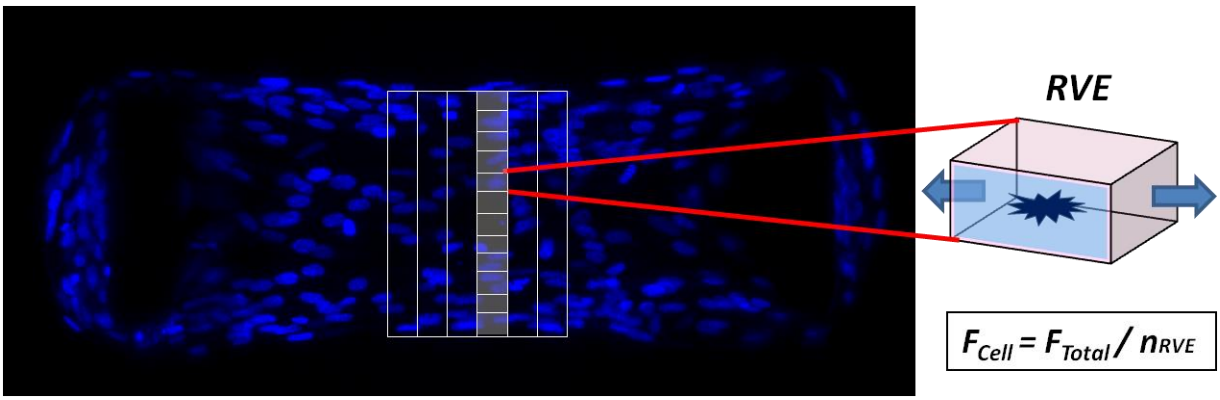

Figure S 1 An RVE includes one cell and surrounding extra cellular matrix. To calculate force per cell, we divided the total tension in the tissue into the average number of RVEs in the cross section, since the tension load is shared by only the cells in parallel.

To calculate average number of RVEs, we made the following assumptions:

1. All of the cells in the maximum projection area are aligned in the direction of tension
2. Cell distribution is homogeneous; cell overlaps and regions without cells are neglected.
3. Aspect ratio of the tissue dimensions and aspect ratio of one RVE is equal.

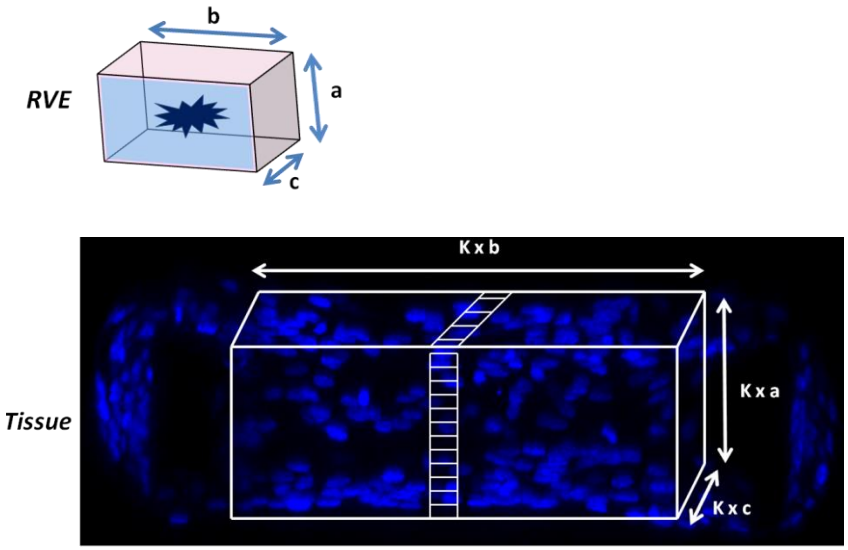

Figure S 2 The total cell number in the middle region of the micro-tissue is taken as the number of RVEs.

$$Numer\ of\ RVEs\ paralel\ to\ cross\ section\ (n_{Parallel\ RVE})\ = K^2$$

$$Total\ numer\ of\ RVEs\ in\ the\ tissue = Total\ number\ of\ cells\ in\ the\ tissue\ (n_{cells})$$

$$n_{cells} = \frac{Volume\ of\ Tissue}{Volume\ of\ RVE} = \frac{K^3 a \times b \times c}{a \times b \times c} = K^3 \qquad K = (n_{cells})^{\frac{1}{3}}$$

(S1)

So, $n_{Parallel\ RVE} = (n_{cells})^{\frac{2}{3}}$

Appendix-III: PDMS Ratios and Heat Treatment for Specific Post Stiffness

Table S 1 PDMS monomer:curing agent ratios and related μ-TUG stiffness determined by uniaxial tensile test.

PDMS monomer : curing agent weight ratio	Heat treatment	Stiffness of the μTUG cantilevers (kPa)
18:1	at 60 ^{0}C for 24 hours	630
10:1	at 110 ^{0}C for 20 minute	1300
10:1	at 110 ^{0}C for 28 hours	2200
4:1	at 60 ^{0}C for 24 hours + at 110 ^{0}C for 48 hours	4200

Appendix-IV: Two-way ANOVA results for homeostatic cell forces on day seven

Table S 2 All Pairwise Multiple Comparison Procedures (Tukey Test):

Effect of TGF-β1 Between Stiffness Groups	TGF-β1 concentration (ng/mL)			
k (nN/nm)	Within 0	Within 0.05	Within 0.5	Within 5
1.01 vs. 0.52	NS	NS	*(p<0.01)	* (p<0.001)
1.01 vs. 0.33	NS	NS	* (p<0.001)	* (p<0.001)
1.01 vs 0.12	NS	NS	* (p<0.001)	* (p<0.001)
0.52 vs 0.33	NS	* (p<0.001)	NS	* (p<0.01)
0.52 vs 0.15	NS	* (p<0.01)	NS	* (p<0.001)
0.33 vs. 0.15	NS	NS	NS	* (p<0.05)

Effect of Stiffness Between TGF-β1 Groups	k (nN/nm)			
TGF-β1 concentration (ng/mL)	Within 0.15	Within 0.33	Within 0.52	Within 1.01
5 vs. 0.5	NS	NS	NS	* (p<0.001)
5 vs. 0.05	NS	NS	NS	* (p<0.001)
5 vs. 0	NS	NS	* (p<0.001)	* (p<0.001)
0.5 vs. 0.05	NS	NS	NS	* (p<0.001)
0.5 vs. 0	NS	NS	* (p<0.001)	* (p<0.001)
0.05 vs. 0	NS	NS	* (p<0.001)	* (p<0.05)

NS: No statistically significant difference.
***: Significantly different with given p value.**

Appendix-V: Micro-tissue Failure Mechanisms

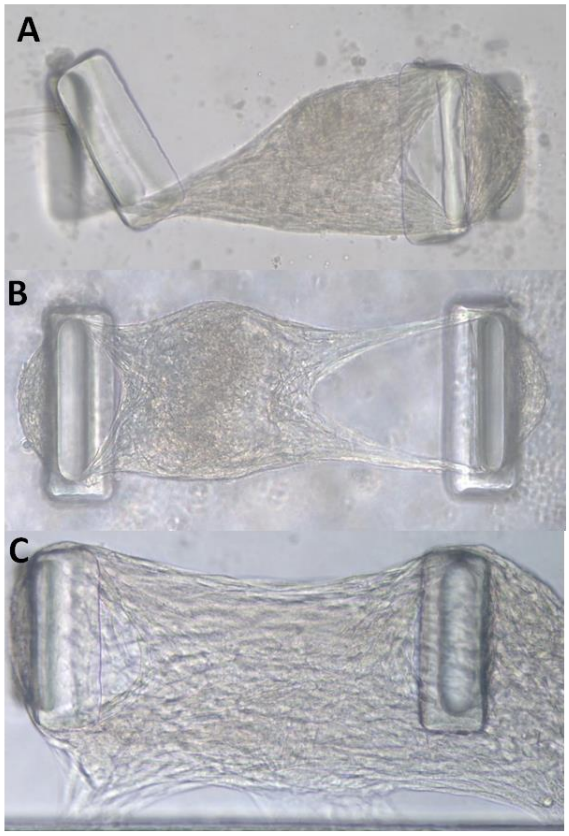

Figure S 3 A) Tissue slipping off the soft cantilever. B) Tissue thinning due to fibrinolysis and/or lack of ECM synthesis. C) Tissue adhered to the PDMS well.

Appendix-VI: Force-Generation Time Course for Different Boundary Btiffness

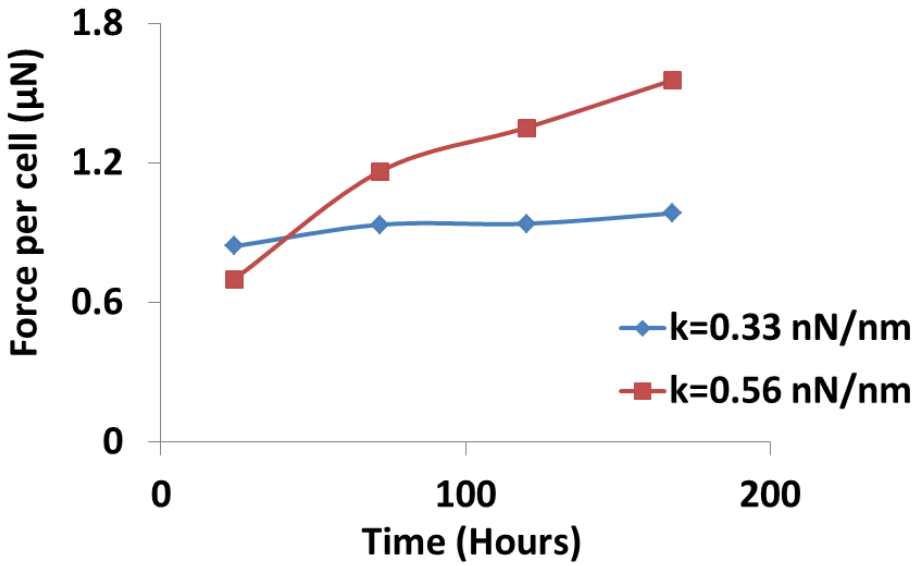

Figure S 4 Cell-generated forces remains almost flat for seven days with 0.33 nN/nm stiff posts, while they keep increasing when posts stiffness is 0.56 nN/nM.

Appendix-VII: Supplementary Force Data

Effect of stiffening boundary real time on force-per-cell values for different post stiffness, media or culture durations.

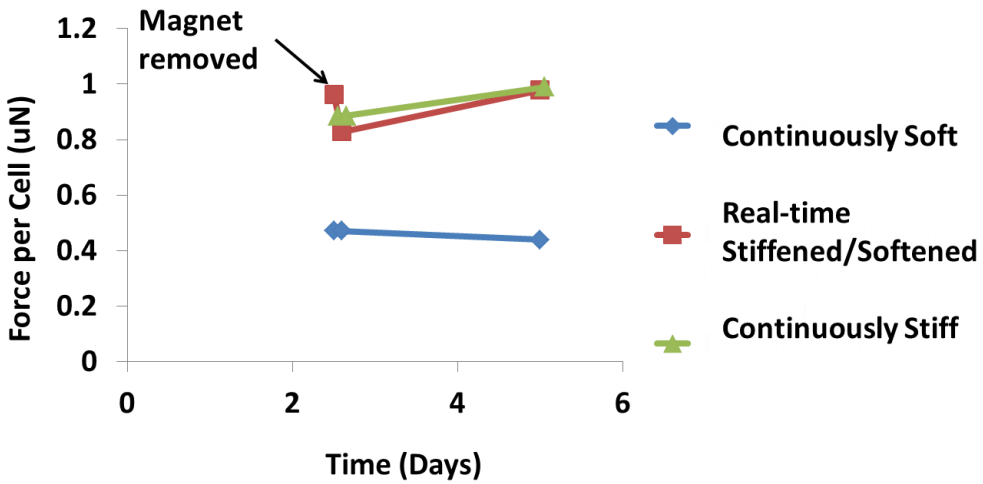

Figure S 5 k= 0.33 nN/nm. Pretreated with 5 ng/mL TGF-β for 4 days. Culture media: DMEM+10%FBS+1ng/mL TGF-β. One of the posts was held with magnetic force for 2 days.

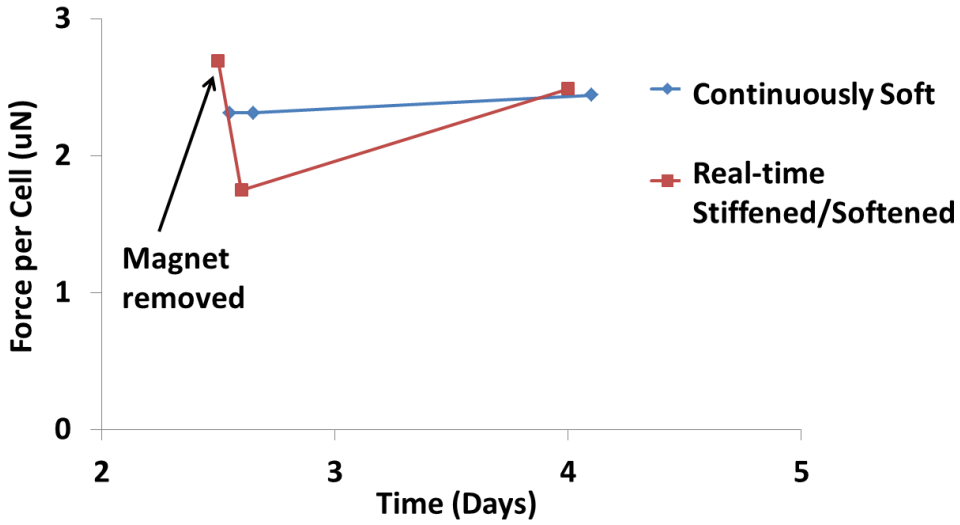

Figure S 6 k= 0.56 nN/nm. No pretreatment TGF-β. Culture media: DMEM+10%FBS+1ng/mL TGF-β. One of the posts was held with magnetic force for 2 days.

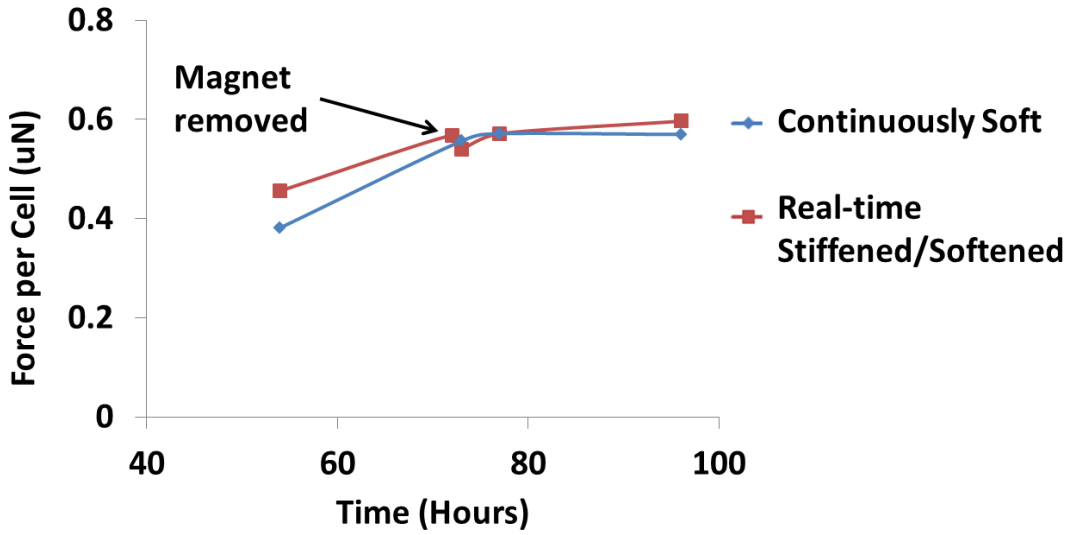

Figure S 7 k= 0.15 nN/nm. No pretreatment TGF-β. Culture media: DMEM+10%FBS+5ng/mL TGF-β. One of the posts was held with magnetic force for 2 days.

Appendix-VIII: α-SMA Distribution Under Very Soft Boundary

α-SMA distribution in micro-tissues with very low micro-posts (k=0.15 nN/nm)

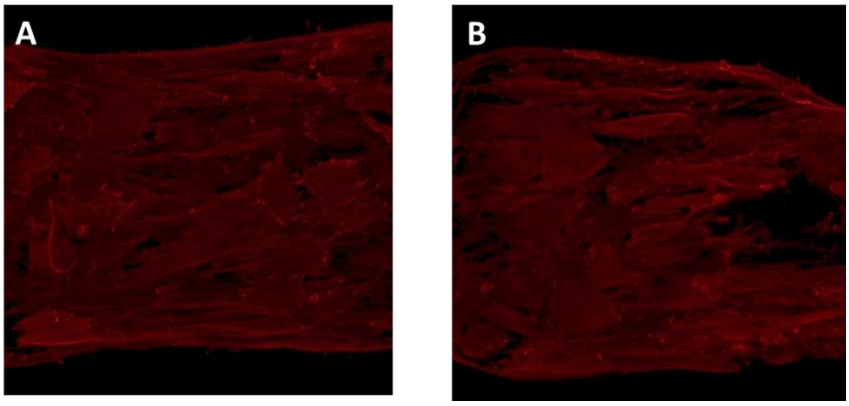

Figure S 8 A: Continuously soft boundary. B: Real-time stiffened and softened boundary. α-SMA stain is not incorporated into stress fibers with very soft micro-posts (k = 0.15 nN/nm).

Appendix- IX: Magnetic Fiels Visualization of the Permanent Magnet

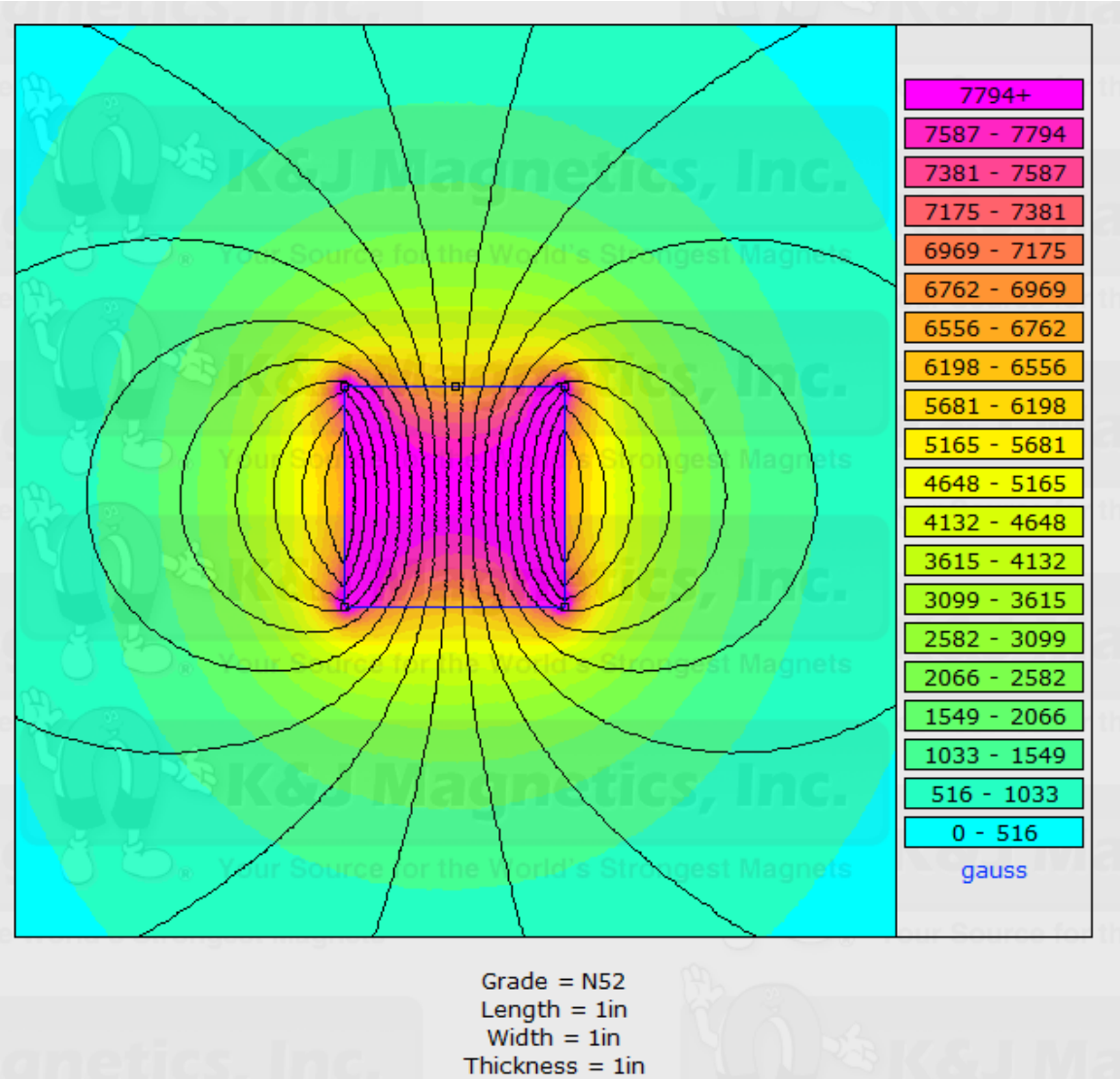

Figure S 9 Magnetic field visualization of NdFeB, Grade N52 permanent magnet (K&J Magnetics, Jamison, PA) in free space.

Appendix- X: Calculation of Micro-Tissue Matrix Modulus

Micro-tissues were stretched by applying magnetic force to the Ni bead glued on top of posts with a permanent magnet as shown in the Figure 4.4-A and B. The force applied by the magnet ($F_{stretch}$) was calculated by determining the deflection of the other post as a result of the stretching $\delta_{stretch}$. The applied force was divided by the initial cross-sectional area of the tissue to calculate the applied engineering stress ($\sigma = F_{stretch}/A$, A is tissue crossectional area). Light distribution patterns on the micro-tissues (Figure 4.4 C) were used to obtain strain distribution by using High Density Mapper (HDM) software (with help of Glenn Gaudette Lab, WPI) (Kelly et al., Medical engineering & physics. 2007;29:154-62). The output displacement gradients from the HDM software were divided by the local initial length (distance between measurements) to calculate the incremental uniaxial engineering strain ($\varepsilon_{stretch}$) in the region of interest (Figure 4.4-B). The tensile stiffness of the micro-tissue was calculated by dividing the change in applied stress by change in local strain (Zhao et al., Advanced Materials, 2013;25:1699-705): E = $\Delta\sigma_{stretch}/\Delta\varepsilon_{stretch}$.

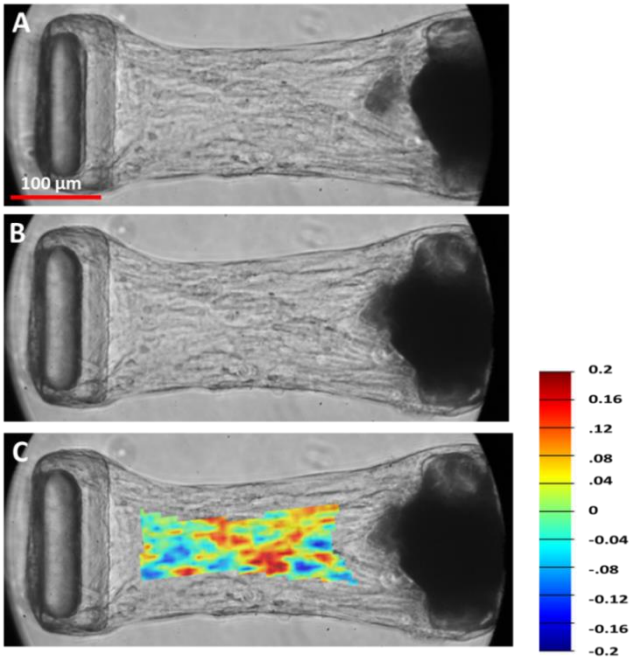

Figure S 10 A: Unstretched micro-tissue (3 days of culture). B: At peak stretch. C: Heat map showing strain distribution on the x-axis over the micro-tissue.

Initial tissue stresses (due to cell-generated forces) in our micro-tissues were 0.86±0.19 for continuously soft boundary and 1.08±0.35 kPa for the real-time stiffened-softened group, which are comparable to initial stress values reported by (Zhao et al., Biomaterials, 35(19), 5056-5064) for 0.3 nN/nm posts stiffness.

The incremental modulus of the micro-tissues with one post hold rigidly from day 2 to day 3 of culture (E = 82.1±51.2 kPa) is approximately double the modulus of micro-tissues cultured between the static posts (E = 37.3±4.9 kPa) (Figure 4.10); however, the difference is not statistically different and the power of the test was low due to low sample numbers (p = 0.207, power = 0.141, n=3 per group).

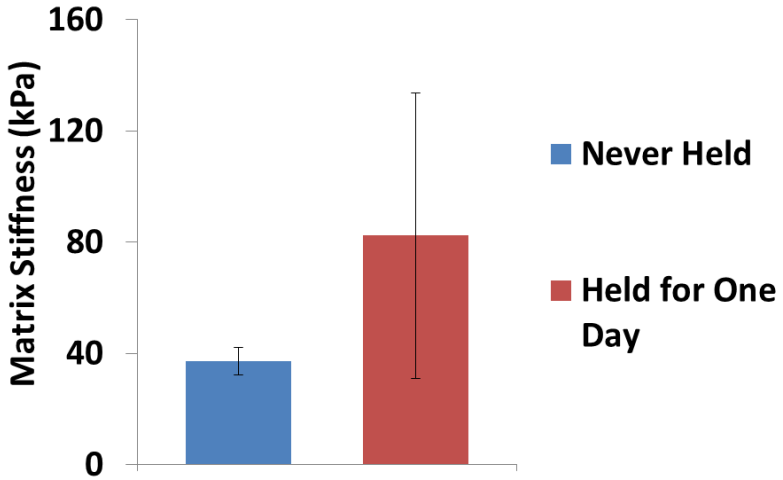

Figure S 11 Matrix stiffness of micro-tissues with one post rigidly hold (effective boundary stiffness increased from 0.165 nN/nm to 0.33 nN/nm after 24 hrs of clulture, then reduced back to 0.165 and mechanical properties measured after an additional 24 hrs) and those with continuously soft posts (k_{eff} = 0.165 entire experiment) (n=3 micro-tissues in each group).

Appendix- XI: Tissue Tensions Before Fully Releasing Gel Boundary

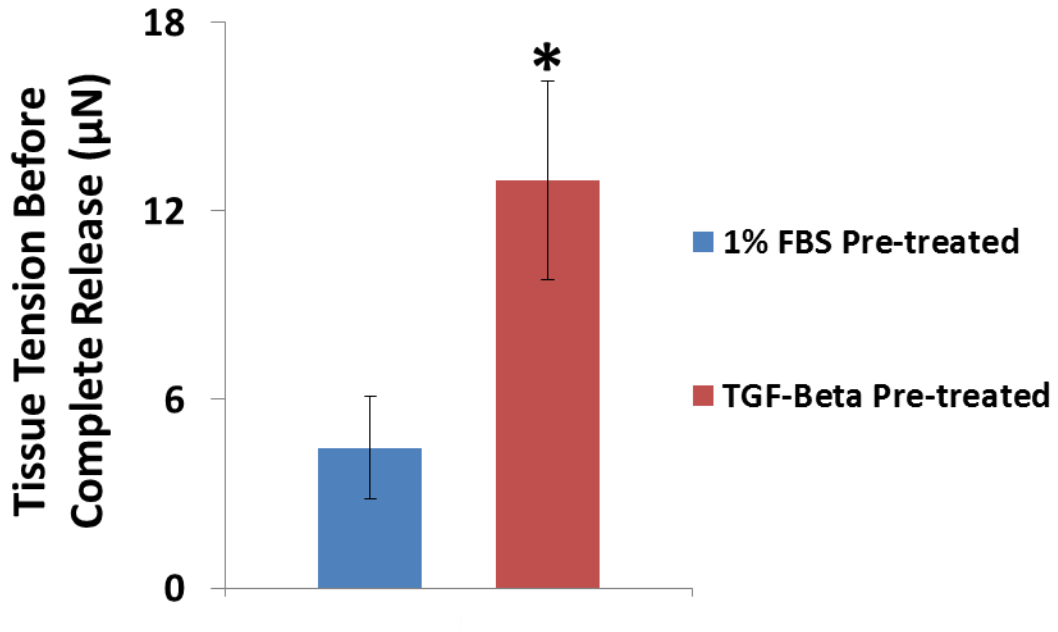

Figure S 12 Tissue tension prior to fully releasing micro-tissues is significantly higher in TGF-β pre-treated group (n=3, *: p< 0.05, t-test)